

**Evidence for a new model of intestinal morphogenesis**

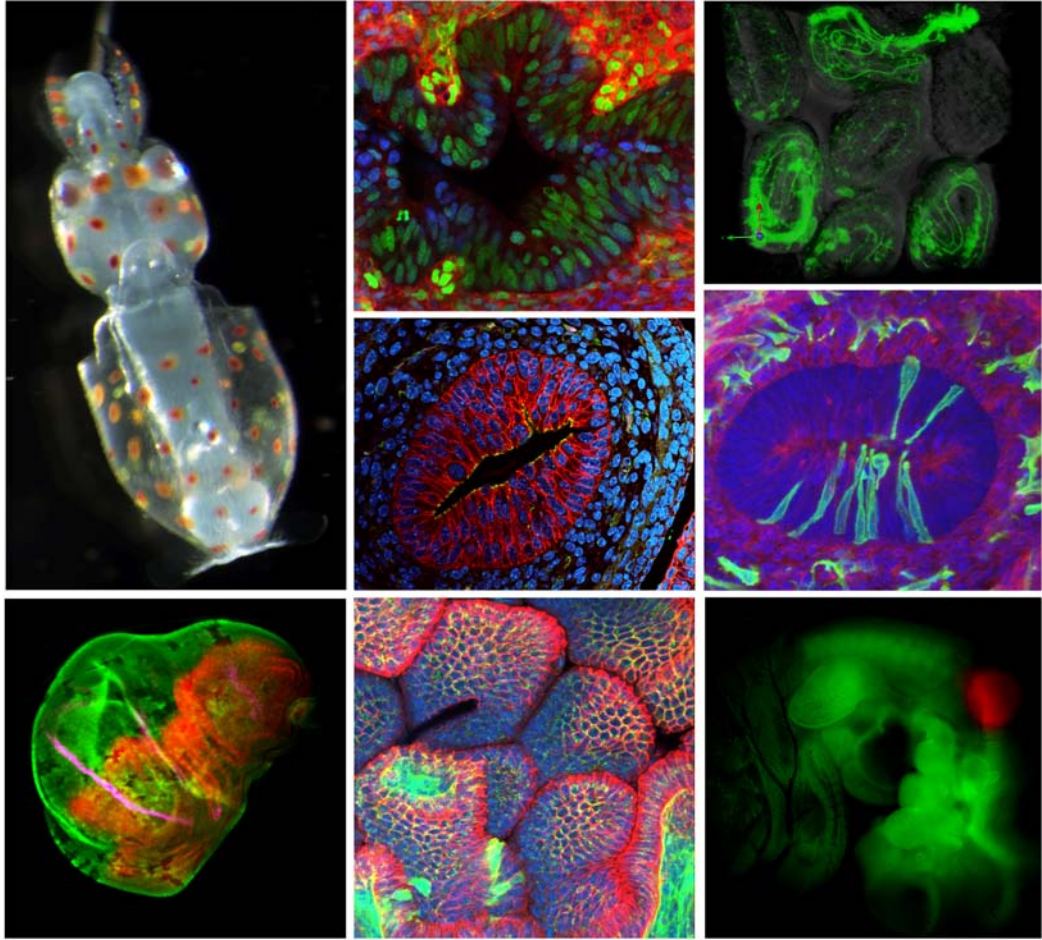
by

Ann Marie Staubach Grosse

A dissertation submitted in partial fulfillment  
of the requirements for the degree of  
Doctor of Philosophy  
(Cellular and Molecular Biology)  
in the University of Michigan  
2011

Doctoral Committee:

Professor Deborah L. Gumucio, Chair  
Professor Sally A. Camper  
Professor Andrzej A. Dlugosz  
Professor Gregory R. Dressler  
Professor Charlotte M. Mistretta



© Ann Marie Staubach Grosse  
2011

I dedicate this thesis to my family, friends, teachers, mentors, and lab.

## **Acknowledgements**

I want to start by thanking the people that first influenced who I am today: my parents. Mom and Dad, thank you for teaching me to work hard and to confront each challenge as it is presented. Your sacrifices have truly provided me with extraordinary opportunities. I am always thankful for your unending love and support (whether cheering during a sporting event or encouraging my pursuit of education and science). I would also like to thank my siblings Adam, Linda, and Gretchen for the past and future memories. I am grateful for the special family bond and friendship that we will always share. Additionally, I would like to thank extended family members including Sue Grosse, Anita Staubach, and Gary Vogt for encouragement and support, especially on the day of my defense.

Second, I would like to thank my husband, Steve. You are my best friend and my support. Thank you for always encouraging me to be my best, listening to my opinions and ideas, and exploring the world with me. Above all, thanks for making me laugh. I love you, and I am excited for what our future holds.

Next, I would like to thank my mentor, Deborah Gumucio. When I started graduate school, I had a lot to learn. Thank you, Deb, for being exceptional, patient leader and motivator. Your passion for teaching, science, and family is truly inspiring. Thank you for the opportunity to work and learn in your lab, and thank you for encouraging me explore science, to develop my scientific thinking, and to find a passion.

I would like to thank all of the Gumucio Lab members for teaching me how to carry out experiments while having fun. I have a number of individuals that I would like to thank personally. My rotation and first memories of the lab were filled with the shenanigans of Kathi, Chris, Blair, and Josh. Thanks to Andrea, Banu, and Neil for teaching me all about Pyrin, Siva, and FMF before we the lab became just guts. Andrea, thanks for the friendship, dessert, advice, and inspiration. Jierong for caring and for always willing to tag, tail, and genotype; you keep the lab running. Thank you Tracy for your sense of humor, your courageous and adventurous personality, and your unconditional love of science. To Asa, Will, Aaron, Mike, Andrea, Xing, Kate, Ajay, and Katherine for the happy hours, journal club, intellectual discussion, lab meetings, ideas, car rides, retreats, lab outings, scientific meetings, and encouragement. To the current members Kate, Michelle, Kara, Neil, Tracy, Jierong, Mark, Lauren, Ajay, and Katherine thanks for the daily camaraderie, lunches, lab gatherings, and support. I would like to offer a very special thanks to Mark and Lauren. My work and this thesis would not be complete without your commitment to the project. Thanks for your hard work, motivation, and ideas. I really enjoyed teaching you all I know about science.

I would like to thank multiple groups and individuals that have helped me develop scientifically. To my thesis committee, your ideas, suggestions, and advice have been a tremendous help. To the many scientific forums at University of Michigan including The Program in Cellular and Molecular Biology, Dev Bio lab group, Organogenesis, Gut Group, and Mouse Club. Thank you for providing a rich scientific environment to present, participate, field questions, ask questions, receive ideas, share reagents, and discuss science. Also, many thanks to my collaborators for talking science, sharing ideas, and providing reagents. Collaborators include but are not limited to Ben Margolis and lab (Jay Piccynski and Mark Schlueter), University of Michigan; Chris Janetopoulos, Vanderbilt University; Jeff Hildebrand, University of Pittsburgh; Santiago Schnell, University of Michigan; Helen McNeill, University of Toronto; and Andrea McClatchey, Harvard University. Also, many thanks to the

faculty and students of the Embryology course for the experience, opportunity, advice, entertainment, and scientific discussion.

There are a number of faculty and support staff throughout the University of Michigan that I would like to offer a special thanks. To the staff of the MIL (Chris Edwards, Dotty Sorenson, Shelley Almburg, Sasha Meshinchi), thank you for teaching me and re-teaching me how to use the microscopes and software. To the Morphology Core staff Marta Dzaman and Maria Ripberger, thank you for teaching me all I know about tissue prep and histology. I would like to thank Jessica and Cathy of the Cell and Molecular Biology program for providing an excellent training program and the support to complete my PhD. Becky Pintar of the Organogenesis Program for running a seamless training program and for being part of our lab for several years. To the Cell and Developmental Biology staff, especially Kristen Hug, for effortlessly taking care of the many unusual administrative requests.

Finally, I would never have made it this far without a great group of friends both in Ann Arbor and in distant cities. To all of my friends (mycircle, Thursday girls, volleyballers, fellow scientists, buffalo gals, medical school crowd, Northside/St. Aidan's) thanks for always going for drinks, vacations, dinners, working out, studying, and just hanging out. Amanda, it was great having a fellow scientist and friend that understands the challenges of marrying a medical student. Maria, thanks for always being outgoing, happy, energetic, adaptable, and willing to talk. Paulette, thanks for studying with me the first two years of graduate school. Steve and I always enjoy hanging out with you and Kevin, and you're your hospitality made the move to Ann Arbor a lot easier. Thanks for your continuous support and encouragement. Ryan, Alex, Mike, Jeff, Nicole, Will, Amanda, Tim, Liz and the medical school crowd, thanks for all of the dinners, football games, and hilarious stories. Also, thanks for always asking me to explain what I study one more time. Buffalo gals, especially Shelby, Monica, and Anna, thanks for staying in touch and being true friends. Our yearly get togethers are never enough. Shelby and Anna, I

would have never survived science classes (especially Pchem) without the two of you. Thanks to my friends since gradeschool Carolyn, Hilary, and Julie for staying in touch and being such great lifetime friends.

The completion of this thesis is an accomplishment that should be attributed to everyone in my life even those not mentioned by name. Thank you.



## Table of contents

Dedication.....	ii
Acknowledgements.....	iii
Lists of Figures.....	viii
List of Abbreviations.....	x
Abstract.....	xi
Chapter	
1. Introduction.....	1
2. Cell dynamics in fetal intestinal epithelium: implications for intestinal growth and morphogenesis.....	35
3. Specialized divisions extend the apical surface of the intestinal lumen and direct the formation of villus structures.....	77
4. The role of Wnt5a and PCP genes in intestinal lengthening and villus formation .....	97
5. Conclusions and Future Directions.....	141

## List of Figures

Figure 1.1. Examples of classical morphogenetic movements used in developmental processes.	21
Figure 1.2. Epithelial cell terminology.	22
Figure 1.3. Pseudostratified epithelia undergo interkinetic nuclear migration (INM).	23
Figure 1.4. Mature epithelial cells have a characteristic AB polarity.	24
Figure 1.5. Multiple examples of lumen formation.	25
Figure 1.6. Intestinal Development.	26
Figure 1.7. PCP phenotypes in <i>Drosophila</i> and Vertebrates.	27
Figure 2.1. Growth in girth and length of the fetal intestine; correlation with histological changes in the proximal duodenum.	61
Figure 2.2. Analysis of cell polarity in the E14.5 intestine.	62
Figure 2.3. The Intestinal epithelium is pseudostratified.	63
Figure 2.4. Intestinal nuclei undergo INM.	64
Figure 2.5. Investigating the mechanisms of epithelial thickening.	65
Figure 2.6. Loss of <i>Shroom3</i> alters epithelial organization.	66
Figure 2.7. Polarity changes in <i>Shroom3</i> null intestines.	67
Figure 2.8. <i>Shroom3</i> is required for organization of the apical actin network during epithelial remodeling.	68
Figure 2.S1. The distal ileum has the same cell shape and cell dynamics pattern as the proximal duodenum.	69

Figure 2.S2. Epithelial cells are pseudostratified.	70
Figure 2.S3. Cell cycle and apoptosis.	71
Figure 2.S4. Shroom3 is expressed in E14.5 intestinal epithelium.	72
Figure 3.1. Lumina are connected.	90
Figure 3.2. At E14.5, pHH3 positive nuclei localize to the tips of forming luminal cracks.	91
Figure 3.3. ZO-1 is the first apical marker during cell division.	92
Figure 3.4. Apical proteins localize to the cytokinetic furrow.	93
Figure 4.1. Growth in length of the fetal intestine.	125
Figure 4.2. Wnt5a expression in the intestine.	126
Figure 4.3. Analysis of villus development and organization.	127
Figure 4.4. Epithelial cell polarity at E16.5.	128
Figure 4.5. Epithelial INM and cell death at E14.5.	129
Figure 4.6. Apical expansion is defective in Wnt5a mutants.	130
Figure 4.7. PCP expression in the intestine.	131
Figure 4.8. Core PCP defects in gut elongation.	132
Figure 4.9. Vangl2;Wnt5a epithelial defects.	133
Figure 4.10. Fat4 PCP defects in gut elongation.	134
Figure 4.11. Epithelial accumulation in Fat4 mutant intestines.	135
Figure 5.1. New model of intestinal morphogenesis.	162
Figure 5.2. The Wnt5a/PCP signaling pathway.	163

## List of Abbreviations

Acetylated  $\alpha$ -tubulin (Ac- $\alpha$ -tub), apicobasal (AB), atypical PKC (aPKC), Blebbistatin (Blebb), Bromodeoxyuridine (BrdU), C57BL/6J (BL6), CaggCreERT2:mT/mG (Cagg;mTmG), Collagen IV (CollIV), convergent extension (CE), crossing division (c-division), Crumbs (Crb), Dachshous (Dchs1), Discs Large (Dlg), Dishevelled (Dvl), E-cadherin (Ecad), embryonic (E), epithelial mesenchymal transition (EMT), extending division (e-division), Four jointed (Fj), Frizzled (Fz), girth division (g-division), hematoxylin and eosin (H&E), interkinetic nuclear migration (INM), intraperitoneal (IP), knockout (KO), Lethal Giant Larvae (Lgl), Mitomycin C (MitoC), myristilated EGFP (mG), myristilated tomato (mT), Nocodazole (Nocod), phospho-Histone H3 (pHH3), PALS1-associated tight junction protein (PATJ), Partitioning deficient (PAR), planar cell polarity (PCP), Protein associated with Lin Seven (PALS1), scanning electron microscopy (SEM), three dimensional (3D), Shroom3<sup>Gt(ROSA)5.3Sor</sup>(Shroom3<sup>Gt</sup>), vacuolar apical compartment (VAC), van Gogh like 2 (Vangl2), wild type (WT), Zona occludens 1 (ZO-1),  $\beta$ -catenin ( $\beta$ -cat),  $\beta$ -galactosidase ( $\beta$ -gal),  $\gamma$ -tubulin ( $\gamma$ -tub)

## Abstract

During vertebrate intestinal development, coordinated morphogenetic movements between E12.5 and E16.5 transform the epithelial layer from a flat surface into evaginating villi and simultaneously generate an intestinal tube of considerable length. However, the genetic and cellular mechanisms driving growth and remodeling of the intestinal epithelium are poorly understood. The currently accepted model for epithelial remodeling proposes that: a) early epithelium is stratified and thickens by adding more cell layers; b) that lumen formation involves *de novo* apical surface generation at isolated secondary lumina; and c) that radial intercalation movements rearrange the epithelial surface into a single layer and generate intestinal length. Using advanced imaging tools and genetic mouse models, the work in this thesis disputes previous assumptions and presents a new model of intestinal morphogenesis. First, the E12.5-E14.5 epithelium is not stratified; rather, it is apicobasally polarized and pseudostratified. The tube grows in girth by progressive cellular elongation driven by actinomyosin and microtubule dependent processes. Second, lumen formation is actually an extension of apical surface from the primary lumen rather than by secondary lumen formation. The driver of luminal expansion is a specialized cell division that we call an extending division, or e-division, in which delivery of apical proteins to the cytokinetic furrow generates

new apical surface. This event effectively expands the apical surface while placing the two daughter cells onto separate villi. We show that Shroom3, an actin binding protein, is required for the formation of a properly organized epithelial surface. Third, length generation does not involve radial intercalation. Instead, we present evidence that planar cell polarity (PCP) is involved in this process. Studies of genetic mouse mutants in known PCP genes, including *Wnt5a*, *Vangl2*, and *Fat4*, lead us to propose that defects in interkinetic nuclear migration as well as oriented cell division give rise to their short gut phenotypes and malformed villi. Together, these data support a new model of epithelial remodeling that has major implications for the mechanistic understanding of intestinal morphogenesis and length generation.

## **Chapter 1**

### **Introduction**

This thesis is focused on a series of morphogenetic processes that occur in mouse mid-fetal life to remodel the intestinal epithelium. The process of remodeling is important because it converts the flat epithelial surface into millions of finger-like villus projections, the functional units of absorption in the adult. Remodeling the epithelium must coordinate mechanisms of lumen expansion, apicobasal polarity, morphogenetic movements, and cell cycle dynamics. In the Introduction, I will first present what is known about these morphogenetic mechanisms as described in other well studied tissues to provide a framework for analyzing intestinal remodeling. Second, I will describe intestinal development in detail, including data that support the existing model of epithelial morphogenesis. Finally, I will introduce my thesis investigations in support of a new theory of intestinal epithelial morphogenesis.

#### **Mechanisms of morphogenesis**

Morphogenesis, the reorganization and coordination of cellular movements to form and shape tissues and organs, is essential to animal development. The cellular dynamics driving morphogenetic mechanisms - including apical constriction, cell

migration, cell division, epithelial mesenchymal transition (EMT), and intercalation- are conserved and control a multitude of developmental processes [reviewed in (Andrew and Ewald, 2009; Keller, 2002; Sawyer et al., 2009)]. In fact, failure of morphogenetic movements early in development contributes to defects in the organization of the body plan, often resulting in a nonviable embryo. Later, developmental morphogenetic defects can lead to congenital birth defects such as spina bifida, cleft palate, cleft lip, gastroschisis, hypospadias, and heart disease (Johnston and Bronsky, 1995; Jones et al., 2009; Kojima et al.; Liu et al., 2003; Mitchell, 2005; Ramsdell, 2005). The same genetic pathways that control morphogenesis during development often cause cancer when mutated in adults (Arsic et al., 2007; Hansson et al., 2004; Logan and Nusse, 2004). The role of cellular dynamics during morphogenesis has been well studied during early embryogenesis when the body axis is organized during gastrulation, but very little is known about the cellular mechanisms driving morphogenesis later during organ development.

### **Classical morphogenesis: Gastrulation and axis elongation**

Aristotle, the first known embryologist, published two opposing theories of embryogenesis in the fourth century B.C.E: pre-formation and epigenesis. The pre-formation theory postulated that embryos were created in the mother as small individuals and only grew larger during development. The theory of epigenesis stated that embryos started as a small mass of tissue and new parts were added throughout development. Aristotle's theories were debated in both the philosophical and scientific communities until the 19<sup>th</sup> century when the invention



of the microscope, the discovery of the cell, the improvement of staining techniques, and the creation of experimental embryology brought about the modern study and understanding of embryology and developmental biology (Gilbert, 2000).

Developmental biologists including Stricker, Haeckel, Spemann, and many others observed and reported the first descriptions of gastrulating embryos in the 1800's and early 1900's. Gastrulation is required to organize the body axis into three different germ layers: ectoderm, mesoderm, and endoderm. In general, ectoderm forms tissues of the skin and nervous system; mesoderm forms muscles, blood, connective tissue, and bones; and endoderm forms the gastrointestinal tract and associated organs (e.g., liver, pancreas, gall bladder, etc.). Initially, the pre-gastrula embryo is made up of two groups of cells: ectoderm and mesendoderm. During mouse gastrulation, cells of the mesendoderm are internalized and the endoderm and the mesoderm soon separate into two individual populations. In general, multiple morphogenetic movements are responsible for the specific arrangement and organization of the germ layers. Without the morphogenetic movements that drive gastrulation, the embryo does not survive. For example, two highly studied morphogenetic movements responsible for driving gastrulation and elongating the body axis are apical constriction and convergent extension (CE).

Apical constriction is a common cellular process that was first recognized in 1902 for its role in the bending of epithelial sheets (Fig. 1.1A). The role of constriction was confirmed using a physical model with brass bars and rubber bands where

increased rubberband tension resulted in a curve or invagination (Lewis, 1947). Throughout the 20<sup>th</sup> century, Vogt, Holfreter, Keller, and many others observed and described apical constriction as a morphogenetic mechanism required during gastrulation (Beetschen, 2001; Haeckel, 1879). Apical constriction is critical for gastrulation in sea urchin sheet invagination, *C. elegans* cell internalization, *Drosophila* ventral furrow invagination, *Xenopus* bottle cell formation, and chick and mouse primitive streak cell ingression [reviewed in (Nowotschin and Hadjantonakis; Sawyer et al., 2009)]. Inhibiting apical constriction results in failure to gastrulate, proving that this constriction is the driving force for cellular internalization.

A second well-studied morphogenetic movement, often used to elongate the anterior posterior body axis, is that of CE (Fig1.1B). During CE, cells from multiple layers intercalate with one another, resulting in a lengthened single layer. In such movements, the direction of intercalation is perpendicular to the direction of tissue lengthening. Thus, CE transforms a short, fat tissue into a long, thin structure. CE movements are used to elongate the body axis in chordates including sea squirts (ascidians), teleost (bony) fish, amphibians, birds, and mammals (Keller, 2002). Within the constraints of a tube, CE movements are termed radial intercalation because multiple concentric layers of cells intercalate in a radial direction to create a single outer layer (Fig 1.1C). For example, radial intercalation was observed in the *Xenopus* archenteron by labeling and tracking cell fates with fluorescein dextran amine. The archenteron started as a short, wide multilayered tube with a small lumen and after radial intercalation, became a lengthened single-layered intestinal

tube with a larger lumen (Chalmers and Slack, 2000). It has been suggested that the mouse intestine also elongates by a radial intercalation process (Cervantes et al., 2008; Yamada et al., 2010), an hypothesis that will be addressed in the context of this thesis.

### **Epithelial cell shape and organization**

Epithelial cells are the building blocks that form flat epithelial sheets such as the skin and the lining of tubular organs such as the gastrointestinal tract. Epithelia are categorized based on the shapes of the individual cells and the organization of those cells within the epithelial layer (Fig. 1.2). When cells exhibit a height to width ratio close to 1.0, they are designated **cuboidal**; when height is greater than width, the cells are referred to as **columnar**; cells with greater width than height are termed **squamous** (Fig. 1.2A). An epithelium composed of a single layer of cells is termed a **simple** (Fig. 1.2B), while a multi-layered epithelium is called **stratified** (Fig. 1.2C). If multiple organizations exist within the same area, the epithelium is **transitional** (Fig. 1.2D). Finally, in a **pseudostratified** (Fig. 1.2E) epithelium, all cells make contact with both the apical and basal surfaces. However, in contrast to a single-layered columnar epithelium, in which all nuclei are aligned, nuclei of the pseudostratified epithelium are staggered, giving the epithelium a layered or stratified appearance.

**A specialized characteristic of pseudostratified epithelia: interkinetic nuclear migration (INM)**

The staggered nuclear appearance of pseudostratified epithelia is a direct result of INM, a process by which nuclei move within the epithelium in concert with the cell cycle (Sauer, 1936). That is, nuclei complete S-phase at the basal epithelial surface, migrate apically during G2, undergo mitosis at the apical surface, and migrate basally during G1 (Fig. 1.3). In the neuroepithelium, the forces that direct basal to apical (adluminal) INM have been well studied; actinomyosin signaling and microtubules have both been implicated as controllers of these movements. Nuclei are moved as a large cargo along microtubules in the direction of the apical centrosome (minus-end-directed), and genetic studies have shown that proteins required to organize microtubules at the centrosome, Cep120, Hook3 and TACCs, are required for this adluminal migration (Ge et al., 2010; Xie et al., 2007). Additionally, adluminal movement is disrupted by interference with the microtubule network, by loss of minus-end-directed microtubular motor proteins, such as dynein, or by loss of proteins such as Lis1 that regulate dynein (Baye and Link, 2008; Del Bene et al., 2008; Feng and Davis, 2000; Gambello et al., 2003; Tsai et al., 2005; Wynshaw-Boris and Gambello, 2001). Despite the strong evidence for the role of microtubules in INM, two studies, one in brain and the other in retinal neuroepithelium, implicate the actinomyosin system in adluminal movement (Norden et al., 2009; Schenk et al., 2009).

The control of apical to basal (abluminal) INM is less well understood. A study in brain neuroepithelium suggests that microtubules are also required for these movements, based on the complete lack of mobility in shRNA-Lis1 treated tissue

(Tsai et al., 2005). However, in the retinal epithelium, actinomyosin was found to control abluminal INM since microtubule inhibited tissue still maintained nuclear migration but actinomyosin inhibition resulted in a lack of INM (Norden et al., 2009).

### **Epithelial polarization**

Intestinal epithelial cells maintain a characteristic apicobasal (AB) polarity that is defined by specific structures and proteins (Fig. 1.4A). Microvilli localize to the apical surface (after E14.5) and the basement membrane is defined at the basal surface. Apical and basolateral surfaces are separated by tight junctions and adherens junctions [reviewed in (Martin-Belmonte and Mostov, 2008; Wang and Margolis, 2007)]. Tight junctions can be identified by the localization of the Zona occludens (ZO-1) protein and function to create a tight seal around the apical epithelial surface. At the lateral surfaces, the epithelial cells are connected to neighboring cells by adherens junctions. The basement membrane is connected to the gut mesenchyme (extracellular matrix) through integrin: cadherin interactions. Intracellular organelles also contain a specific polarization in epithelial cells. The nucleus in a mature polarized epithelium usually drops to the basal surface, while the Golgi is positioned apical to the nucleus. The structure of the epithelial layer and maintenance of the tube is dependent on proper localization of AB polarity complexes [reviewed in (Bryant and Mostov, 2008; Iden and Collard, 2008)]. The Golgi function to sort protein containing vesicles to the apical surface in columnar epithelia or to the lateral surface in pseudostratified epithelia, using polarized microtubules, thus

establishing and maintaining polarity (Ku et al., 1999; Rodriguez-Boulan and Nelson, 1989).

Three conserved AB polarity complexes are responsible for epithelial polarization; incorporation and mutual exclusion of protein complexes into specific membrane domains defines AB polarity of the epithelial cell. The Crumbs (Crb) and Partitioning deficient (PAR) complexes localize apically while the Scribble complex localizes basolaterally in epithelial cells [reviewed in (Martin-Belmonte and Mostov, 2008; Nelson, 2009; Wang and Margolis, 2007)]. The Crb complex was first identified in *Drosophila* and is composed of Crb3, Protein associated with Lin Seven 1 (PALS1), and PALS1 associated tight junction protein (PATJ). The PAR complex components, discovered in *C. elegans*, are PAR3, PAR6, and atypical protein kinase C (aPKC; Fig. 1.4B). The Scribble complex was discovered in *Drosophila* and consists of Scribble, Discs Large (Dlg), and Lethal Giant Larvae (Lgl). Delivery of AB polarity proteins occurs through polarized vesicular trafficking (Jaulin et al., 2007). Loss of function mutations in Scribble or Crb complexes in *Drosophila* results in AB polarity defects (Bilder et al., 2003; Tanentzapf and Tepass, 2003) while deletion of the PAR complex results in improper junction formation (Georgiou et al., 2008).

### **Tube and lumen formation**

Tubes are defined as AB polarized epithelia that surround a central lumen. There are numerous mechanisms by which tubes can establish and expand the lumen

[reviewed in (Andrew and Ewald, 2009)]; several of the most pertinent will be discussed here.

*Polarized precursors wrap into a tube during primary neural tube formation.* In the case of the primary neural tube, the epithelial sheet is AB polarized prior to tube formation and pseudostratified after tube formation (Fig. 1.5A). AB elongation and apical constriction of medial cells causes the epithelium to bend to form a simple tube (Andrew and Ewald, 2009; Lubarsky and Krasnow, 2003; Pilot and Lecuit, 2005; Sawyer et al., 2009). Both AB elongation and apical constriction of the neuroepithelium to create the neural tube depends on Shroom3, a PDZ binding domain-containing protein that localizes to the apical adherens junction (Haigo et al., 2003; Hildebrand, 2005; Lee et al., 2009; Lee et al., 2007; Nishimura and Takeichi, 2008; Taylor et al., 2008). The neuroepithelial cells change shape through Shroom3-mediated control of  $\gamma$ -tubulin and F-actin at the apical surface (Colas and Schoenwolf, 2001; Haigo et al., 2003; Hildebrand, 2005; Hildebrand and Soriano, 1999; Lee et al., 2009; Lee et al., 2007). Shroom3 also functions to apically constrict epithelial cells of other tissues such as the lens and *Xenopus* gut epithelium (Chung et al., 2010; Plageman et al., 2010).

*Secondary lumen formation and coalescence.* Another relevant mode of tube formation is observed in the zebrafish intestine (Fig. 1.5B). In the zebrafish gut, the tube is formed from a solid rod of unpolarized precursors that undergo lumen formation by cord hollowing, a mechanism where small apical surfaces form *de*

*nov*o, enlarge, and fuse to form a single central lumen (Ng et al., 2005). The expansion process requires the formation of tight junctions followed by fluid transport between the tight junctions; some of the genes required for these processes have been identified (Bagnat et al., 2007). Mouse intestinal lumen formation is also believed to involve secondary lumen (Mathan et al., 1976). Histological studies suggest that small luminal pockets called secondary lumina, defined by newly formed apical surfaces, form in the deep layers of the stratified epithelium (Mathan et al., 1976). Expansion and coalescence of the secondary lumina then create a unified luminal space.

*Lumen formation by temporary stratification and cellular rearrangement.* The formation of tubular branching in both pancreatic acini and ducts of the mammary glands are also relevant to our studies. In these tissues, the tubes adopt a temporarily stratified organization (Ewald et al., 2008; Villasenor et al., 2011). Within the stratified layer, the bottom layer is basally polarized and the layer closest to the lumen is apically polarized, while cells in between are unpolarized. Reorganization of this stratified layer occurs by cellular rearrangement, migration, and re-polarization. In the pancreas, a microlumen forms *de novo* at the center of a rosette between multiple apically constricted cells; these lumina are then connect to form a ramified ductal system (Fig. 1.5C) (Villasenor et al., 2011).

*Co-opting cytokinesis to create an apical surface.* During a specific developmental window, a specialized type of cell division is required to create a lumen in the



developing zebrafish neural keel (Tawk et al., 2007). This mitotic event, called a crossing- (or c-) division, occurs at the extending luminal surface (Fig. 1.5D). A nucleus on one side of the keel moves toward the center of the forming keel and undergoes mitosis. One daughter of the mitotic event crosses over to the other side of the keel during cytokinesis. In doing so, the two daughters deposit the apical surface protein, Pard3, at the cytokinetic furrow between the two cells. This creates an apical or luminal space between the two sister cells and sets up the mirror symmetry of the neural tube (Ciruna et al., 2006; Tawk et al., 2007). The co-option of cytokinesis to form a luminal surface is also seen *in vitro* in both MDCK cysts and epithelial Caco2 organoid cultures. Biochemical studies have demonstrated that maintenance of the luminal surface is driven by vesicular delivery of apical membranes (Fig. 1.5E) (Ferrari et al., 2008; Jaffe et al., 2008; Martin-Belmonte et al., 2007; Schluter et al., 2009). During the first cell division, abscission occurs symmetrically, with the midbody localized to the central point between the two daughter cells (Jaffe et al., 2008). Subsequent cell divisions maintain the central lumen by asymmetrically localizing midbodies to the luminal side of the cell (Jaffe et al., 2008). Inhibiting apically localized proteins (PTEN, Cdc42, Pard3, Crb3) in MDCK cysts, Caco-2 organoids, and the neural keel results in ectopic lumina or lack of lumen formation (Jaffe et al., 2008; Martin-Belmonte et al., 2007; Tawk et al., 2007).

These examples, demonstrating the similarities and differences that characterize previously studied epithelial morphogenetic mechanisms in epithelial tubes, will aid

our study of the processes driving morphogenic change in the intestine. The aim of the work described in this thesis is to discover the genetic and cellular mechanisms required to remodel the epithelial layer in the mouse embryonic intestinal tube in midfetal life. Below, we review the formation of the intestine and the existing data about its remodeling.

### **Intestinal Organogenesis**

After gastrulation, a series of poorly understood morphogenetic movements transform a flat sheet of endoderm into a primitive gut tube (Franklin et al., 2008; Kimura et al., 2006; Lawson and Schoenwolf, 2003; Rosenquist, 1971; Tam et al., 2007; Tremblay and Zaret, 2005). By embryonic day (E) 9.5, the tubular gut is comprised of a single layer of polarized endodermal epithelium, wrapped by mesoderm; epithelial/mesenchymal crosstalk is important throughout intestinal development and patterning [reviewed in (Kedinger et al., 1998)]. At this time, patterning on the anterior/posterior axis has already established broad domains for foregut, midgut, and hindgut (Spence et al., 2011; Wells and Melton, 1999; Zorn and Wells, 2009). At E10, organ buds grow out from the endodermal epithelium and develop into thyroid, liver, pancreas, lungs and other gut-associated organs [reviewed in (Spence et al., 2011; Wells and Melton, 1999; Zorn and Wells, 2009)]. This thesis will specifically focus on the morphogenesis of the small intestinal epithelium.

For maximum absorptive capacity, the adult intestine is lined with fingerlike projections called villi and invaginations called crypts. Villi are formed during the epithelial remodeling of the embryonic intestine, while crypts are formed after birth (Fig. 1.6). The villi contain differentiated cells including absorptive enterocytes and secretory goblet and enteroendocrine cells, while the crypt houses the Paneth cells as well as the stem and progenitor cells. The adult intestine is constantly regenerative and has the unique ability to turn over its epithelial layer every 4-5 days. To do this, the crypt progenitors divide to create new epithelial cells that differentiate and travel up the villus. Once at the top of the villus, epithelial cells are sloughed off by apoptosis and released into the lumen. Adult intestinal regenerative ability, epithelial barrier function, absorptive function, as well as immune response in the mature intestine are areas of intense study. Much less is known, however, about how the villus structure of the intestine is generated during fetal life. Understanding how the villi are formed and organized could offer insight into treatments for the many diseases associated with malabsorption such as celiac disease and short bowel syndrome.

### **Intestinal epithelial morphogenesis**

Intestinal epithelial morphogenesis has been studied histologically in several species, including mouse, rat, pig, sheep and human (Dekaney et al., 1997; Madara et al., 1981; Mathan et al., 1976; Matsumoto et al., 2002; Toyota et al., 1989; Trahair and Robinson, 1986; Trier and Moxey, 1979). In the mouse, the intestinal tube at E9.5 is a single-layered, AB polarized epithelium surrounding a central lumen.

Between E9.5 and E14.5 (the time prior to epithelial remodeling and formation of villi), the epithelial layer of the tube thickens progressively. Mathan *et al.* describe the process of intestinal epithelial thickening in the fetal rat as a stratification event, in which the undifferentiated epithelial cells increase to as many as 8 cell layers thick (Mathan et al., 1976). Just prior to remodeling, a change occurs within the deepest cell layers of the epithelium. Here, membrane bound cytoplasmic vesicles associate with unusually long tight junctional complexes that form on neighboring plasma membranes. In the center of the long lateral junctions, small isolated lumina, also known as secondary lumina, form *de novo* (Madara et al., 1981; Mathan et al., 1976). Cytoplasmic vacuoles continuously fuse to enlarge the secondary lumina until they join with the central primary lumen. By E16.5, the lumina are connected and the epithelium resolves to a single columnar layer lining the villi. These light and electron microscopy studies established the theory that intestinal epithelial remodeling occurs by a temporary stratification event followed by *de novo* secondary lumen formation and coalescence.

Two more recent genetic studies of mouse intestinal morphogenesis further support the stratified epithelial paradigm. The first study identifies *Ezrin*, which encodes an apically localized scaffolding protein, as a gene required for proper lumen formation (Saotome et al., 2004). In *Ezrin* deficient mice, villi are connected and lumina exist as islands throughout the epithelium. The authors conclude that secondary lumina form, but improper polarization in the absence of *Ezrin* results in failed coalesce with the primary lumen.

A second study examines the role of *Wnt5a*, a non-canonical Wnt ligand, in intestinal lengthening (Cervantes et al., 2008). The *Wnt5a* null mouse intestine is shorter than that of its wild type (WT) littermates, with greater epithelial thickness at E11.5. To investigate this thickening and short gut phenotype, the authors tracked nuclei after Bromodeoxyuridine (BrdU) labeling. BrdU positive cells were observed throughout the epithelial layer, interspersed with non-labeled cells in WT tissue. In contrast, excess BrdU positive nuclei collected at the luminal surface in *Wnt5a* null intestines (Cervantes et al., 2008) leading the authors to conclude that cells of the stratified intestinal epithelium temporarily delaminate to divide, but that their radial re-intercalation is compromised in the *Wnt5a* mutants. The authors propose that radial intercalation drives gut elongation between E11.5 and E12.5 and that compromising these movements is responsible for the short gut phenotype; they observe no additional epithelial defects after this time (Cervantes et al., 2008).

Most intestinal studies agree with the temporary stratification model of gut morphogenesis, but a few investigations call this theory into question. In human embryos, the duodenal epithelium is described as pseudostratified (Matsumoto et al., 2002), but the morphological data still support the notion that coalescence of secondary lumina is involved in creating the final luminal space. In contrast, two studies, one in the pig and the other in sheep, report no observation of secondary lumen formation (Dekaney et al., 1997; Trahair and Robinson, 1986).

At the start of my work, the current understanding of intestinal morphogenesis was, at best, conflicting and incomplete. Both the organization of the intestinal epithelium and the process of lumen formation during epithelial remodeling were unclear. The current dogma of intestinal development was put forth based on light and electron microscopic analysis of histologic sections. In this two dimensional view, a pseudostratified epithelium with stacked nuclei could be easily mistaken for the similar looking multi-layered stratified layer. Therefore, we set out to re-evaluate embryonic intestinal cell shape and morphogenesis using more modern experimental techniques. Our study addressed several specific questions:

- 1) Is the epithelium AB polarized throughout remodeling?
- 2) What is the shape and organization of the epithelial layer between E12.5 and E16.5?
- 3) Is there a specific pattern or compartmentalization of proliferative cells in the unremodeled epithelium?
- 4) Is cell shape change required for the organization and remodeling of the epithelium?
- 5) Are secondary lumina involved in epithelial remodeling? If not, what is the mechanism for luminal expansion during epithelial remodeling?

Studies designed to answer questions #1-4 above are addressed in Chapter 2 of this thesis. Question #5 is considered in Chapter 3. As outlined in those Chapters, the results of these analyses were surprising and indicated that many of the previous

assumptions about cell shape and intestinal remodeling are incorrect.

### **Role of planar cell polarity (PCP) signaling in intestinal remodeling and lengthening**

The PCP pathway controls tissue polarity and coordinates the behavior of multiple cells in the plane of the epithelium. PCP pathway molecules and interactions were discovered in *Drosophila* to control the direction of individual actin-rich hair extensions on epidermal cells of the fly wing (Fig. 1.7A) and organization of photoreceptors in ommatidia of the compound eye (Fig. 1.7B)(Gubb and Garcia-Bellido, 1982; Vinson and Adler, 1987). Flies with mutations in the core PCP genes exhibit disrupted planar organization in both the wing and the eye, but AB polarity and cell identity remain unaffected. The core PCP genes are identified as *Frizzled* (Visel et al.), a seven-pass transmembrane receptor; *Dishevelled* (Dsh; mammalian orthologue is Dvl), a cytoplasmic signaling protein; *Strabismus* or *van Gogh* (Vang), membrane proteins; *Flamingo*, a membrane protein with cadherin like domains; and *Prickle*, a cytoplasmic protein. In *Drosophila*, the asymmetric localization of these proteins imparts cytoskeletal changes that are propagated across the epithelium, thus organizing the tissue. The originating polarity signal or ligand in *Drosophila* is unknown. A multitude of tissue-specific effectors continue the signaling pathway downstream of the core PCP proteins and eventually modify the localization and organization of the cytoskeletal network to coordinate planar polarity and morphogenetic movements.

In vertebrates, the analysis of *Xenopus*, zebrafish, and mouse reveal that orthologues of *Drosophila* core PCP genes are responsible for actin rich bundle organization of stereocilia in the the mammalian inner ear similar to *Drosophila* (Fig. 1.7C).

Additionally, PCP genes are required in morphogenetic movements of CE and neural tube closure, a role unique to vertebrates (Fig. 1.7D). Altered Wnt/Fz signaling results in modified cytoskeletal organization in *Xenopus* CE (Collier and Gubb, 1997; Habas et al., 2001; Park et al., 2006; Wallingford et al., 2000), chick neural tube apical constriction (Kinoshita et al., 2008), and zebrafish ciliogenesis (Oishi et al., 2006).

Data suggest that the polarity initiating ligands in vertebrates are part of the non-canonical Wnt family. Both *Wnt11/silberblick* and *Wnt5/pipetail* in zebrafish are required for CE (Heisenberg et al., 2000; Kilian et al., 2003). In mice, genetic knockouts of *Wnt5a* are associated with disorganized stereocilia in the cochlea and defects in outgrowth of many organs, including short intestines (Cervantes et al., 2008; Qian et al., 2007; Yamaguchi et al., 1999). Genetic crosses of *Wnt5a* and *Looptail* (*Vangl2* mutant mice) result in an enhanced stereocilia phenotype suggesting that *Wnt5a* is acting in the core PCP pathway in mice (Qian et al., 2007).

A more recent addition to the PCP pathway is *Fat4*, a protein that signals either upstream of the core PCP genes or in parallel to that pathway (Saburi et al., 2008). Large cadherins *Fat* and *Dachsous* (Ds; mammalian orthologue is *Dchs1*) along with the Golgi-associated kinase, four jointed (*Fj*; mammalian orthologue is *Fjx1*) make



up the *Fat/Ds* cassette. It is important to note that the *Fat/Ds* cassette also signals in a PCP independent manner through the Hippo pathway to control tissue growth.

The Hippo pathway [reviewed in (Sopko and McNeill, 2009)] is beyond the scope of this thesis. Only PCP dependent functions of the Fat pathway will be discussed.

The *Fat* PCP phenotypes were identified in *Drosophila* tissues to alter oriented cell division and organ development (Baena-Lopez et al., 2005; Casal et al., 2002; Matakatsu and Blair, 2004; Rawls et al., 2002; Simon, 2004; Yang et al., 2002; Zeidler et al., 1999). Similarly, recent studies have identified the role of mammalian orthologue *Fat4* in mammalian kidney development to orient cell division responsible for elongating the kidney tubules (Saburi et al., 2008). *Fat4* interacts with both *Vangl2* and *Fjx1*, resulting in more severe cystic phenotypes. *Fat4*<sup>-/-</sup> and *Fat4*<sup>-/-</sup>;*Vangl2*<sup>Lp/+</sup> animals display defective stereocilia in the inner ear, validating the model as a PCP phenotype. Additionally, large cystic structures are observed in the kidney, characteristic of polycystic kidney disease (Saburi et al., 2008).

Furthermore, *Fat4* and *Dchs1* have been identified as broadly required for proper mammalian development in multiple organs including skeleton, kidney, lung, heart, and intestine (Mao et al., 2011). In the gastrointestinal tract specifically, both *Fat4* and *Dchs1* mutant mice demonstrate short gut phenotypes but no morphogenetic or cellular mechanisms were identified (Mao et al., 2011).

Because *Wnt5a* and *Fat4* mutant intestines have been demonstrated to be short (Cervantes et al., 2008; Mao et al., 2011), these pathways may be important in

mouse intestinal development. We asked the following questions to probe the genetic mechanisms driving intestinal epithelial morphogenesis and remodeling:

- 1) Is *Wnt5a* required for mouse embryonic epithelial morphogenesis including AB polarity, planar polarity, and epithelial remodeling?
- 2) Does *Wnt5a* interact genetically with *Fat4* or *Vangl2*?

Studies designed to evaluate the above questions are examined in Chapter 4 of this thesis. The results establish that *Wnt5a* is required for proper epithelial morphogenesis and may interact with the PCP pathways in gut lengthening and villus development.

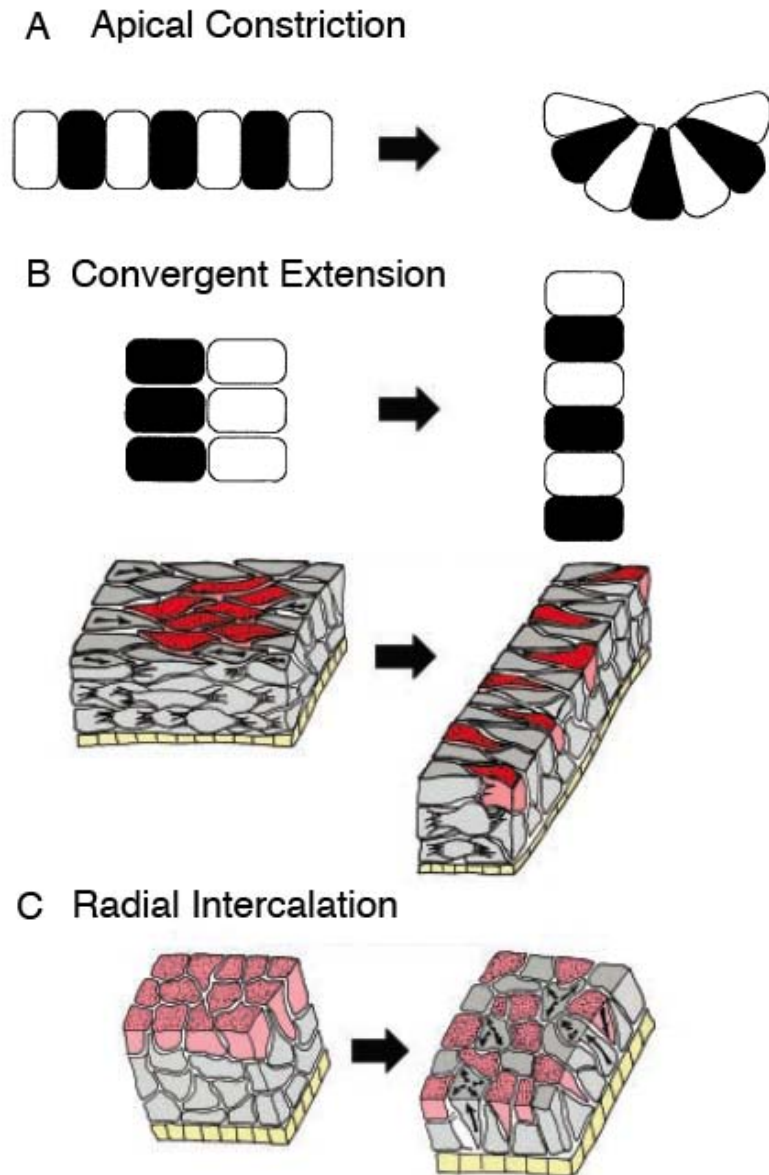


**Figure 1.1. Examples of classical morphogenetic movements used in developmental processes.** A) Apical constriction controls bending of an epithelial sheet. B) CE occurs when multiple cell layers intercalate to transform a short, fat tissue into a long, thin structure. C) Radial Intercalation is the CE movement within a tube. Concentric layers of cells intercalate along the radial axis. [Reproduced with permission from (Keller, 2002; Wallingford et al., 2002)]

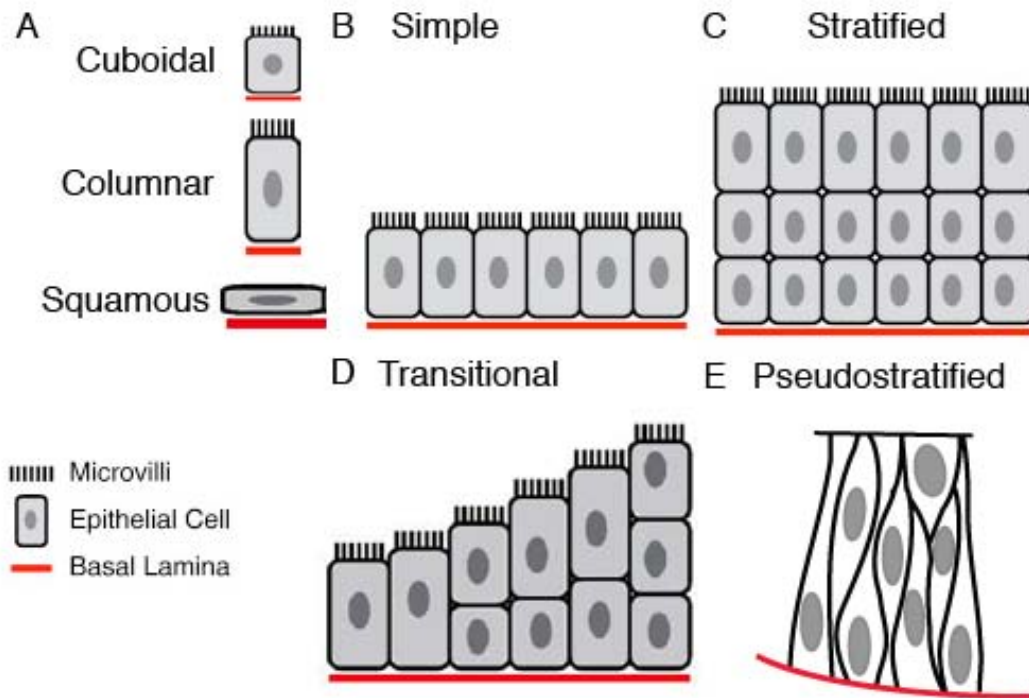


**Figure 1.2. Epithelial cell terminology.** A) Epithelial cell shape is based on height to width ratios. Cuboidal cells exhibit equal height to width. Columnar cells have greater height than width. Squamous cells have a shorter height and longer width. Epithelial cell terminology is also based on the structure within a sheet. B) A simple epithelium is single-layered. C) A stratified epithelium is multi-layered. D) A transitional epithelium is made up of several organizations in close proximity. E) A pseudostratified epithelium is a densely packed, single layer of cells with staggered nuclei. [Panels A-D reproduced with permission from (Andrew and Ewald, 2009)]

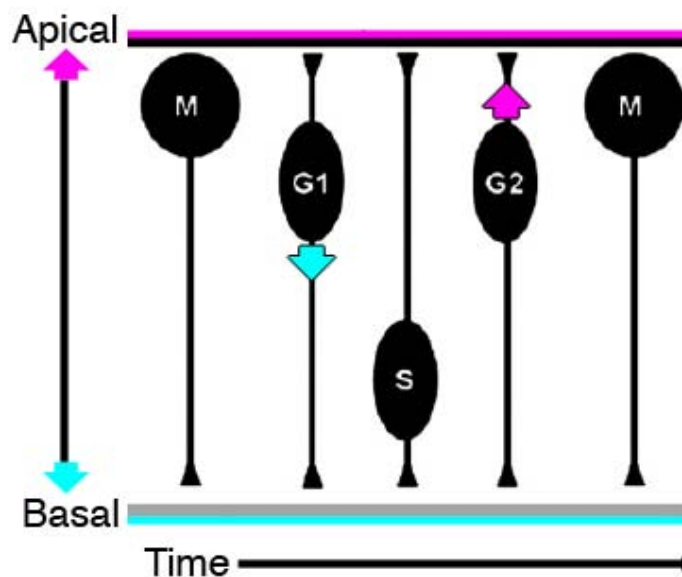


**Figure 1.3. Pseudostratified epithelia undergo interkinetic nuclear migration (INM).** Nuclei migrate between the basal and apical surfaces in coordination with the cell cycle. This schematic demonstrates the nuclear localization of a single nucleus in time. Mitosis occurs at the apical surface, nuclei of daughter cells in G1 migrate basally, S-phase occurs at the basal side, G2 nuclei migrate apically, and once at the apical surface, cells again enter mitosis and divide. [Reproduced with permission from (Baye and Link, 2008)]

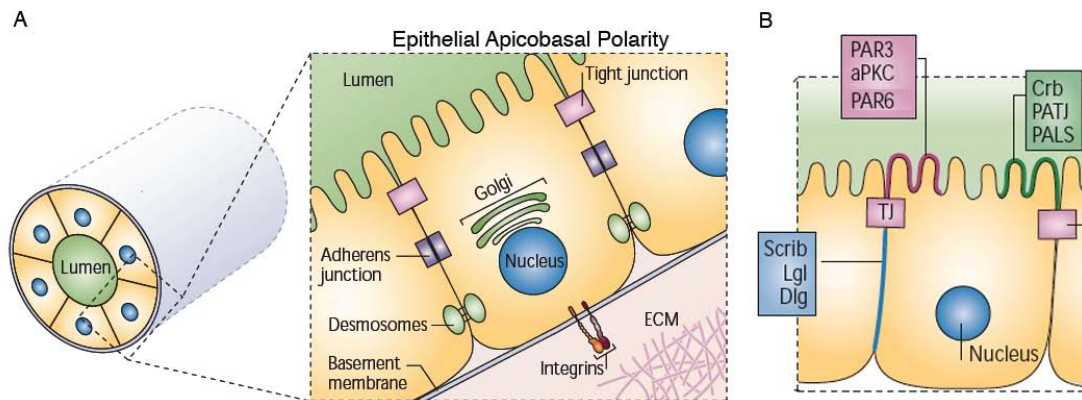


**Figure 1.4. Mature epithelial cells have a characteristic AB polarity.** A) AB polarity of the mature epithelium of a tube consists of an apical surface adjacent to the lumen (shown in this schematic with microvilli), tight junctions at the junction between the apical and lateral surfaces, adherens junctions connect the lateral surfaces of neighboring cells, a basement membrane at the basal side, a basal nucleus, and a Golgi apparatus apical to the nucleus. B) AB polarity is set up by expression of one complex of polarity proteins and exclusion of the others. The PAR complex (PAR3, aPKC, PAR6) and the Crumbs complex (Crb, PATJ, PALS) are recruited to the apical surface, while the Scribble complex (Scribble, Dlg, Lgl) localizes to the basolateral surface. [Reproduced/adapted with permission from (Bryant and Mostov, 2008; Iden and Collard, 2008)]

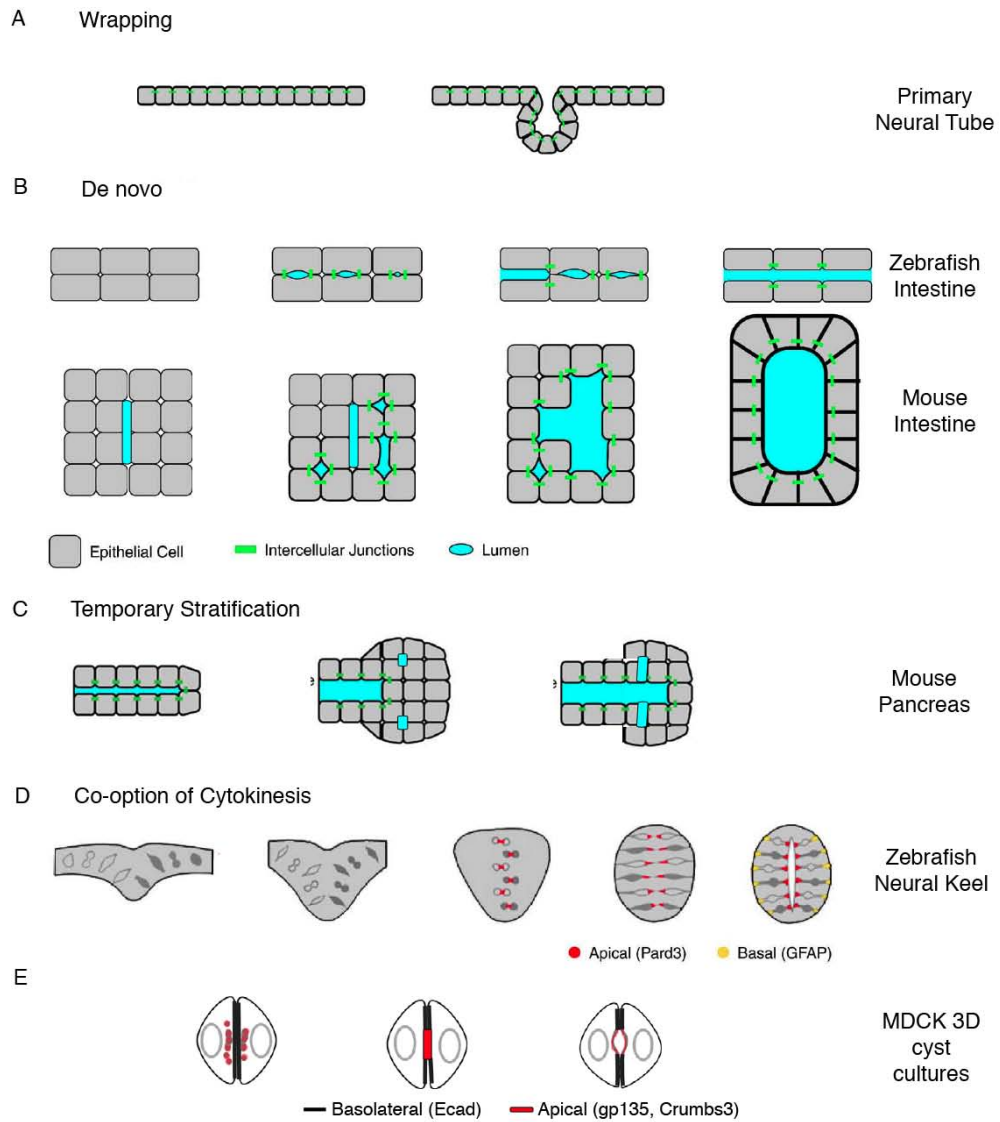


**Figure 1.5. Multiple examples of lumen formation.** A) Wrapping: polarized precursors during primary neural tube formation apically contract at hinge points to wrap into a tube. B) *De novo* lumen formation: unpolarized precursors create apical surface *de novo*. These isolated apical surfaces, termed secondary lumina coalesce to form a single lumen. The existing data for zebrafish and mouse intestine support this method. C) Temporary stratification: the mouse pancreatic ducts start out as simple polarized tubes. Pancreatic buds temporarily stratify and a combination of secondary lumen formation, apical constriction, and cellular rearrangements result in ductal branching. D-E) Co-option of cytokinesis: The zebrafish neural keel and cultured MDCK cysts deliver apical proteins to the cytokinetic furrow to create a lumen between the daughter cells. The zebrafish neural keel model is unique in that the two daughter cells are separated, one on either side of the newly formed lumen, establishing the mirror symmetry of the neural tube. [Reproduced/adapted with permission from (Andrew and Ewald, 2009; Ferrari et al., 2008)]

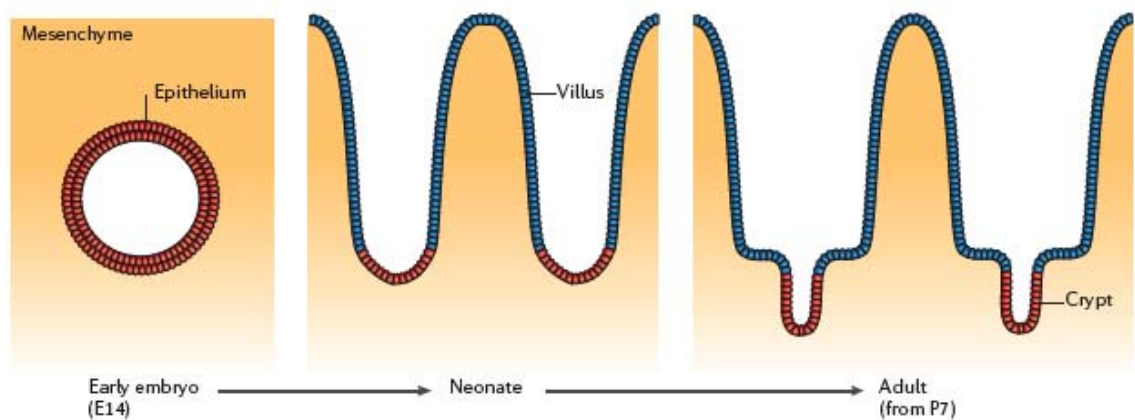


**Figure 1.6. Intestinal Development.** A) The embryonic intestine starts as a simple tube with a smooth apical surface; the epithelium is highly proliferative at this stage (red). Most studies suggest that this early epithelium is stratified. Through a series of remodeling events, villi form and evaginate into the lumen, while the epithelium remodels to a simple columnar form. After villus emergence, the stem cell zone is localized to the intervillus or pre-crypt region (red) and the differentiated cells (blue) are found on the villus proper. At P7, the stem cell zone invaginates to form crypts (red); this organization of the intestine is maintained from P7 through adult life. [Reproduced with permission from (Crosnier et al., 2006)]



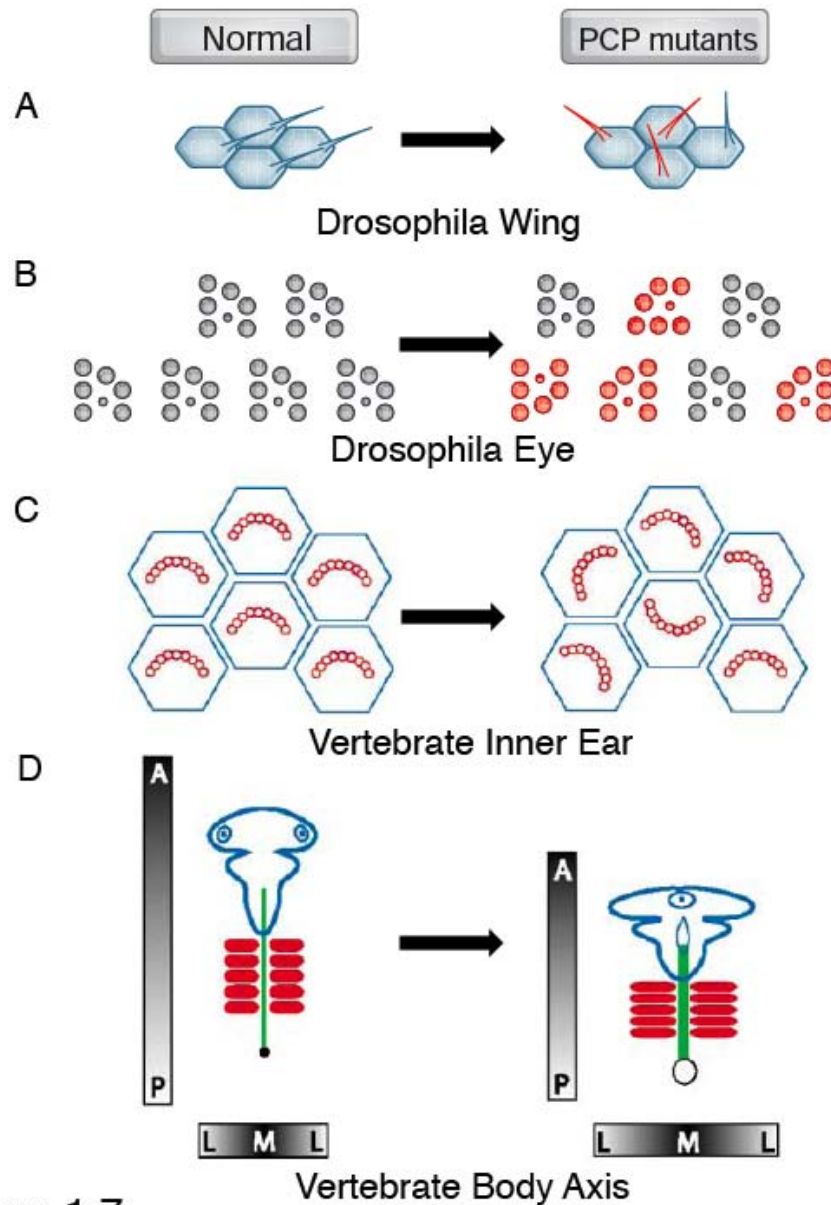


**Figure 1.7. PCP phenotypes in *Drosophila* and Vertebrates.** PCP proteins were identified in *Drosophila* to control the organization of the actin-rich hairs on the *Drosophila* wing (A) as well as the organization of groups of cells in the *Drosophila* complex eye (B). In vertebrates, PCP orthologues regulate the organization of the actin-rich stereocilia (C). However, the additional role of PCP in vertebrate CE movements during body axis elongation (D) suggests differences from the *Drosophila* pathway. A: anterior, P: posterior, L: lateral, M: medial [Reproduced with permission from (McNeill, 2009; Veeman et al., 2003)]

## **Literature Cited**

- Andrew, D. J. and Ewald, A. J.** (2009). Morphogenesis of epithelial tubes: Insights into tube formation, elongation, and elaboration. *Dev Biol*.
- Arsic, D., Beasley, S. W. and Sullivan, M. J.** (2007). Switched-on Sonic hedgehog: a gene whose activity extends beyond fetal development--to oncogenesis. *J Paediatr Child Health* **43**, 421-3.
- Baena-Lopez, L. A., Baonza, A. and Garcia-Bellido, A.** (2005). The orientation of cell divisions determines the shape of Drosophila organs. *Curr Biol* **15**, 1640-4.
- Bagnat, M., Cheung, I. D., Mostov, K. E. and Stainier, D. Y.** (2007). Genetic control of single lumen formation in the zebrafish gut. *Nat Cell Biol* **9**, 954-60.
- Baye, L. M. and Link, B. A.** (2008). Nuclear migration during retinal development. *Brain Res* **1192**, 29-36.
- Beetschen, J. C.** (2001). Amphibian gastrulation: history and evolution of a 125 year-old concept. *Int J Dev Biol* **45**, 771-95.
- Bilder, D., Schober, M. and Perrimon, N.** (2003). Integrated activity of PDZ protein complexes regulates epithelial polarity. *Nat Cell Biol* **5**, 53-8.
- Bryant, D. M. and Mostov, K. E.** (2008). From cells to organs: building polarized tissue. *Nat Rev Mol Cell Biol* **9**, 887-901.
- Casal, J., Struhl, G. and Lawrence, P. A.** (2002). Developmental compartments and planar polarity in Drosophila. *Curr Biol* **12**, 1189-98.
- Cervantes, S., Yamaguchi, T. P. and Hebrok, M.** (2008). Wnt5a is essential for intestinal elongation in mice. *Dev Biol*.
- Chalmers, A. D. and Slack, J. M.** (2000). The Xenopus tadpole gut: fate maps and morphogenetic movements. *Development* **127**, 381-92.
- Chung, M. I., Nascone-Yoder, N. M., Grover, S. A., Drysdale, T. A. and Wallingford, J. B.** (2010). Direct activation of Shroom3 transcription by Pitx proteins drives epithelial morphogenesis in the developing gut. *Development* **137**, 1339-49.
- Ciruna, B., Jenny, A., Lee, D., Mlodzik, M. and Schier, A. F.** (2006). Planar cell polarity signalling couples cell division and morphogenesis during neurulation. *Nature* **439**, 220-4.
- Colas, J. F. and Schoenwolf, G. C.** (2001). Towards a cellular and molecular understanding of neurulation. *Dev Dyn* **221**, 117-45.
- Collier, S. and Gubb, D.** (1997). Drosophila tissue polarity requires the cell-autonomous activity of the fuzzy gene, which encodes a novel transmembrane protein. *Development* **124**, 4029-37.
- Crosnier, C., Stamatakis, D. and Lewis, J.** (2006). Organizing cell renewal in the intestine: stem cells, signals and combinatorial control. *Nat Rev Genet* **7**, 349-59.
- Dekaney, C. M., Bazer, F. W. and Jaeger, L. A.** (1997). Mucosal morphogenesis and cytodifferentiation in fetal porcine small intestine. *Anat Rec* **249**, 517-23.
- Del Bene, F., Wehman, A. M., Link, B. A. and Baier, H.** (2008). Regulation of neurogenesis by interkinetic nuclear migration through an apical-basal notch gradient. *Cell* **134**, 1055-65.

**Ewald, A. J., Brenot, A., Duong, M., Chan, B. S. and Werb, Z.** (2008). Collective epithelial migration and cell rearrangements drive mammary branching morphogenesis. *Dev Cell* **14**, 570-81.

**Feng, Y. and Davis, N. G.** (2000). Akr1p and the type I casein kinases act prior to the ubiquitination step of yeast endocytosis: Akr1p is required for kinase localization to the plasma membrane. *Mol Cell Biol* **20**, 5350-9.

**Ferrari, A., Veligodskiy, A., Berge, U., Lucas, M. S. and Kroschewski, R.** (2008). ROCK-mediated contractility, tight junctions and channels contribute to the conversion of a preapical patch into apical surface during isochoric lumen initiation. *J Cell Sci* **121**, 3649-63.

**Franklin, V., Khoo, P. L., Bildsoe, H., Wong, N., Lewis, S. and Tam, P. P.** (2008). Regionalisation of the endoderm progenitors and morphogenesis of the gut portals of the mouse embryo. *Mech Dev* **125**, 587-600.

**Gambello, M. J., Darling, D. L., Yingling, J., Tanaka, T., Gleeson, J. G. and Wynshaw-Boris, A.** (2003). Multiple dose-dependent effects of Lis1 on cerebral cortical development. *J Neurosci* **23**, 1719-29.

**Ge, X., Frank, C. L., Calderon de Anda, F. and Tsai, L. H.** (2010). Hook3 interacts with PCM1 to regulate pericentriolar material assembly and the timing of neurogenesis. *Neuron* **65**, 191-203.

**Georgiou, M., Marinari, E., Burden, J. and Baum, B.** (2008). Cdc42, Par6, and aPKC regulate Arp2/3-mediated endocytosis to control local adherens junction stability. *Curr Biol* **18**, 1631-8.

**Gilbert, S. F.** (2000). *Developmental Biology* Sinauer Associates.

**Gubb, D. and Garcia-Bellido, A.** (1982). A genetic analysis of the determination of cuticular polarity during development in *Drosophila melanogaster*. *J Embryol Exp Morphol* **68**, 37-57.

**Habas, R., Kato, Y. and He, X.** (2001). Wnt/Frizzled activation of Rho regulates vertebrate gastrulation and requires a novel Formin homology protein Daam1. *Cell* **107**, 843-54.

**Haeckel, E.** (1879). *The Evolution of Man*, (ed).

**Haigo, S. L., Hildebrand, J. D., Harland, R. M. and Wallingford, J. B.** (2003). Shroom induces apical constriction and is required for hinge-point formation during neural tube closure. *Curr Biol* **13**, 2125-37.

**Hansson, E. M., Lendahl, U. and Chapman, G.** (2004). Notch signaling in development and disease. *Semin Cancer Biol* **14**, 320-8.

**Heisenberg, C. P., Tada, M., Rauch, G. J., Saude, L., Concha, M. L., Geisler, R., Stemple, D. L., Smith, J. C. and Wilson, S. W.** (2000). Silberblick/Wnt11 mediates convergent extension movements during zebrafish gastrulation. *Nature* **405**, 76-81.

**Hildebrand, J. D.** (2005). Shroom regulates epithelial cell shape via the apical positioning of an actomyosin network. *J Cell Sci* **118**, 5191-203.

**Hildebrand, J. D. and Soriano, P.** (1999). Shroom, a PDZ domain-containing actin-binding protein, is required for neural tube morphogenesis in mice. *Cell* **99**, 485-97.

**Iden, S. and Collard, J. G.** (2008). Crosstalk between small GTPases and polarity proteins in cell polarization. *Nat Rev Mol Cell Biol* **9**, 846-59.

- Jaffe, A. B., Kaji, N., Durgan, J. and Hall, A.** (2008). Cdc42 controls spindle orientation to position the apical surface during epithelial morphogenesis. *J Cell Biol* **183**, 625-33.
- Jaulin, F., Xue, X., Rodriguez-Boulan, E. and Kreitzer, G.** (2007). Polarization-dependent selective transport to the apical membrane by KIF5B in MDCK cells. *Dev Cell* **13**, 511-22.
- Johnston, M. C. and Bronsky, P. T.** (1995). Prenatal craniofacial development: new insights on normal and abnormal mechanisms. *Crit Rev Oral Biol Med* **6**, 25-79.
- Jones, K. L., Benirschke, K. and Chambers, C. D.** (2009). Gastroschisis: etiology and developmental pathogenesis. *Clin Genet* **75**, 322-5.
- Kedinger, M., Duluc, I., Fritsch, C., Lorentz, O., Plateroti, M. and Freund, J. N.** (1998). Intestinal epithelial-mesenchymal cell interactions. *Ann N Y Acad Sci* **859**, 1-17.
- Keller, R.** (2002). Shaping the vertebrate body plan by polarized embryonic cell movements. *Science* **298**, 1950-4.
- Kilian, B., Mansukoski, H., Barbosa, F. C., Ulrich, F., Tada, M. and Heisenberg, C. P.** (2003). The role of Ppt/Wnt5 in regulating cell shape and movement during zebrafish gastrulation. *Mech Dev* **120**, 467-76.
- Kimura, W., Yasugi, S., Stern, C. D. and Fukuda, K.** (2006). Fate and plasticity of the endoderm in the early chick embryo. *Dev Biol* **289**, 283-95.
- Kinoshita, N., Sasai, N., Misaki, K. and Yonemura, S.** (2008). Apical accumulation of Rho in the neural plate is important for neural plate cell shape change and neural tube formation. *Mol Biol Cell* **19**, 2289-99.
- Kojima, Y., Kohri, K. and Hayashi, Y.** Genetic pathway of external genitalia formation and molecular etiology of hypospadias. *J Pediatr Urol* **6**, 346-54.
- Ku, N. O., Zhou, X., Toivola, D. M. and Omary, M. B.** (1999). The cytoskeleton of digestive epithelia in health and disease. *Am J Physiol* **277**, G1108-37.
- Lawson, A. and Schoenwolf, G. C.** (2003). Epiblast and primitive-streak origins of the endoderm in the gastrulating chick embryo. *Development* **130**, 3491-501.
- Lee, C., Le, M. P. and Wallingford, J. B.** (2009). The shroom family proteins play broad roles in the morphogenesis of thickened epithelial sheets. *Dev Dyn* **238**, 1480-91.
- Lee, C., Scherr, H. M. and Wallingford, J. B.** (2007). Shroom family proteins regulate gamma-tubulin distribution and microtubule architecture during epithelial cell shape change. *Development* **134**, 1431-41.
- Lewis, W. H.** (1947). Mechanism of invagination. *Anat Rec* **97**, 139-156.
- Liu, J., Zhang, L., Wang, D., Shen, H., Jiang, M., Mei, P., Hayden, P. S., Sedor, J. R. and Hu, H.** (2003). Congenital diaphragmatic hernia, kidney agenesis and cardiac defects associated with Slit3-deficiency in mice. *Mech Dev* **120**, 1059-70.
- Logan, C. Y. and Nusse, R.** (2004). The Wnt signaling pathway in development and disease. *Annu Rev Cell Dev Biol* **20**, 781-810.
- Lubarsky, B. and Krasnow, M. A.** (2003). Tube morphogenesis: making and shaping biological tubes. *Cell* **112**, 19-28.
- Madara, J. L., Neutra, M. R. and Trier, J. S.** (1981). Junctional complexes in fetal rat small intestine during morphogenesis. *Dev Biol* **86**, 170-8.

**Mao, Y., Mulvaney, J., Zakaria, S., Yu, T., Morgan, K. M., Allen, S., Basson, M. A., Francis-West, P. and Irvine, K. D.** (2011). Characterization of a Dchs1 mutant mouse reveals requirements for Dchs1-Fat4 signaling during mammalian development. *Development* **138**, 947-57.

**Martin-Belmonte, F., Gassama, A., Datta, A., Yu, W., Rescher, U., Gerke, V. and Mostov, K.** (2007). PTEN-mediated apical segregation of phosphoinositides controls epithelial morphogenesis through Cdc42. *Cell* **128**, 383-97.

**Martin-Belmonte, F. and Mostov, K.** (2008). Regulation of cell polarity during epithelial morphogenesis. *Curr Opin Cell Biol* **20**, 227-34.

**Matakatsu, H. and Blair, S. S.** (2004). Interactions between Fat and Dachshous and the regulation of planar cell polarity in the Drosophila wing. *Development* **131**, 3785-94.

**Mathan, M., Moxey, P. C. and Trier, J. S.** (1976). Morphogenesis of fetal rat duodenal villi. *Am J Anat* **146**, 73-92.

**Matsumoto, A., Hashimoto, K., Yoshioka, T. and Otani, H.** (2002). Occlusion and subsequent re-canalization in early duodenal development of human embryos: integrated organogenesis and histogenesis through a possible epithelial-mesenchymal interaction. *Anat Embryol (Berl)* **205**, 53-65.

**McNeill, H.** (2009). Planar cell polarity and the kidney. *J Am Soc Nephrol* **20**, 2104-11.

**Mitchell, L. E.** (2005). Epidemiology of neural tube defects. *Am J Med Genet C Semin Med Genet* **135C**, 88-94.

**Nelson, W. J.** (2009). Remodeling epithelial cell organization: transitions between front-rear and apical-basal polarity. *Cold Spring Harb Perspect Biol* **1**, a000513.

**Ng, A. N., de Jong-Curtain, T. A., Mawdsley, D. J., White, S. J., Shin, J., Appel, B., Dong, P. D., Stainier, D. Y. and Heath, J. K.** (2005). Formation of the digestive system in zebrafish: III. Intestinal epithelium morphogenesis. *Dev Biol* **286**, 114-35.

**Nishimura, T. and Takeichi, M.** (2008). Shroom3-mediated recruitment of Rho kinases to the apical cell junctions regulates epithelial and neuroepithelial planar remodeling. *Development* **135**, 1493-502.

**Norden, C., Young, S., Link, B. A. and Harris, W. A.** (2009). Actomyosin is the main driver of interkinetic nuclear migration in the retina. *Cell* **138**, 1195-208.

**Nowotschin, S. and Hadjantonakis, A. K.** Cellular dynamics in the early mouse embryo: from axis formation to gastrulation. *Curr Opin Genet Dev* **20**, 420-7.

**Oishi, I., Kawakami, Y., Raya, A., Callol-Massot, C. and Izpisua Belmonte, J. C.** (2006). Regulation of primary cilia formation and left-right patterning in zebrafish by a noncanonical Wnt signaling mediator, duboraya. *Nat Genet* **38**, 1316-22.

**Park, T. J., Haigo, S. L. and Wallingford, J. B.** (2006). Ciliogenesis defects in embryos lacking inturnd or fuzzy function are associated with failure of planar cell polarity and Hedgehog signaling. *Nat Genet* **38**, 303-11.

**Pilot, F. and Lecuit, T.** (2005). Compartmentalized morphogenesis in epithelia: from cell to tissue shape. *Dev Dyn* **232**, 685-94.

**Plageman, T. F., Jr., Chung, M. I., Lou, M., Smith, A. N., Hildebrand, J. D., Wallingford, J. B. and Lang, R. A.** (2010). Pax6-dependent Shroom3 expression regulates apical constriction during lens placode invagination. *Development* **137**, 405-15.

**Qian, D., Jones, C., Rzdzińska, A., Mark, S., Zhang, X., Steel, K. P., Dai, X. and Chen, P.** (2007). Wnt5a functions in planar cell polarity regulation in mice. *Dev Biol* **306**, 121-33.

**Ramsdell, A. F.** (2005). Left-right asymmetry and congenital cardiac defects: getting to the heart of the matter in vertebrate left-right axis determination. *Dev Biol* **288**, 1-20.

**Rawls, A. S., Guinto, J. B. and Wolff, T.** (2002). The cadherins fat and dachsous regulate dorsal/ventral signaling in the *Drosophila* eye. *Curr Biol* **12**, 1021-6.

**Rodriguez-Boulan, E. and Nelson, W. J.** (1989). Morphogenesis of the polarized epithelial cell phenotype. *Science* **245**, 718-25.

**Rosenquist, G. C.** (1971). The location of the pregut endoderm in the chick embryo at the primitive streak stage as determined by radioautographic mapping. *Dev Biol* **26**, 323-35.

**Saburi, S., Hester, I., Fischer, E., Pontoglio, M., Eremina, V., Gessler, M., Quaggin, S. E., Harrison, R., Mount, R. and McNeill, H.** (2008). Loss of Fat4 disrupts PCP signaling and oriented cell division and leads to cystic kidney disease. *Nat Genet* **40**, 1010-5.

**Saotome, I., Curto, M. and McClatchey, A. I.** (2004). Ezrin is essential for epithelial organization and villus morphogenesis in the developing intestine. *Dev Cell* **6**, 855-64.

**Sauer, F. C.** (1936). The Interkinetic migration of embryonic epithelial nuclei. *J Morphol.* **60**, 1-11.

**Sawyer, J. M., Harrell, J. R., Shemer, G., Sullivan-Brown, J., Roh-Johnson, M. and Goldstein, B.** (2009). Apical constriction: A cell shape change that can drive morphogenesis. *Dev Biol.*

**Schenk, J., Wilsch-Brauninger, M., Calegari, F. and Huttner, W. B.** (2009). Myosin II is required for interkinetic nuclear migration of neural progenitors. *Proc Natl Acad Sci U S A* **106**, 16487-92.

**Schluter, M. A., Pfarr, C. S., Pieczynski, J., Whiteman, E. L., Hurd, T. W., Fan, S., Liu, C. J. and Margolis, B.** (2009). Trafficking of Crumbs3 during cytokinesis is crucial for lumen formation. *Mol Biol Cell* **20**, 4652-63.

**Simon, M. A.** (2004). Planar cell polarity in the *Drosophila* eye is directed by graded Four-jointed and Dachsous expression. *Development* **131**, 6175-84.

**Sopko, R. and McNeill, H.** (2009). The skinny on Fat: an enormous cadherin that regulates cell adhesion, tissue growth, and planar cell polarity. *Curr Opin Cell Biol* **21**, 717-23.

**Spence, J. R., Lauf, R. and Shroyer, N. F.** (2011). Vertebrate intestinal endoderm development. *Dev Dyn* **240**, 501-20.

**Tam, P. P., Khoo, P. L., Lewis, S. L., Bildsoe, H., Wong, N., Tsang, T. E., Gad, J. M. and Robb, L.** (2007). Sequential allocation and global pattern of movement of the definitive endoderm in the mouse embryo during gastrulation. *Development* **134**, 251-60.

**Tanentzapf, G. and Tepass, U.** (2003). Interactions between the crumbs, lethal giant larvae and bazooka pathways in epithelial polarization. *Nat Cell Biol* **5**, 46-52.

**Tawk, M., Araya, C., Lyons, D. A., Reugels, A. M., Girdler, G. C., Bayley, P. R., Hyde, D. R., Tada, M. and Clarke, J. D.** (2007). A mirror-symmetric cell division that orchestrates neuroepithelial morphogenesis. *Nature* **446**, 797-800.

**Taylor, J., Chung, K. H., Figueroa, C., Zurawski, J., Dickson, H. M., Brace, E. J., Avery, A. W., Turner, D. L. and Vojtek, A. B.** (2008). The scaffold protein POSH regulates axon outgrowth. *Mol Biol Cell* **19**, 5181-92.

**Toyota, T., Yamamoto, M. and Kataoka, K.** (1989). Light and electron microscope study on developing intestinal mucosa in rat fetuses with special reference to the obliteration of the intestinal lumen. *Arch Histol Cytol* **52**, 51-60.

**Trahair, J. and Robinson, P.** (1986). The development of the ovine small intestine. *Anat Rec* **214**, 294-303.

**Tremblay, K. D. and Zaret, K. S.** (2005). Distinct populations of endoderm cells converge to generate the embryonic liver bud and ventral foregut tissues. *Dev Biol* **280**, 87-99.

**Trier, J. S. and Moxey, P. C.** (1979). Morphogenesis of the small intestine during fetal development. *Ciba Found Symp*, 3-29.

**Tsai, J. W., Chen, Y., Kriegstein, A. R. and Vallee, R. B.** (2005). LIS1 RNA interference blocks neural stem cell division, morphogenesis, and motility at multiple stages. *J Cell Biol* **170**, 935-45.

**Veeman, M. T., Axelrod, J. D. and Moon, R. T.** (2003). A second canon. Functions and mechanisms of beta-catenin-independent Wnt signaling. *Dev Cell* **5**, 367-77.

**Villasenor, A., Chong, D. C., Henkemeyer, M. and Cleaver, O.** (2011). Epithelial dynamics of pancreatic branching morphogenesis. *Development* **137**, 4295-305.

**Vinson, C. R. and Adler, P. N.** (1987). Directional non-cell autonomy and the transmission of polarity information by the frizzled gene of *Drosophila*. *Nature* **329**, 549-51.

**Visel, A., Blow, M. J., Li, Z., Zhang, T., Akiyama, J. A., Holt, A., Plajzer-Frick, I., Shoukry, M., Wright, C., Chen, F. et al.** (2009). ChIP-seq accurately predicts tissue-specific activity of enhancers. *Nature* **457**, 854-8.

**Wallingford, J. B., Fraser, S. E. and Harland, R. M.** (2002). Convergent extension: the molecular control of polarized cell movement during embryonic development. *Dev Cell* **2**, 695-706.

**Wallingford, J. B., Rowning, B. A., Vogeli, K. M., Rothbacher, U., Fraser, S. E. and Harland, R. M.** (2000). Dishevelled controls cell polarity during *Xenopus* gastrulation. *Nature* **405**, 81-5.

**Wang, Q. and Margolis, B.** (2007). Apical junctional complexes and cell polarity. *Kidney Int* **72**, 1448-58.

**Wells, J. M. and Melton, D. A.** (1999). Vertebrate endoderm development. *Annu Rev Cell Dev Biol* **15**, 393-410.

**Wynshaw-Boris, A. and Gambello, M. J.** (2001). LIS1 and dynein motor function in neuronal migration and development. *Genes Dev* **15**, 639-51.

**Xie, Z., Moy, L. Y., Sanada, K., Zhou, Y., Buchman, J. J. and Tsai, L. H.** (2007). Cep120 and TACCs control interkinetic nuclear migration and the neural progenitor pool. *Neuron* **56**, 79-93.

- Yamada, M., Udagawa, J., Matsumoto, A., Hashimoto, R., Hatta, T., Nishita, M., Minami, Y. and Otani, H.** (2010). Ror2 is required for midgut elongation during mouse development. *Dev Dyn* **239**, 941-53.
- Yamaguchi, T. P., Bradley, A., McMahon, A. P. and Jones, S.** (1999). A Wnt5a pathway underlies outgrowth of multiple structures in the vertebrate embryo. *Development* **126**, 1211-23.
- Yang, C. H., Axelrod, J. D. and Simon, M. A.** (2002). Regulation of Frizzled by fat-like cadherins during planar polarity signaling in the Drosophila compound eye. *Cell* **108**, 675-88.
- Zeidler, M. P., Perrimon, N. and Strutt, D. I.** (1999). The four-jointed gene is required in the Drosophila eye for ommatidial polarity specification. *Curr Biol* **9**, 1363-72.
- Zorn, A. M. and Wells, J. M.** (2009). Vertebrate endoderm development and organ formation. *Annu Rev Cell Dev Biol* **25**, 221-51.



## Chapter 2

### Cell dynamics in fetal intestinal epithelium: implications for intestinal growth and morphogenesis\*

#### Summary:

The cellular mechanisms driving growth and remodeling of the early intestinal epithelium are poorly understood. Current dogma suggests that the murine fetal intestinal epithelium is stratified, that villi are formed by an epithelial remodeling process involving *de novo* formation of apical surface at secondary lumina, and that a major intestinal lengthening mechanism is radial intercalation of stratified cells. Here, we investigate cell polarity, cell cycle dynamics, and cell shape in the fetal murine intestine between E12.5 and embryonic day (E) 14.5. We show that, contrary to previous assumptions, this epithelium is pseudostratified. Furthermore, epithelial nuclei exhibit interkinetic nuclear migration, a process wherein nuclei move in concert with the cell cycle, from the basal side (where DNA is synthesized) to the apical surface (where mitosis takes place); such nuclear movements were previously misinterpreted as radial intercalation of cells. We further demonstrate that growth of epithelial girth between E12.5 and E14.5 is driven by microtubule-

---

\* This chapter represents a submitted manuscript: Grosse AS, Pressprich MF, Curley LB, Margolis B, Hildebrand JD, and DL Gumucio (2011). "Cell dynamics in fetal intestinal epithelium: implications for intestinal growth and morphogenesis."

and actinomyosin-dependent apicobasal elongation, rather than by progressive epithelial stratification as was previously thought. Finally, we demonstrate that the actin-binding protein Shroom3 is critical for maintenance of a properly organized pseudostratified epithelium. In mice lacking Shroom3, the apical surface is expanded and the apical actin network is highly ramified during villus emergence. These results favor an alternative model of intestinal morphogenesis in which the epithelium remains single-layered and apicobasally polarized throughout early intestinal development.

### **Introduction:**

When formed at E9.5, the murine primitive gut tube possesses a central lumen surrounded by a polarized, endodermally-derived epithelium [reviewed in (Wells and Melton, 1999; Zorn and Wells, 2009)]. Over the next five days, the epithelium progressively increases in girth (Mathan et al., 1976; Matsumoto et al., 2002). At E14.5, the thickened epithelium begins a drastic remodeling process whereby the previously flat luminal surface is converted into villi, finger-like epithelial projections with mesenchymal cores.

Careful histological studies of specimens from multiple species have provided an outline of morphological events involved in this process (Babyatsky, 2003; Dauca et al., 1990; Hashimoto et al., 1999; Madara et al., 1981; Mathan et al., 1976; Matsumoto et al., 2002; Toyota et al., 1989). In the majority of these investigations, the intestinal epithelial organization is characterized as multilayered (i.e., stratified)

(Babyatsky, 2003; Dauca et al., 1990; Hashimoto et al., 1999; Madara et al., 1981; Mathan et al., 1976; Toyota et al., 1989), though rare studies indicate that it is single-layered (i.e., pseudostratified) (Matsumoto et al., 2002). Multiple recent mechanistic studies of villus formation and intestinal growth accept the more common stratified paradigm and interpret experimental data in this context (Cervantes et al., 2008; Kim et al., 2007; Saotome et al., 2004). However, no careful analysis of cell shape and cell dynamics in the intestinal epithelium has been previously carried out despite the fact that these factors have important implications for cell cycle compartmentalization, patterns of intestinal growth and mechanisms of epithelial remodeling.

Cell cycle compartmentalization is quite different in stratified and pseudostratified epithelia. For example, in the esophagus, a stratified epithelium of the GI tract, the basal-most layer contains stem and transient amplifying cells, which together provide the mitotic compartment. As cells leave the basal layer and move toward the luminal surface, they withdraw from the cell cycle and differentiate [reviewed in (Croagh et al., 2008)]. In the transiently stratified epithelium of the branching mammary gland, mitotic cells are distributed throughout the multiple cell layers of the terminal end bud (Ewald et al., 2008). In contrast, in pseudostratified epithelia, such as the embryonic neural tube or developing retina, the cell cycle is uniquely tied to a process called interkinetic nuclear migration (INM)(Sauer, 1936). During INM, nuclei near the basement membrane synthesize DNA, then travel apically while in G2 phase, undergo mitosis at the apical surface and travel back to the basal

surface in G1 phase. Thus, while mitotic figures are either basally located or distributed in stratified epithelia, mitosis is an apical event in pseudostratified epithelia. Due to their constant apicobasal (AB) movement, nuclei appear staggered in a pseudostratified epithelium (Miyata, 2008). INM, and by implication, nuclear staggering, is a consequence of cell proliferation since agents that inhibit proliferation interrupt INM (Baye and Link, 2008; Ueno et al., 2006).

Mechanisms driving growth of intestinal girth are also predicted to differ in stratified vs. pseudostratified epithelia. Stratified epithelia increase girth by adding cell layers, while pseudostratified epithelia thicken by progressive elongation of epithelial cells (Miyata, 2008). It has been shown that AB elongation of pseudostratified epithelial cells in the developing neural tube depends on Shroom3, a PDZ binding domain-containing protein that localizes to the apical adherens junction (Haigo et al., 2003; Hildebrand, 2005; Hildebrand and Soriano, 1999). Interestingly, Shroom3 also controls apical constriction, another attribute shared by most pseudostratified epithelia (Haigo et al., 2003; Hildebrand, 2005; Lee et al., 2009; Lee et al., 2007; Nishimura and Takeichi, 2008; Taylor et al., 2008).

The exact nature of cell shape and cell polarity in the early intestine also impacts our interpretation of the mechanisms driving the drastic remodeling of intestinal surface that occurs at E14.5. A stratified epithelium would remodel by cell reorganization and *de novo* polarization of central cells; indeed, existing models favor this strategy [see Fig. 7E in (Saotome et al., 2004) and Fig. 1A in (Kim et al.,

2007)]. These models are supported by ultrastructural studies that link initiation of epithelial remodeling to the *de novo* formation of apical surfaces at so-called secondary lumina located deep within stratified epithelial layers (Madara et al., 1981; Mathan et al., 1976; Toyota et al., 1989) and by recent studies in the zebrafish (Bagnat et al., 2007) and mouse intestine (Saotome et al., 2004) that pinpoint some of the genes required for this process. Dynamic changes in cell polarity and fusion of a network of secondary lumina in the context of a transient stratified epithelium were recently shown to drive formation of murine pancreatic acini (Villasenor et al., 2010). However, in a pseudostratified epithelium, in which all cells already have an apical surface facing the lumen, a more likely mechanism driving remodeling would be cell shape change, coupled with expansion of the existing luminal surface.

Together, these highlights reveal the importance of cell shape, cell polarity, and cell cycle dynamics in understanding early intestinal epithelial morphogenesis. Here, we provide the first comprehensive analysis of cell dynamics in the early murine intestinal epithelium. We establish a new model of intestinal morphogenesis wherein the epithelial tube maintains its polarization throughout epithelial thickening and remodeling. We show definitively that the early intestinal epithelium is pseudostratified, undergoes INM, and grows in girth by progressive AB elongation that is dependent upon microtubules and actomyosin signaling. In accord with this, we demonstrate that the actomyosin signaling protein, Shroom3, is an important controller of the pseudostratified shape. In the absence of Shroom3, apical surfaces are expanded, and the epithelium is disorganized. During intestinal remodeling,

Shroom3 is further required to properly arrange the apical F-actin network at the surface of emerging villi.

## **Results:**

*Growth of the early intestinal epithelium.* To document growth in girth in the early intestinal epithelium we examined C57Bl6/J (BL6) mice at E12.5, E14.5, and E16.5 (Fig. 2.1). Epithelial girth was recorded as distance from the basement membrane to the apical surface in intestinal cross sections from the proximal duodenum, just distal to the pancreatic duct (Fig. 2.1) and from the distal ileum just proximal to the cecum (Fig. 2.S1A-D). In both areas, epithelial growth in thickness between E12.5 and E14.5 is associated with an increase in the number of stacked nuclei; girth drops precipitously upon remodeling (Fig. 2.1B-D; Fig. 2.S1B-D). Increased nuclear layers could be due to increasing stratification of the intestinal epithelium or might reflect progressive packing of nuclei in a pseudostratified epithelium. To further explore these alternatives, we investigated AB polarity and cell shape.

*Cell polarity in the early intestinal epithelium.* To define the state of epithelial polarization during epithelial thickening, markers that detect apical [atypical PKC (aPKC), Ezrin,  $\beta$ -actin, Crumbs3, Zona occludens 1 (ZO-1)], basal [collagen IV (CollIV)] and lateral [E-cadherin (Ecad)] cell surfaces were examined by confocal imaging of vibratome-sectioned intestines. All five apical proteins are confined to the luminal surface of the epithelium at both E12.5 and E14.5 (Fig. 2.1B,C; Fig. 2.2A-E). Occasionally, small regions of apical staining are seen in deeper regions of the

epithelium (e.g., Fig. 2.2D). However, when examined in the context of the entire z-stack, these regions are always contiguous with the central lumen. We found no evidence for isolated apical surfaces in deep regions of the epithelium. As expected, the basal marker (CollIV) was found exclusively at the circumference of the epithelial tube (Fig. 2.2C) while Ecad staining was located at the lateral surfaces (Fig. 2.2B,E). This distribution of polarity markers is consistent with a pseudostratified epithelium. However, a similar distribution of markers would be seen in stratified epithelia in which central cells lack both apical and basal polarity (Mailleux et al., 2008; Sternlicht, 2006; Tucker, 2007; Villasenor et al., 2010; Walker et al., 2008). To further investigate this, we examined the Golgi marker, gm130. Long, laterally positioned Golgi structures were seen (Fig. 2.2F), a staining pattern that is more consistent with a pseudostratified cell shape than a stratified one.

In a pseudostratified epithelium, cells are highly elongated and densely packed; all cells touch both basal and apical surfaces and the apical footprint of each cell is very small (Miyata, 2008). In contrast, in a stratified epithelium with multiple cell layers, dramatic apical constriction of luminal cells is not required. To assess apical constriction, intestines were stained with the centrosomal marker,  $\gamma$ -tubulin ( $\gamma$ -tub). In cells that are not dividing, the centrosome is positioned at the center of the apical surface; centrosome to centrosome distance reflects the apical cell size. As shown in Fig. 2.3A, centrosomes are densely packed at the luminal surface of BL6 epithelium, suggesting that cells are highly constricted.

Apical cell footprints were also traced in 100  $\mu\text{m}$  vibratome slices of E14.5 duodenal tissue stained with ZO-1, a tight junction marker. Using 3D reconstruction software, a portion of the luminal surface was rebuilt from the confocal z-stack, revealing numerous small apical footprints (Fig. 2.3B). The few large footprints are mitotic cells, as discussed further below. This ZO-1 pattern closely resembles that seen in the neural tube (Miyata, 2008), a known pseudostratified epithelium.

*Tracing cellular shapes confirms that the intestinal epithelium is pseudostratified.* We took several different approaches to visualize whole cells in the context of the intact epithelium. First, scanning electron microscopy (SEM) of E13.5 epithelium revealed epithelial cells stretching across the AB axis (Fig. 2.S2A). Second, in cultured intestines, 24 hours after electroporation of a lumenally injected plasmid encoding CMV-EGFP, reconstructed confocal z-stacks from vibratome sections showed that cells expressing EGFP were touching both basal and apical surfaces (Fig. 2.S2B); nuclei of these cells were positioned basally in some cases and apically in others. Identical results were seen when E14.5 intestinal lumens from BL6 animals were injected with a fine micellar mixture of DiI-labeled oil in PBS and cultured on a transwell membrane for 8 hours prior to confocal imaging (Fig. 2.S2C).

These data are consistent with the idea that at least some cells of the early intestinal epithelium are pseudostratified. However, these techniques may favor the labeling of cells that touch the apical surface, leaving open the possibility that a population of basally oriented cells exist that do not stretch apically or that a population of central



cells may exist without touching either the basal or apical surfaces. Thus, as a third approach, we utilized mT/mG reporter mice [mTmG; (Muzumdar et al., 2007)] that express myristilated tomato DsRed in cell membranes in the absence of Cre and myristilated CMV-EGFP (Hepker et al.) in membranes after Cre recombination. mTmG mice were mated with CaggCreERT2 [Cagg; (Hayashi and McMahon, 2002)] mice, and pregnant dams were gavaged with tamoxifen 24 hours prior to sacrifice. In Cagg;mTmG offspring, mG-labeled membranes of single cells were readily observed in the background of mT-labeled cells. A movie of a confocal z-stack (Fig. 2.3 and Movie 2.1) reveals that individual cells are highly elongated and stretch across multiple sections within the z-stack, accounting for the fact that 2D images of histological sections rarely capture whole cells and instead give the false appearance of stratification. Reconstructions of multiple z-slices from E12.5 (Fig. 2.3C) and E14.5 (Fig. 2.3D,E) confirm that the majority of the cells stretch entirely across the girth of the epithelium. Quantitation of 259 cells from the E14.5 z-stacks reveals that 83% of EGFP positive cells stretch from the apical surface to the basement membrane (Fig. 2.3F). Another 4% touch only the apical surface. Generally, these cells are rounded and may represent dividing cells. Finally, 13% of cells at the edges of the z-stack could not be unequivocally analyzed. We found no clear evidence for the presence of basally located cells that do not touch the apical surface and no evidence for centrally located cells that touch neither the basal nor the apical surface. Identical results were seen in the distal ileum (Fig. 2.S1E-G).

Together, the data from polarity studies and from multiple different labeling techniques are congruent and indicate that the early intestinal epithelium thickens between E12.5 and E14.5 by progressive cell elongation and progressive pseudostratification rather than addition of cellular layers. Therefore, the murine intestinal tube is maintained throughout this period as a single layer of AB polarized epithelium.

*Cell cycle dynamics in the early intestinal epithelium.* Pseudostratified epithelia are typically highly proliferative and undergo a unique process known as INM, wherein nuclei move back and forth between apical and basal surfaces in concert with the cell cycle (Miyata, 2008; Sauer, 1936; Ueno et al., 2006). To determine whether the early intestinal epithelium shares these characteristics, intestinal sections from E14.5 BL6 mice were stained for Ki67, a marker that is present on cells in all phases of the cell cycle except G0. As shown in Fig. 2.S3A, the majority of epithelial cells are actively cycling. Caspase 3 staining revealed very little apoptosis (Fig 2.S3B).

To further examine cell cycle compartmentalization, pregnant dams were intraperitoneally (IP) injected at E14.5 with a pulse of Bromodeoxyuridine (BrdU), a thymidine analog; 20 minutes later, the same dams were IP injected with a thymidine chase to quench BrdU uptake. Nuclei in S-phase incorporate BrdU and their movement can be subsequently tracked over time. We recorded the number and location of labeled nuclei at 40, 120, and 200 minutes post BrdU injection in the proximal duodenum (Fig. 2.4) and distal ileum (Fig. 2.S1H-J). In both areas, at 40

minutes, most labeled nuclei are found close to the basal surface of the epithelium (Fig. 2.4A). With time, nuclei localize to progressively apical locations (Fig. 2.4A-C, quantified in Fig. 2.4D). Co-staining with a marker for mitotic cells, phospho-histone-H3 (pHH3), reveals that at 40 minutes, none of the nuclei are stained with both BrdU and pHH3 (Fig. 2.4A, inset). At 120 minutes, most mitotic nuclei are still unlabeled with BrdU (Fig. 2.4B, inset) but rare double-labeling is detected. However, at 200 minutes post-BrdU, the majority of nuclei are labeled with both pHH3 and BrdU (Fig. 2.4C, inset), indicating that between 120 and 200 minutes is required to traverse the S-G2-M phases of the cell cycle in the early intestinal epithelium. Finally, we found that mitosis takes place exclusively at the luminal (apical) surface (Fig. 2.4E), as it does in other pseudostratified epithelia (Miyata, 2008; Sauer, 1936; Ueno et al., 2006). Together, these data demonstrate that the pseudostratified intestinal epithelium undergoes INM.

*Mechanisms controlling growth of epithelial girth in the early intestine. Cell*

elongation and INM occur concurrently during epithelial thickening, suggesting that INM movements and progressive staggering of cell nuclei could be responsible for the growth of epithelial girth. To test this, we interrupted the cell cycle in cultured intestines; previous studies have shown that cell cycle progression is required for INM (Ueno et al., 2006). E14.0 intestines were dissected from BL6 mice, placed into culture on transwell membranes and treated with 5  $\mu$ g/mL Mitomycin C (MitoC), an agent that crosslinks DNA in S-phase, inhibiting cell cycle progression. After 15 hours, control intestines retained nuclear staggering, with 3-4 layers of nuclei

visible (Fig. 2.5A). In contrast, epithelial cells in MitoC-treated intestines took on a more columnar shape without nuclear staggering (Fig. 2.5B). Interestingly, the change in cell shape did not affect epithelial thickness. Thus, cell cycle progression, nuclear movement, and progressive nuclear staggering are not required for the maintenance of intestinal girth.

In other systems, both microtubule dynamics and actomyosin signaling have been implicated in the control of cell height (Levina et al., 2001; Picone et al., 2010). Thus, we tested whether either of these cytoskeletal signaling systems are critical for intestinal epithelial cell elongation. Intestinal organ cultures from Cagg;mTmG mice (E14.0) were treated with the myosin IIB inhibitor, Blebbistatin (Blebb) or the microtubule polymerizing inhibitor, Nocodazole (Nocod). Blebb was used at 5  $\mu$ M, a concentration previously shown to not affect the cell cycle (Schenk et al., 2009). After 15 hours of culture, control intestines retained their pseudostratified morphology, with 3-4 nuclear layers visible (Fig. 2.5C). However, Blebb-treated intestines exhibited drastically diminished cell height (Fig. 2.5D). Nuclear staggering was intact in treated intestines, with 2-3 nuclear layers visible, and mitotic figures were found at the apical surface. These findings imply that, in the intestinal epithelium, cell elongation, but not INM, requires actomyosin signaling.

Cell height was also reduced in cultured E14.0 Cagg;mTmG intestines treated with 1  $\mu$ M Nocod (Fig. 2.5E,F). Since Nocod can block cells in metaphase due to a failure of spindle formation, rounded cells at the luminal surface after 15 hours of culture

confirmed the apical localization of mitosis. In Fig. 2.5E, one of the rounded mitotic cells expressing mG has a long process that connects to the basal surface. In the neural tube, similar long processes connect dividing cells to the basement membrane (Das et al., 2003; Miyata et al., 2001; Saito et al., 2003). Nuclear stacking in Nocod-treated intestines was diminished to a row of mitotic cells at the apical surface and a row of non-mitotic cells at the basal surface. Although Nocod may have inhibited apical to basal INM, the data above demonstrate that blocking INM entirely with MitoC does not affect cell height. Thus, the Nocod data imply a role for microtubules in cell lengthening. We conclude that the growth of girth in the intestinal epithelium is due to progressive cell lengthening of pseudostratified cells and that maintenance of epithelial cell height requires the microtubular network as well as actomyosin signaling.

*Shroom3 is required for cell organization in the intestinal epithelium.* Shroom3 is a PDZ-containing protein that localizes to the apical surface of pseudostratified epithelial cells, where it directs both apical constriction and AB elongation via control of actomyosin signaling and  $\gamma$ -tub organization (Hildebrand, 2005; Hildebrand and Soriano, 1999; Lee et al., 2007; Plageman et al., 2010). Recently, *Shroom3* was shown to be important in epithelial cell shape in the *Xenopus* gut (Chung et al., 2010), however, the cellular impact on morphogenesis was not investigated in that study. In the mouse, *Shroom3* is expressed in the E8.5 gut (Hildebrand and Soriano, 1999) but expression at later stages has not been examined and the role of Shroom3 in mouse intestinal development is unknown.

We first examined *Shroom3* expression in the E14.5 intestine using the gene trap mouse line, *Shroom<sup>Gt(ROSA)5.3Sor</sup>* (hereafter referred to as *Shroom<sup>Gt</sup>*), in which a  $\beta$ -galactosidase ( $\beta$ -gal) reporter gene is spliced into *Shroom3* transcript, allowing detection of *Shroom3* expression via X-gal staining (Hildebrand and Soriano, 1999). We found that in *Shroom<sup>Gt/+</sup>* mice, intestinal epithelial cells are  $\beta$ -gal positive; *Shroom3* activity appears greatest in the proximal intestine (Fig. 2.S4). Variability in  $\beta$ -gal staining from cell to cell suggests that *Shroom3* expression levels might be dynamically regulated.

To investigate the actions of *Shroom3* during intestinal morphogenesis, we stained intestinal sections from WT and *Shroom3<sup>Gt/Gt</sup>* mice with Ecad as a marker of cell shape and aPKC and CollIV as markers of apical and basal surfaces, respectively. In the absence of *Shroom3*, the epithelium is disorganized, with many rounded cells located at the luminal surface, some of which display pynknotic nuclei (Fig. 2.6B); Caspase 3 staining confirms the presence of apoptotic cells (Fig. 2.S3C). Surprisingly, epithelial girth did not appear to be significantly altered in *Shroom3* deficient mice. In fact, due to the presence of rounded luminal cells, girth was increased in some areas. These results suggest that *Shroom3* either does not play a role in cellular elongation in mouse intestinal epithelium or that *Shroom2*, which is expressed in the intestinal epithelium (J.H., data not shown) and can drive apical constriction and cell elongation (Lee et al., 2009), plays a partially redundant role with *Shroom3* in shaping cells of the developing intestine.

To determine whether rounded luminal cells in *Shroom3* mice were indicative of increased mitotic activity, we examined pHH3 staining. In WT intestines, mitotic cells localize to the apical surface (Fig. 2.6C and Fig. 2.4E). In *Shroom3* null intestines, rounded central cells are negative for pHH3. Rather pHH3-positive mitotic nuclei are found beneath clumps of rounded cells (Fig. 2.6D). Interestingly, analysis of the apical marker, aPKC, reveals that the mitotic cells in *Shroom3* mice are in fact adjacent to apical surfaces that stretch beneath the rounded central cells (Fig. 2.6B,F). Together, these findings, along with the dynamic *Shroom3* expression pattern, lead us to posit a critical need for *Shroom3* as cells complete mitosis and shift from their rounded condition to re-establish an elongated and apically constricted shape. Cells that fail to reassume their pseudostratified shape may lose their attachment to the basal surface and undergo anoikis, detectable here by increased Caspase 3 staining (Fig. 2.S3C).

*Shroom3 is required for apical constriction in the pseudostratified intestinal epithelium.* It has been reported that in MDCK cells, *Shroom3* is required for apical constriction, but its loss does not affect AB polarity (Hildebrand, 2005). Indeed, aPKC expression is expanded but remains apical in *Shroom3* null mouse intestines (Fig. 2.6E,F). Analysis of additional cell polarity markers reveals that ZO-1 expression is expanded and somewhat irregular, but still apical (Fig. 2.7A,B). The lateral marker, Ecad, emphasizes the altered geometry and shape of the luminal epithelial cells (Fig. 2.7C,D). However, while Ecad is absent from the apical surface of

control intestinal cells (Fig. 2.7C), it is present apically on several rounded cells in the *Shroom3* intestines (Fig. 2.7D). Apical expansion is confirmed by analysis of  $\gamma$ -tub staining. In control intestines, centrosomes are densely packed together, a reflection of the highly constricted apical surfaces (Fig. 2.7E). In contrast, in *Shroom3<sup>Gt/Gt</sup>* tissue, the increased distance between centrosomes confirms the loss of apical constriction (Fig. 2.7F).

*The apical surfaces of emerging villi are disorganized in the absence of Shroom3*

Beginning at E14.5, villus formation begins and is accompanied by drastic remodeling of the epithelium. We predicted that the increased girth, branching luminal surface, and abnormal polarity in the thickened *Shroom3<sup>Gt/Gt</sup>* intestine would result in irregular epithelial remodeling. Since *Shroom3* is known to localize to adherens junctions and organize the apical actin network in neural epithelium and MDCK cells (Hildebrand, 2005; Hildebrand and Soriano, 1999), we tested whether apical actin distribution is altered in *Shroom3* deficient intestinal cells. Thus, we stained E15.5 WT and *Shroom3<sup>Gt/Gt</sup>* intestines with the F-actin binding toxin, phalloidin. In control littermates the apical surfaces of emerging villi are brightly stained with phalloidin (Fig. 2.8A). In *Shroom3* null mice, the F-actin network is expanded and ramified making it difficult to discern the surfaces of individual villi (Fig. 2.8B). Reconstructed surface renderings of phalloidin staining (Fig. 2.8C,D and Movie 2.2, 2.3) demonstrate that in control mice, the apical actin network from contiguous cells forms a smooth sheet over each emerging villus (Fig. 2.8C). In contrast, the apical actin network of *Shroom3* deficient intestines appears



rough and highly disorganized (Fig. 2.8D). Together, our data indicate that Shroom3 signaling is required to maintain the single-layered, pseudostratified epithelium and to properly shape the smooth apical surface of emerging villi.

## **Discussion**

Numerous studies in rat, mouse, sheep, pig, and rabbit have characterized the intestinal epithelium as stratified prior to villus remodeling (Cervantes et al., 2008; de Santa Barbara et al., 2003; Dekaney et al., 1997; Dekaney et al., 2007; Hashimoto et al., 1999; Kim et al., 2007; Madara et al., 1981; Mathan et al., 1976; Saotome et al., 2004; Sbarbati, 1982; Toofanian and Targowski, 1982; Toyota et al., 1989). In all of these studies, the histological and microscopic techniques used were unable to capture the entirety of the extremely long, thin epithelial cells that stretch from basal to apical surfaces. Through genetic labeling techniques and 3D reconstruction, we demonstrate that the early mouse intestinal epithelium is in fact pseudostratified and relies, in part, on Shroom3 to maintain orderly pseudostratification. This revised model of intestinal organization, in which the intestinal tube maintains its AB polarity and its pseudostratified shape during early growth and during the initiation of villus morphogenesis, has enormous implications for the interpretation of previous and future functional studies of the developing intestine.

Our findings challenge the notion that secondary lumen formation is a central driver of intestinal remodeling, as previously suggested by early morphological studies

(Mathan et al., 1976) and by the finding of malformed and fused villi in Ezrin null mice (Saotome et al., 2004). In both cases, the starting point for hypothesis building was the idea that the intestinal epithelium is stratified. However, our examination of confocal z-stacks from vibratome sections with multiple different apical markers revealed no unequivocal example of a true secondary lumen that was not connected to the primary lumen. The actual mechanism that drives intestinal remodeling and villus formation remains to be determined, but the fused villi seen in Ezrin null mice (Saotome et al., 2004) suggest that this is tied to apical surface generation. In light of the studies described here, it will be important to revisit that model as a tool to investigate the mechanisms of luminal expansion.

Knowledge that the early murine intestinal epithelium is pseudostratified also demands that current models concerning intestinal lengthening be re-examined. On the basis of the phenotypic comparison of wild type and *Wnt5a* null mice, Cervantes *et al.* posited that the intestine grows in length via radial intercalation of stratified epithelial cells (Cervantes et al., 2008). Specifically, BrdU labeling patterns in WT E11.5 intestines led to the proposal that cells delaminate from the basal lamina, forming a temporarily stratified epithelium. Delaminated cells were posited to divide and then re-intercalate into the basal epithelial layer, expanding it lengthwise. In *Wnt5a* null mice, BrdU labeled cells accumulate at the luminal surface. Hence, intestines exhibit increased girth, but severely reduced length, suggesting a defect in radial intercalation movements. Mice lacking Ror2, a receptor that binds Wnt5a, also exhibited a thickened epithelial phenotype and again, radial

intercalation was posited to be the mechanism (Yamada et al., 2010). From our current study, it is now clear that the authors were observing INM, but interpreting nuclear movements as cellular movements in the context of an incorrect stratified epithelial model. Indeed, radial intercalation is not possible in the context of a pseudostratified epithelium since cells are already in a single layer.

In this regard, it is interesting that many pseudostratified epithelia (e.g., the developing neural tube, retina and as demonstrated here, the intestinal epithelium) are rapidly proliferating tissues. It has been speculated that, in the neural tube, pseudostratification and INM are adaptations that allowed increasingly dense packing of actively proliferating progenitors, needed for expanding the number of differentiated neurons and thus, the size of the brain (Miyata, 2008; Smart, 1972). In the intestine, pseudostratification (and INM) may similarly allow tight packing of a bolus of tall, thin progenitor cells that, when re-shaped to columnar during epithelial remodeling, would quickly and efficiently extend intestinal length. It will be important to test whether factors interfering with INM also interfere with progenitor expansion and intestinal lengthening. Indeed, we are currently investigating the kinetics of cell cycle and efficiency of INM in the *Wnt5a* model.

The mechanisms controlling the growth of intestinal girth have not been previously identified. Our studies reveal that progressive cell elongation of pseudostratified cells drives this aspect of epithelial growth. Further, the elongated shape of these pseudostratified cells requires an intact microtubule network as well as actomyosin

signaling. Interestingly, both of these cytoskeletal systems have been shown to be regulated by members of the Shroom family in other pseudostratified epithelia (Dietz et al., 2006; Haigo et al., 2003; Hildebrand, 2005; Hildebrand and Soriano, 1999; Lee et al., 2009; Lee et al., 2007; Plageman et al., 2010). We provide here the first detailed study of the critical role of murine Shroom3 in intestinal cell shape. Deletion of *Shroom3* greatly expands apical surface area; cells with increased surface area are rounded and located centrally. Rounded central cells were also seen in *Xenopus* intestine after transfection of dominant negative Shroom3 (Chung et al., 2010), suggesting that *Shroom3* plays an evolutionarily conserved role in intestinal epithelial morphology.

In *Shroom3* null intestines, some cells retained their normal elongated shapes. Compensation by intestinally expressed *Shroom2* could potentially explain this conundrum, since the cytoskeletal signaling properties of Shroom2 and Shroom3 are similar (Lee et al., 2009). Overall, our data indicate that Shroom3 is primarily responsible for two critical aspects at the apical surface: apical constriction of pseudostratified cells prior to intestinal remodeling and organization of the apical actin network in contiguous cells at the interface of emerging villi. Since *Shroom3* expression appears to be dynamic, the appearance of rounded and apoptotic cells at the central lumen, with mitotic cells beneath them, leads us to further speculate that Shroom3 expression is important for the re-establishment of the pseudostratified shape in post-mitotic cells.

The studies described here represent the first comprehensive analysis of cell shape, cell cycle dynamics, and cell polarity in the early intestinal epithelium. All data are congruent with the conclusions that the epithelium is pseudostratified, that increasing cell height is responsible for epithelial thickening, and that *Shroom3* drives apical surface dynamics and modulates cell shape in the developing intestine. Given the established role for Shroom proteins in cell shape and remodeling of many epithelia, an obvious next question is: What upstream factors control *Shroom3* (and *Shroom2*) expression levels in the developing gut? Recent studies indicate that *Pax6* is upstream of *Shroom3* in the developing mouse lens placode (Plageman et al., 2010), while *Pitx* transcription factors have been identified as regulators of *Shroom3* in *Xenopus* gut and neural tube (Chung et al., 2010). *Pitx1* and *Pitx2* as well as *Pax6* (weak) and *Pax7* are epithelially expressed in the E14.5 mouse intestine ([www.genepaint.org](http://www.genepaint.org)). It will be important to determine whether any of these transcription factors are involved in remodeling of the E14.5 intestine through dynamic regulation of Shroom signaling.

## **Materials and Methods:**

### *Mice*

Embryonic tissues were obtained from the following mouse lines: C57BL6/J (Jackson Labs 000664), mTmG (Jackson labs 007576), CaggCreERT2 (Jackson Labs 004682), and *Shroom*<sup>3Gt(ROSA)5.3Sor</sup> (Jeff Hildebrand). Pregnant females with Cagg;mTmG embryos were gavaged 12-24 hours prior to sacrifice with 250 mL of

20 mg/mL tamoxifen dissolved in EtOH and corn oil. Length from the pylorus through the colon was measured on images of intestines dissected from BL6 embryos, using a Leica MZ12.5 stereo microscope, Leica DFC290 camera, and Leica Applications Suite software.

### *Genotyping PCR*

Genotyping PCR was performed with the GoTaq PCR kit (Promega M7122) and primers from idtdna.com. All PCR cycles were hot start. mTmG and CaggCre genotyping protocols can be obtained from the Jackson Lab website.

Shroom<sup>Gt(ROSA)<sup>5.3</sup>Sor</sup> primers: Shrm3R1: GAGTTTGTCTCAACCGCGAGC, Shrm3R5: GAGCACTGGCTGCTCTTCTAG, Shrm3F11: GGTGACTGAGGAGTAGAGTCC.

Shroom<sup>Gt(ROSA)<sup>5.3</sup>Sor</sup> reaction concentrations: 1mM dNTP, 2mM MgCl<sub>2</sub>, 0.1uM each primer, 0.02U/μL Taq. CaggCreERT2 PCR cycle: 94°C 30 s, 58°C 30 sec, 62°C 2 s, repeat for 32 cycles.

### *Tissue preparation*

Tissues were fixed 1 hour to overnight in 4% paraformaldehyde and prepared for paraffin, OCT, or agarose embedding. For paraffin, tissue was rinsed with PBS, dehydrated in ethanol, and infused with paraffin. For OCT, tissue was washed with PBS, incubated overnight in 30% sucrose, and embedded in OCT. Agarose samples were rinsed in 1x PBS and embedded in 7% low melt agarose. Cagg;mTmG samples were always vibratome embedded since paraffin processing quenched fluorescence. Paraffin blocks were sectioned at 5 μm, OCT blocks were sectioned at 10μm, and

agarose embedded tissue was vibratome sectioned at 100  $\mu\text{m}$ . Sections were stained and imaged on an Olympus FluoView 500 laser scanning confocal microscope or Nikon eclipse E800 widefield fluorescent microscope.

### *Immunostaining*

Sections were deparaffinized in xylene, rehydrated, washed with PBS, and boiled in 10mM sodium citrate at pH=6 for antigen retrieval. Sections were incubated for 30 minutes in blocking buffer (1% BSA, 10% goat serum, and 0.3% Triton X-100 in TBS). Primary antibodies (details below) were diluted in blocking buffer and incubated overnight at 4°C. Molecular Probes Alexafluor conjugated secondary antibodies (Invitrogen; 1:1000; 488, 568, 647) with 10  $\mu\text{g}/\text{mL}$  Hoechst (Invitrogen) were diluted in blocking buffer for 30 minutes at RT; slides were mounted with Prolong Gold (Invitrogen).

Vibratome sections were permeabilized in 0.5% Triton X-100 in PBS, blocked (4% goat serum and 0.1% Tween 20 in PBS), incubated with primary antibody at 4°C overnight, incubated with Molecular Probes Alexafluor conjugated secondary antibodies (Invitrogen; 1:1000) and 10  $\mu\text{g}/\text{mL}$  Hoechst (Invitrogen) for 45 minutes at RT, and mounted with Prolong Gold between two glass coverslips. Images were obtained on an Olympus FluoView 500 laser scanning confocal microscope. Z-stacks were 3D reconstructed using Bitplane Imaris software.

### *X-gal staining*

Cryostat sections were air dried, washed in PBS, and stained for 2 hours to O/N in the dark at 37°C in X-gal stain solution: 1 mM MgCl<sub>2</sub>, 5 mM K<sub>4</sub>Fe(CN)<sub>6</sub>, 5 mM K<sub>3</sub>Fe(CN)<sub>6</sub> and 1 mg/ml X-gal in PBS. Stained sections were counter-stained in eosin, dehydrated and mounted using Permount (Fisher Scientific).

### *Antibodies*

β-actin-FITC (Sigma F3022, 1:1000), BrdU (Accurate Chemical and Scientific Corp clone BU1/75, 1:200), BrdU (DSHB clone G3G4, 1:400), Casp 3 (R&D AF835, 1:500), CollIV (Millipore AB756P, 1:500), Crumbs3 (Dr. Ben Margolis, 1:5000), Ecad (Invitrogen ECCD2 13-1900, 1:1000), Ecad (BD 610181, 1:1000), Ezrin [Thermo Scientific MS-661-P1, 1:100; blocking from M.O.M. kit (Vector Labs)], gm130 (BD 610822; 1:250), Ki67 (Thermo Scientific rm-9106-S1, 1:400), Phalloidin-488 (Molecular Probes A12379, 1:50), pHH3 (Millipore 6-570, 1:400), pHH3 (Millipore 05-806; 1:200), PKCζ (aPKC; Santa Cruz sc-216, 1:500), γ-tubulin (Sigma T5326, 1:500; block overnight), ZO-1 (Invitrogen 33-9100; 1:1000).

### *BrdU labeling studies*

Pregnant females were IP injected with a pulse of 50 mg/kg BrdU, chased at various times with 500 mg/kg thymidine. Tissues were paraffin embedded and stained with anti-BrdU. BrdU positive nuclei were counted manually, and significance was determined using ANOVA and unpaired t-tests.

### *Organ culture*



Fetal intestines were dissected in warm 1xPBS and cultured in Bgjb culturing media (Gibco) with 1% Pen/Strep and 5mg/mL ascorbic acid on transwell plates (Costar 3428) at 37°C with 5% CO<sub>2</sub>. Intestines were cultured for 15 hours at the air/liquid interface in the presence or absence of MitoC (5 mg/mL), Blebb (5 mM), or Nocod (0.1-1 mM) prior to fixation, embedding, sectioning and immunostaining.

### *Electroporation*

E13.5-14 BL6 intestines were dissected into ice cold 1xPBS. Intestinal lumens were injected with 1 µg/µL pEGFP-C1 (Clontech) using a pulled glass needle and immediately electroporated with three pulses of 35 V (50ms on, 500ms off) using a low voltage, square wave electroporator (Abud et al., 2004). Intestines were cultured for 24-48 hours on transwell plates, agarose embedded, stained, and imaged. DNA for electroporation was purified using the Qiagen endofree plasmid maxi kit.

### *SEM*

Intestinal tissue samples were fixed in Bouin's solution and dehydrated in EtOH followed by hexamethyldisilazane. Samples were critical point dried and mounted using double-sided tape. The intestinal surface was exposed by cracking with a sharp razor blade. Samples were then coated with gold/palladium under vacuum and imaged on an AMRAY 1910 Field Emission Scanning Electron Microscope (FEG-SEM) using X-STREAM imaging software.

## **Acknowledgements**

The authors are grateful for excellent technical assistance provided by Chris Edwards, Shelley Almburg, Dotty Sorenson, and Sasha Meshinchi in the Microscopy and Image Analysis Laboratory as well as Marta Dzaman and Maria Ripberger in the Organogenesis Morphology Core at the University of Michigan. We thank Drs. Kate Walton and Åsa Kolterud for helpful discussions. The work was supported by NIH R01 DK065850 and NIH R56 DK089933 to DLG, DK69605 to BM, and by the Organogenesis Training Program (NIH T32-HD007505 to ASG).

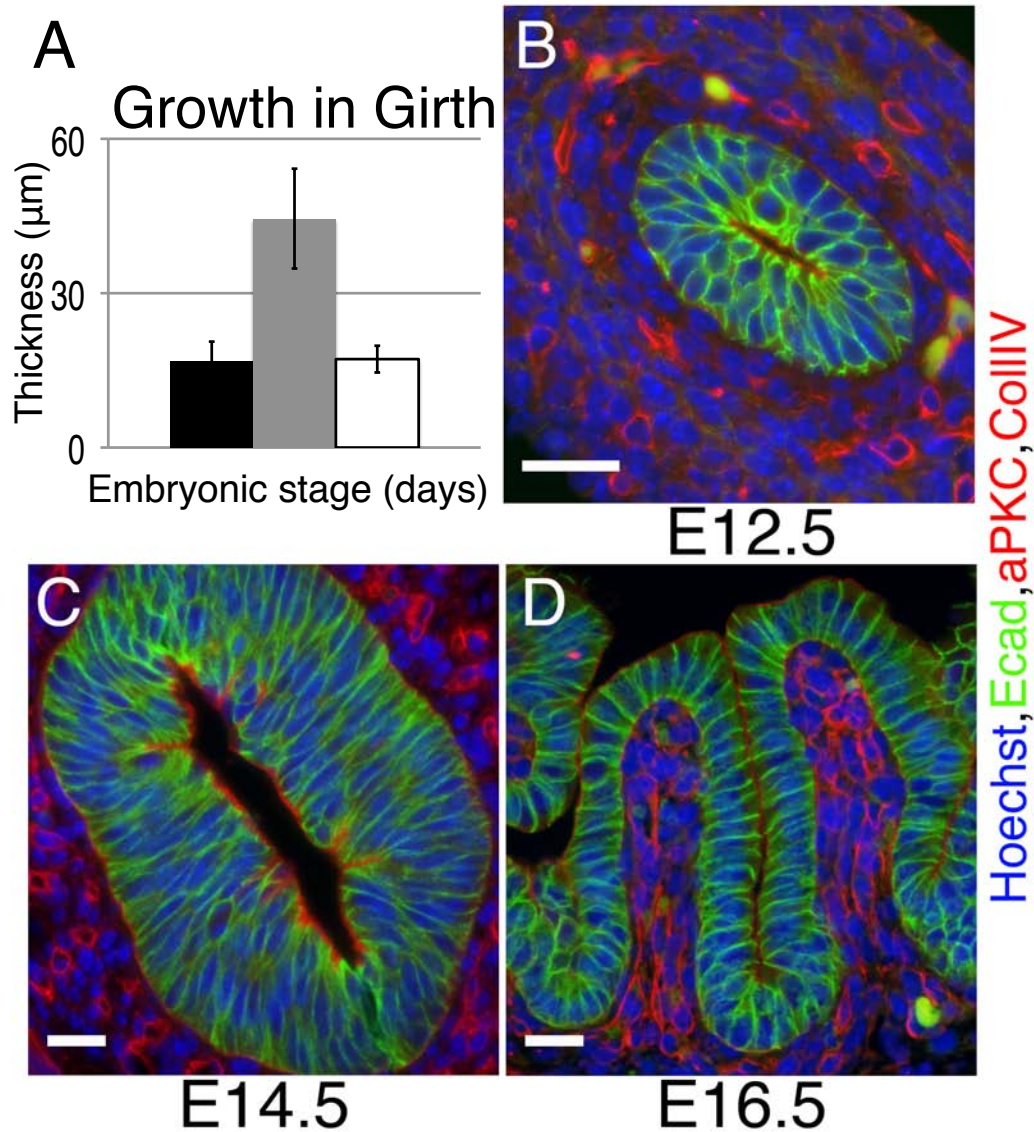


**Figure 2.1. Growth in girth and length of the fetal intestine; correlation with histological changes in the proximal duodenum.** A) Measurement of intestinal epithelial thickness at E12.5, 14.5, and 16.5 (n=6 for each time point). B-D) Intestinal sections stained with Hoechst (blue), Ecad (green), aPKC (red), and CollIV (red) were used to measure girth (double headed arrows). Error bars = SD. Scale bars = 20 $\mu\text{m}$ . \*p<0.001.

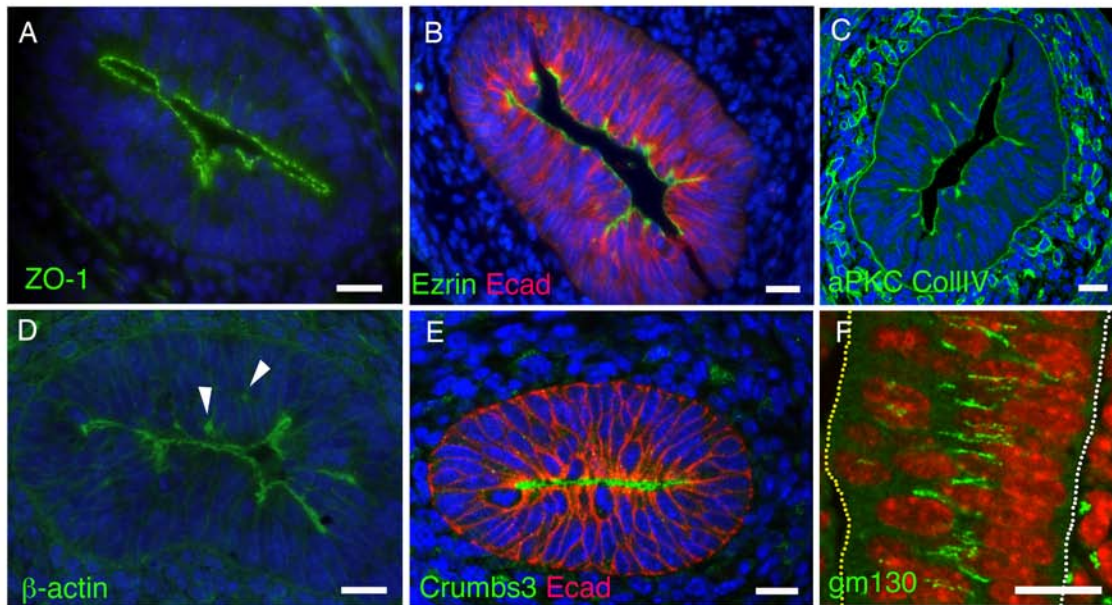


**Figure 2.2. Analysis of cell polarity in the E14.5 intestine.** Apical proteins ZO-1 (A), Ezrin (B), aPKC (C),  $\beta$ -actin (D), and Crumbs (E) localize to the luminal surface. Occasional apical staining deeper within the epithelium (white arrow heads in (D)) is also connected to the primary lumen (see text). CollIV (C) stains the basement membrane surrounding the epithelial layer, while Ecad (B, E) outlines the lateral surface. Gm130 (F) stains Golgi that extend along the lateral surface. Apical and basal are marked by dotted yellow and white lines, respectively. Scale bars = 20  $\mu$ m.

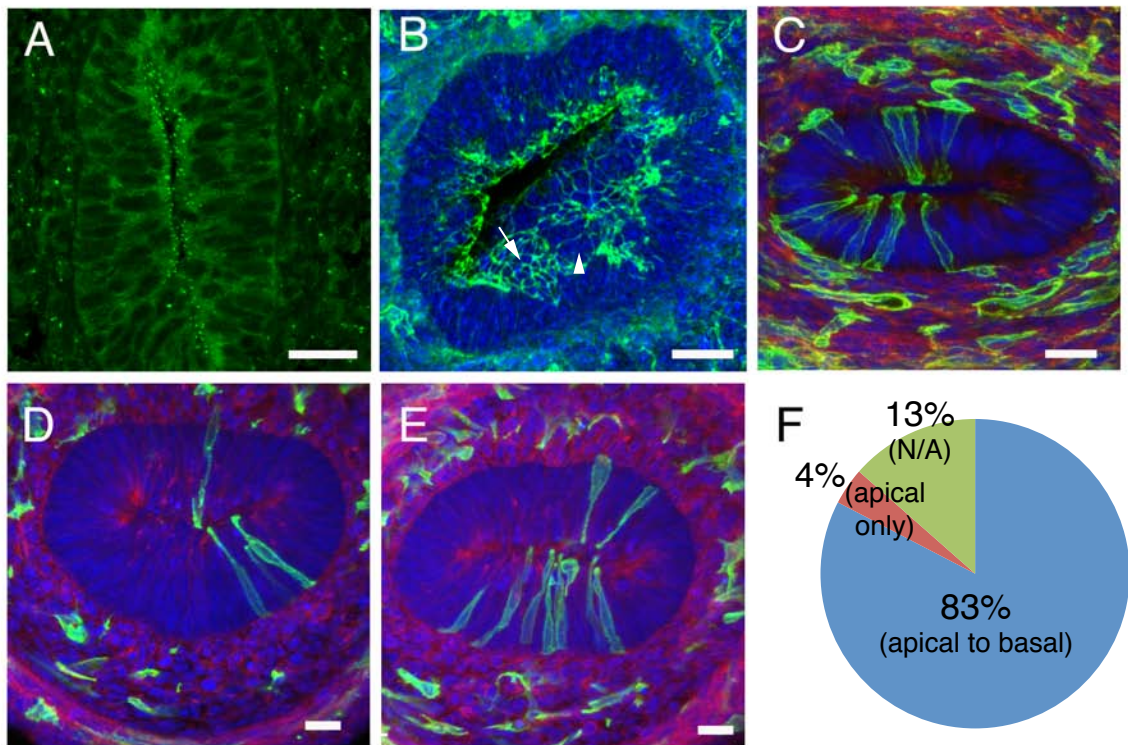


**Figure 2.3. The Intestinal epithelium is pseudostratified.** A) Centrosomes stained with  $\gamma$ -tub concentrate at the apical surface. B) A 3D reconstructed confocal z-stack from a vibratome sectioned intestine stained with ZO-1 (green) and Hoechst (blue) reveals many small apical footprints (arrow) and a large mitotic apical footprint (arrowhead). C-E) Reconstructed confocal z-stacks from vibratome sectioned Cagg;mTmG fetal intestines show shapes of individual EGFP positive epithelial cells at E12.5 (C) and E14.5 (D,E). Movie 2.1 is a video of E,F) Quantification of 259 E14.5 EGFP positive cells from Cagg;mTmG 3D reconstructions reveal that the epithelium is pseudostratified. Scale bars = 20  $\mu$ m.



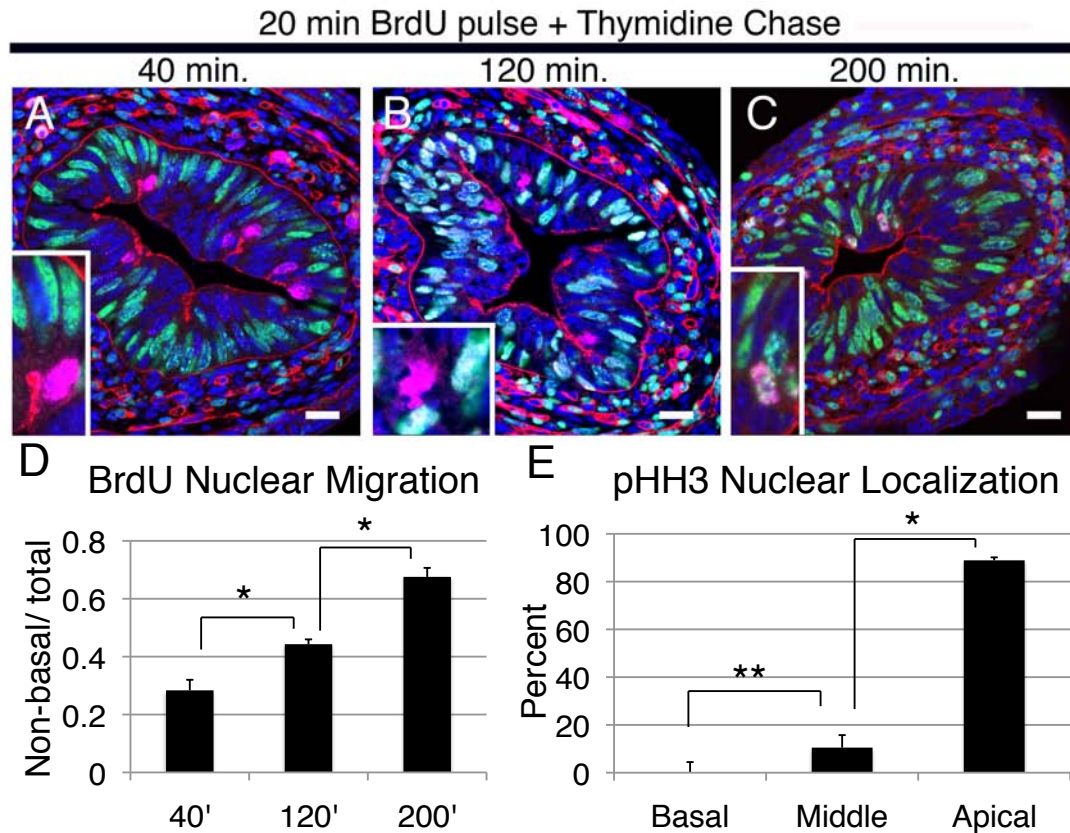


**Figure 2.4. Intestinal nuclei undergo INM.** BrdU was used to track nuclear movement (see text). A-C) Intestinal sections were stained with Hoechst (blue), BrdU (green), aPKC (red), CollIV (red), and pHH3 (pink). After 40 minutes (A), BrdU is visible in S-phase nuclei along the basement membrane; mitotic (pHH3 positive) nuclei are not BrdU positive (inset). After 120 (B) and 200 minutes (C), BrdU positive nuclei progressively migrate toward the apical surface. Costaining of pHH3 and BrdU is rare at 120 minutes and frequent at 200 minutes (insets). D) Quantification of the proportion of non-basal BrdU positive nuclei reveals progressive apical migration. Error bars = S.D.; n=4 intestines. E) Quantification of pHH3 positive nuclei demonstrates that mitosis occurs at the apical surface (n=4 intestines, error bars = S.D.). \*p<0.01, \*\*p<0.05

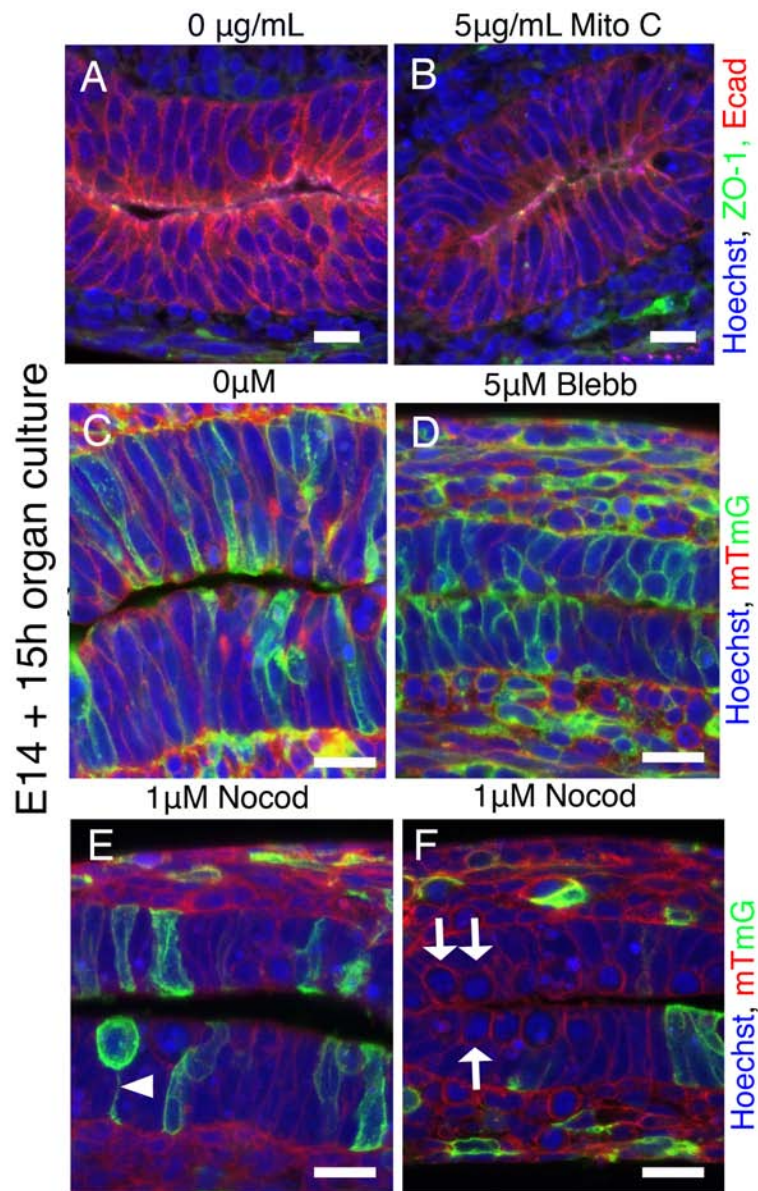


**Figure 2.5. Investigating the mechanisms of epithelial thickening.** A-C) BL6 E14 intestines, cultured on transwell membranes at the air liquid interface for 15 hours. A) Untreated intestine, with 3-4 nuclear layers. B) Treatment with MitoC causes loss of nuclear stacking, but no change in epithelial height. Ecad (red), ZO-1 (green), and Hoechst (blue) (C-F) Cagg;mTmG intestines cultured with no drug addition (C); 5  $\mu$ M Blebb (D), or 1  $\mu$ M Nocod (E,F). Intestinal epithelial cell height is greatly shortened after drug treatment, but intestines retain stacked nuclei. Treatment of duodenal (E) and ileal (F) samples with Nocod suspends cells in metaphase as seen by rounded apical cells (arrows). Dividing cells maintain connection to the basement membrane (arrowhead).

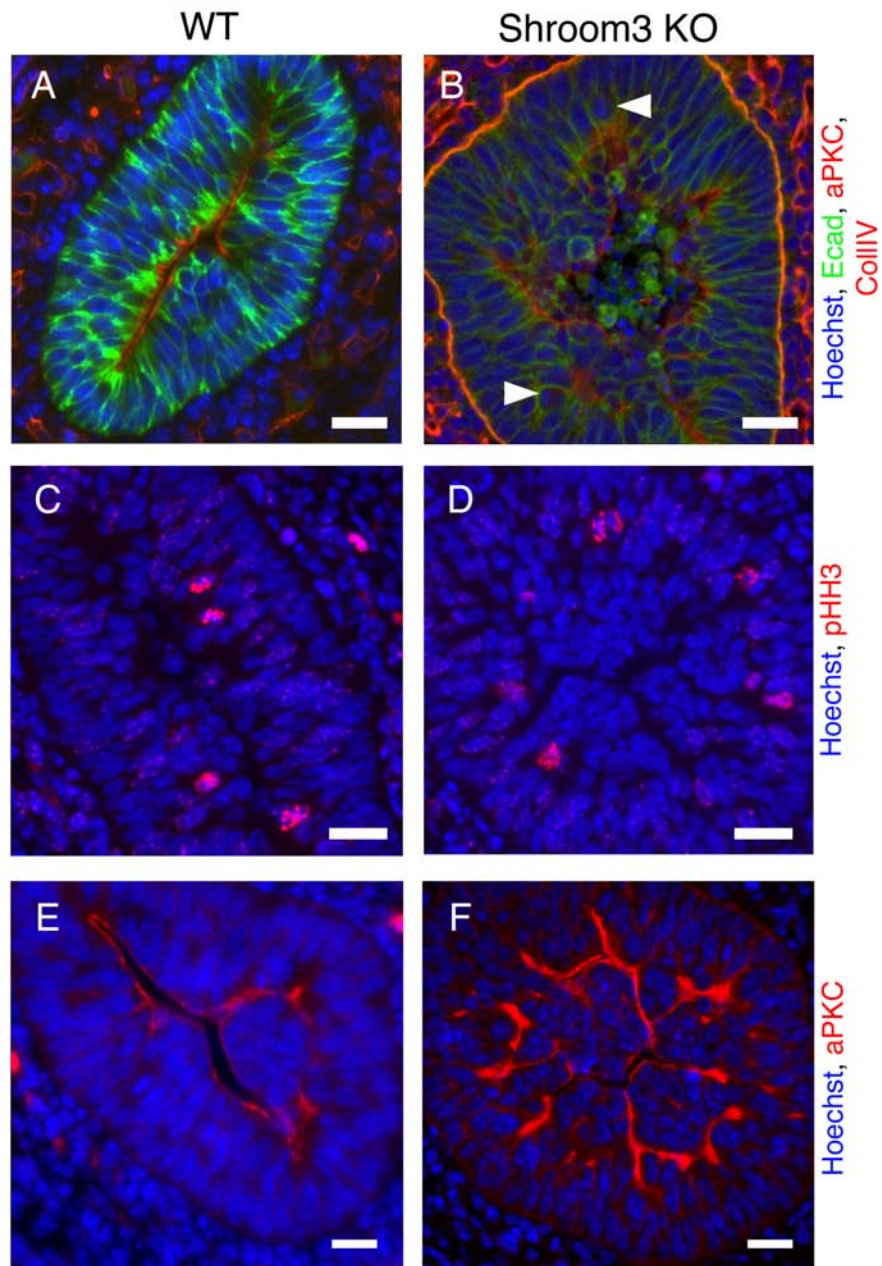


**Figure 2.6. Loss of *Shroom3* alters epithelial organization.** A,B) In *Shroom3* deficient intestines (B), rounded cells fill the lumen; some are pyknotic. Many rounded cells exhibit expanded apical staining. Mitotic cells are located near apically stained regions, beneath rounded cells (arrowheads). Hoechst (blue), Ecad (green), aPKC (red), and CollIV (red). C,D) Mitotic nuclei (pHH3, red) are at the luminal surface of WT controls, but beneath rounded nuclei in the *Shroom3* knockout. E,F) Expanded apical surface in *Shroom3* null mice is seen by aPKC staining (red). Nuclei are stained with Hoechst (blue).



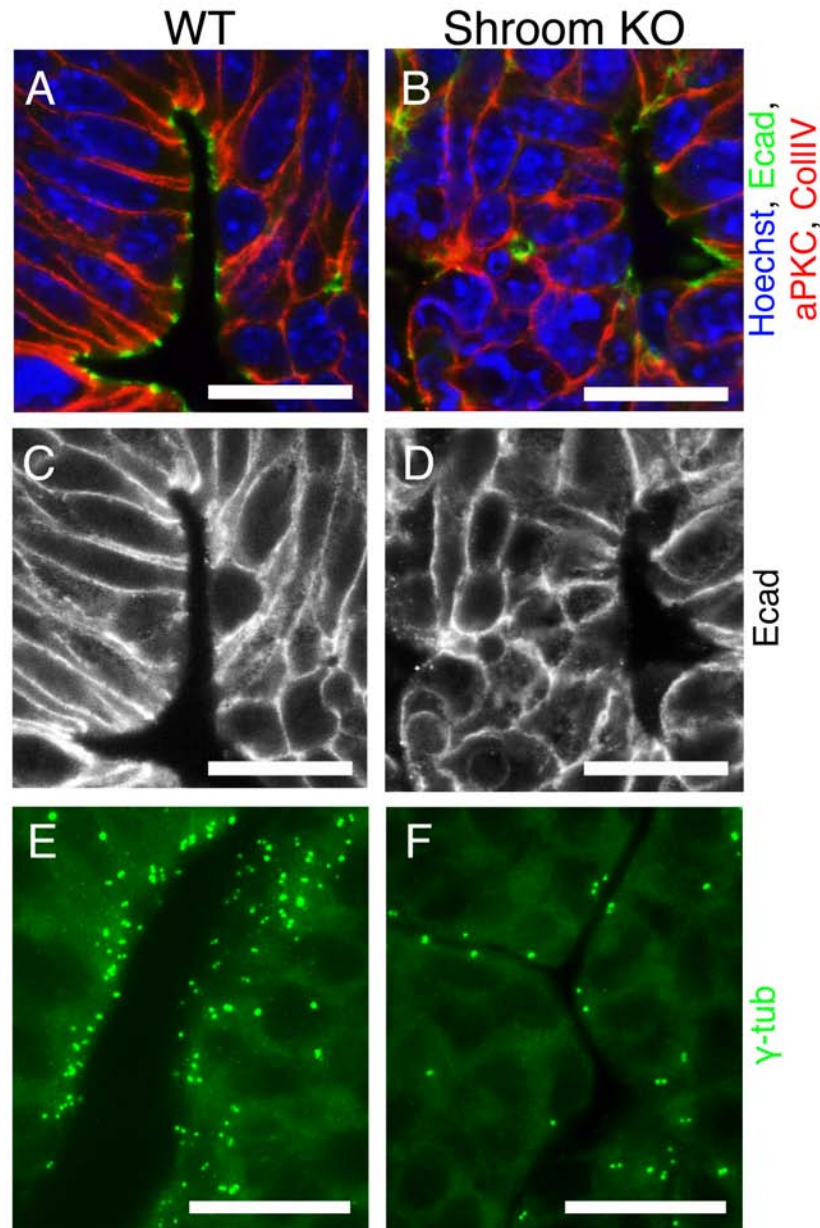


**Figure 2.7. Polarity changes in *Shroom3* null intestines.** A,B) ZO-1 staining. WT intestines exhibit punctate staining at tight junctions. B) Irregular and expanded ZO-1 expression in *Shroom3* null intestines still localizes apically. C,D) Ecad staining. In WT embryos (C) cells are elongated and apically constricted. In the absence of *Shroom3* (D), central cells are rounded and luminal surfaces show Ecad staining. E,F)  $\gamma$ -tub staining. Expanded apical surface is emphasized by greater distance between  $\gamma$ -tub (green) stained centrosomes in *Shroom3* null intestines (F) compared to WT controls (E).  $\gamma$ -tub images are from three consecutive images over  $5\mu\text{m}$ , rebuilt using Helicon Focus.

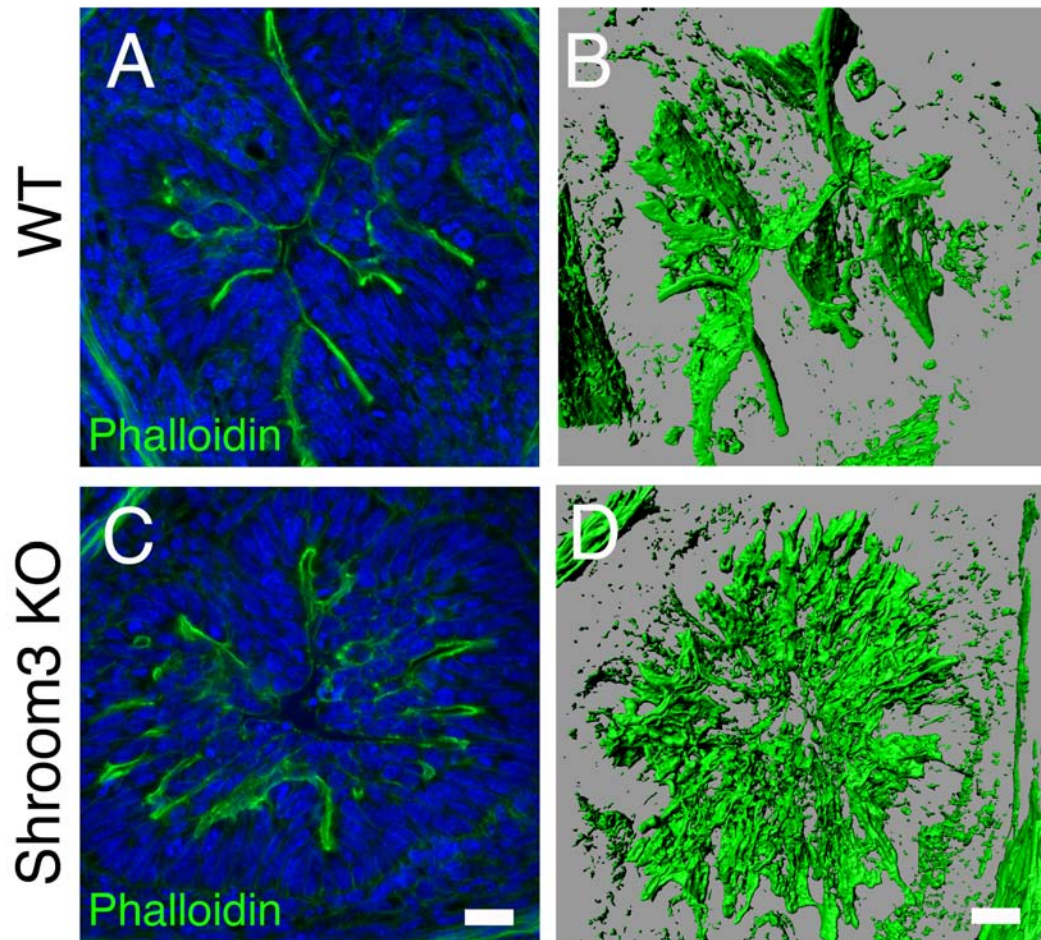


**Figure 2.8. *Shroom3* is required for organization of the apical actin network during epithelial remodeling.** A-D) E15.5 intestines from *Shroom3<sup>Gt/+</sup>* (A,B) and *Shroom3<sup>Gt/Gt</sup>* (C,D) animals initiate villus formation. A,C) Strong phalloidin (green) staining detects the F-actin network at the apical surface. B,D) 3D surface renderings of phalloidin confocal z-stacks. A sheet-like apical actin network covers emerging villi in *Shroom3<sup>Gt/+</sup>* intestines (B) while this network is disorganized and highly branched in *Shroom3<sup>Gt/Gt</sup>* intestines (D). These images rotate in Movies 2.2, 2.3.



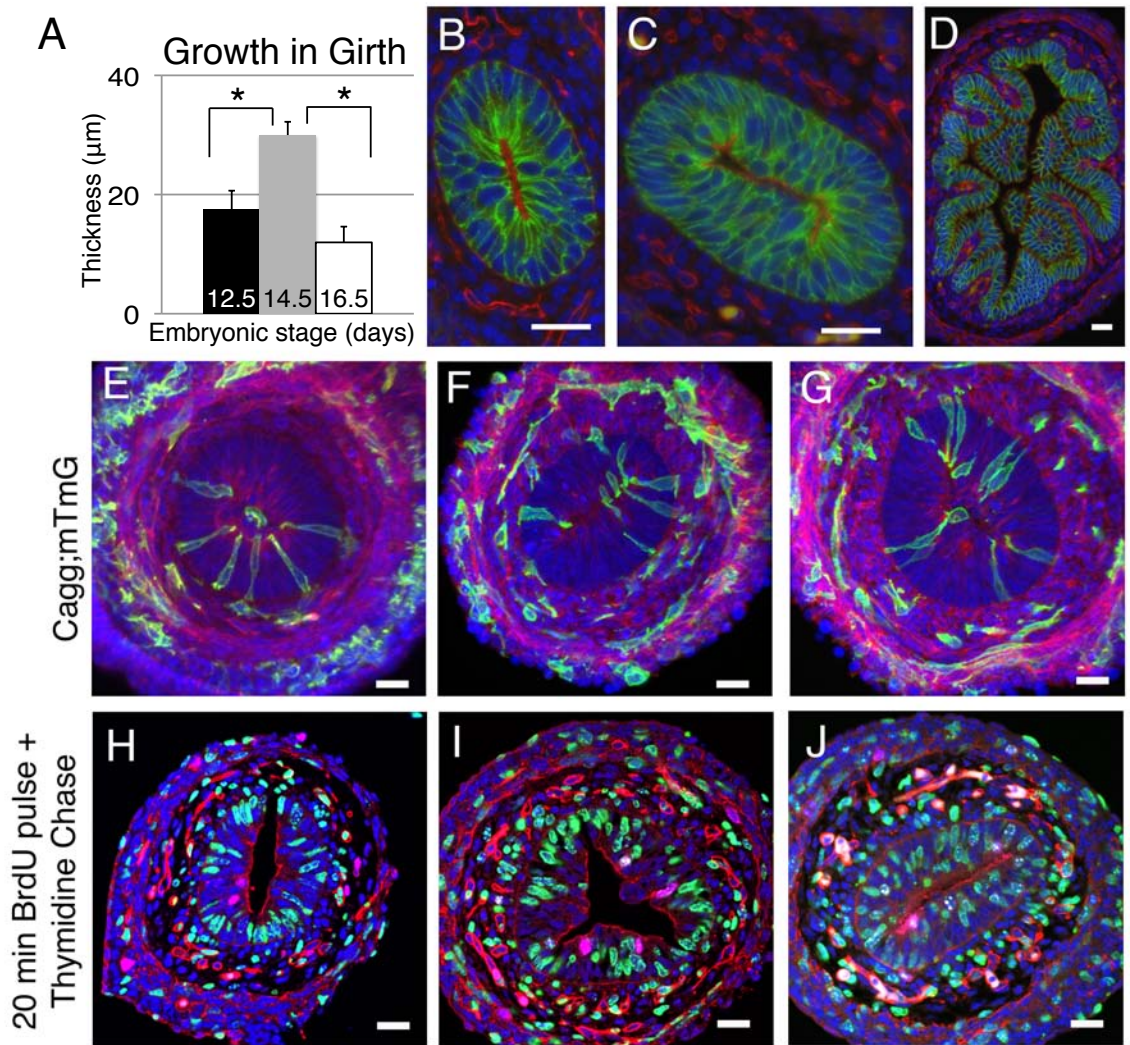


**Figure 2.S1. The distal ileum has the same cell shape and cell dynamics pattern as the proximal duodenum.** A-D) Girth measurements reflect the results in Fig. 1E-F) Using the same methods as Fig. 3, ileal epithelium is pseudostratified. H-J) As in Fig. 4, the epithelium undergoes INM.

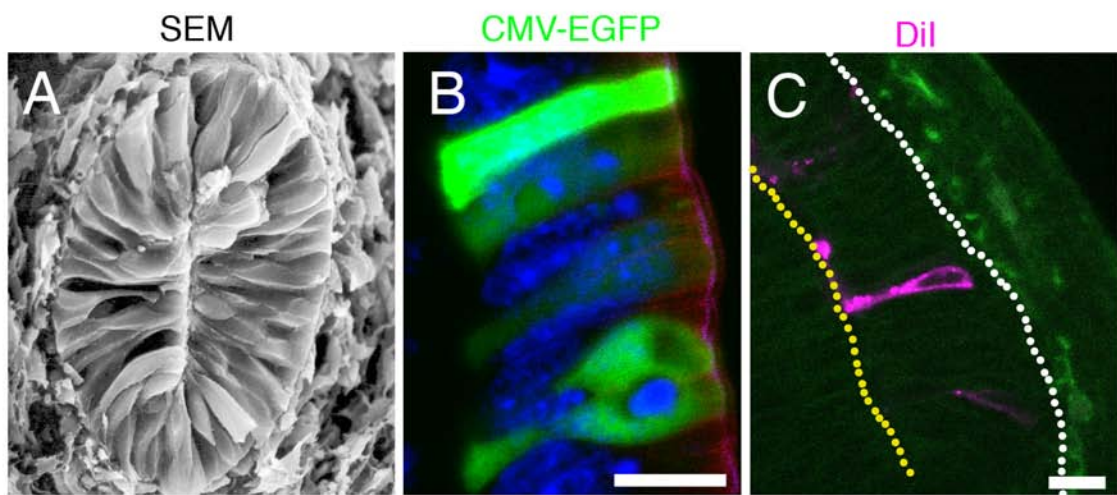


**Figure 2.S2. Epithelial cells are pseudostratified.** A) Individual cells of an E13.5 intestine visualized by SEM stretch the width of the epithelium. B) pEGFP-C1 vector was electroporated into the intestinal epithelium. EGFP-positive epithelial cells touched apical and basal surfaces. Vibratome sections expressed EGFP and were stained with Hoechst (blue) and aPKC (pink). C) DiI oil mixed with PBS was injected into the lumen. A stained cell (pink) stretches from the basement membrane (white dotted line) to the lumen (yellow dotted line).

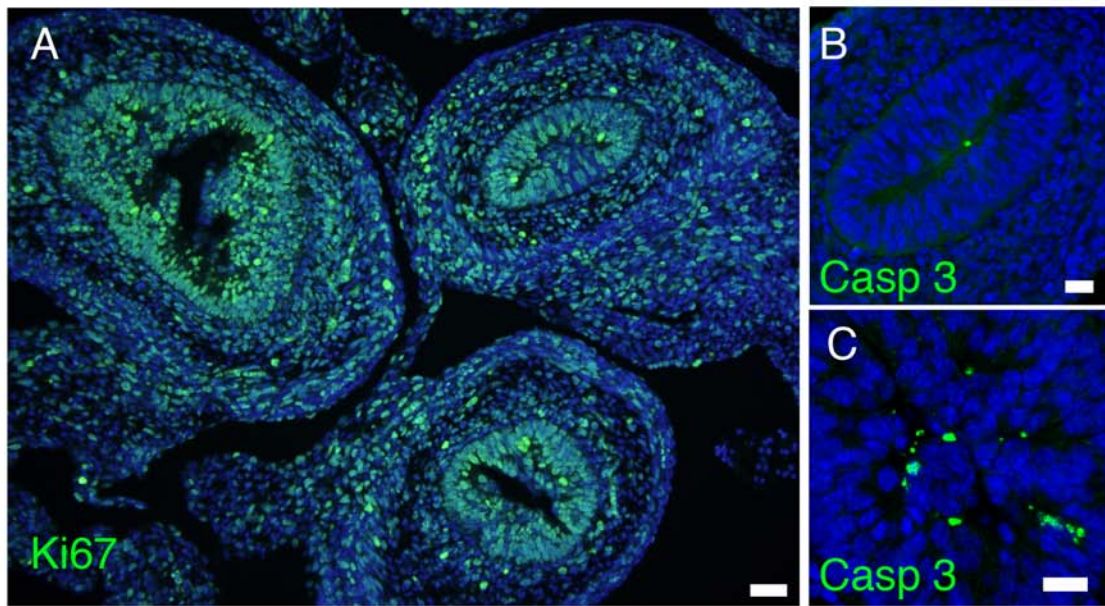


**Figure 2.S3. Cell cycle and apoptosis.** A) E14.5 C57BL6/J Intestinal epithelium stained with Ki67 (green) and Hoechst (blue). Most cells are cycling. B) Caspase3 (green) staining of C57BL6/J intestine reveals rare apoptotic cells. C) Apoptotic cells are more numerous in *Shroom3* null intestines.

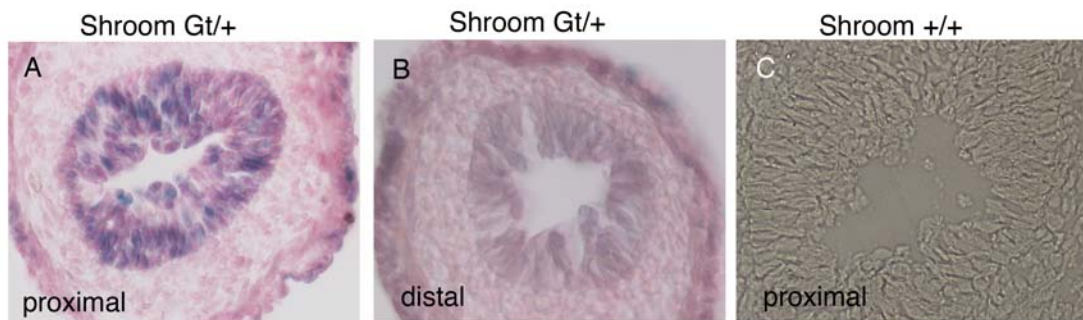


**Figure 2.S4. Shroom3 is expressed in E14.5 intestinal epithelium.** A) *Shroom<sup>Gt/+</sup>* intestinal sections were stained with X-gal (blue) and eosin (pink). *Shroom3* is expressed strongly within the epithelium of the proximal duodenum. B) Expression is weak in distal ileum. C) Tissue from WT littermate controls were X-gal negative.



## **Literature cited**

**Abud, H. E., Lock, P. and Heath, J. K.** (2004). Efficient gene transfer into the epithelial cell layer of embryonic mouse intestine using low-voltage electroporation. *Gastroenterology* **126**, 1779-87.

**Babyatsky, M. W. a. P., D.K.** (2003). Growth and development of the gastrointestinal tract. Philadelphia, PA: Lippincott Williams & Williams.

**Bagnat, M., Cheung, I. D., Mostov, K. E. and Stainier, D. Y.** (2007). Genetic control of single lumen formation in the zebrafish gut. *Nat Cell Biol* **9**, 954-60.

**Baye, L. M. and Link, B. A.** (2008). Nuclear migration during retinal development. *Brain Res* **1192**, 29-36.

**Cervantes, S., Yamaguchi, T. P. and Hebrok, M.** (2008). Wnt5a is essential for intestinal elongation in mice. *Dev Biol*.

**Chung, M. I., Nascone-Yoder, N. M., Grover, S. A., Drysdale, T. A. and Wallingford, J. B.** (2010). Direct activation of Shroom3 transcription by Pitx proteins drives epithelial morphogenesis in the developing gut. *Development* **137**, 1339-49.

**Croagh, D., Thomas, R. J., Phillips, W. A. and Kaur, P.** (2008). Esophageal stem cells--a review of their identification and characterization. *Stem Cell Rev* **4**, 261-8.

**Das, T., Payer, B., Cayouette, M. and Harris, W. A.** (2003). In vivo time-lapse imaging of cell divisions during neurogenesis in the developing zebrafish retina. *Neuron* **37**, 597-609.

**Dauca, M., Bouziges, F., Colin, S., Kedingler, M., Keller, M. K., Schilt, J., Simon-Assmann, P. and Haffen, K.** (1990). Development of the vertebrate small intestine and mechanisms of cell differentiation. *Int J Dev Biol* **34**, 205-18.

**de Santa Barbara, P., van den Brink, G. R. and Roberts, D. J.** (2003). Development and differentiation of the intestinal epithelium. *Cell Mol Life Sci* **60**, 1322-32.

**Dekaney, C. M., Bazer, F. W. and Jaeger, L. A.** (1997). Mucosal morphogenesis and cytodifferentiation in fetal porcine small intestine. *Anat Rec* **249**, 517-23.

**Dekaney, C. M., Fong, J. J., Rigby, R. J., Lund, P. K., Henning, S. J. and Helmrath, M. A.** (2007). Expansion of intestinal stem cells associated with long-term adaptation following ileocecal resection in mice. *Am J Physiol Gastrointest Liver Physiol* **293**, G1013-22.

**Dietz, M. L., Bernaciak, T. M., Vendetti, F., Kielec, J. M. and Hildebrand, J. D.** (2006). Differential actin-dependent localization modulates the evolutionarily conserved activity of Shroom family proteins. *J Biol Chem* **281**, 20542-54.

**Ewald, A. J., Brenot, A., Duong, M., Chan, B. S. and Werb, Z.** (2008). Collective epithelial migration and cell rearrangements drive mammary branching morphogenesis. *Dev Cell* **14**, 570-81.

**Haigo, S. L., Hildebrand, J. D., Harland, R. M. and Wallingford, J. B.** (2003). Shroom induces apical constriction and is required for hinge point formation during neural tube closure. *Curr Biol* **13**, 2125-37.

**Hashimoto, H., Ishikawa, H. and Kusakabe, M.** (1999). Development of vascular networks during the morphogenesis of intestinal villi in the fetal mouse. *Kaibogaku Zasshi* **74**, 567-76.

**Hayashi, S. and McMahon, A. P.** (2002). Efficient recombination in diverse tissues by a tamoxifen-inducible form of Cre: a tool for temporally regulated gene activation/inactivation in the mouse. *Dev Biol* **244**, 305-18.

**Hepker, J., Blackman, R. K. and Holmgren, R.** (1999). Cubitus interruptus is necessary but not sufficient for direct activation of a wing-specific decapentaplegic enhancer. *Development* **126**, 3669-77.

**Hildebrand, J. D.** (2005). Shroom regulates epithelial cell shape via the apical positioning of an actomyosin network. *J Cell Sci* **118**, 5191-203.

**Hildebrand, J. D. and Soriano, P.** (1999). Shroom, a PDZ domain-containing actin-binding protein, is required for neural tube morphogenesis in mice. *Cell* **99**, 485-97.

**Kim, B. M., Mao, J., Taketo, M. M. and Shivdasani, R. A.** (2007). Phases of canonical Wnt signaling during the development of mouse intestinal epithelium. *Gastroenterology* **133**, 529-38.

**Lee, C., Le, M. P. and Wallingford, J. B.** (2009). The shroom family proteins play broad roles in the morphogenesis of thickened epithelial sheets. *Dev Dyn* **238**, 1480-91.

**Lee, C., Scherr, H. M. and Wallingford, J. B.** (2007). Shroom family proteins regulate gamma-tubulin distribution and microtubule architecture during epithelial cell shape change. *Development* **134**, 1431-41.

**Levina, E. M., Kharitonova, M. A., Rovinsky, Y. A. and Vasiliev, J. M.** (2001). Cytoskeletal control of fibroblast length: experiments with linear strips of substrate. *J Cell Sci* **114**, 4335-41.

**Madara, J. L., Neutra, M. R. and Trier, J. S.** (1981). Junctional complexes in fetal rat small intestine during morphogenesis. *Dev Biol* **86**, 170-8.

**Mailleux, A. A., Overholtzer, M. and Brugge, J. S.** (2008). Lumen formation during mammary epithelial morphogenesis: insights from in vitro and in vivo models. *Cell Cycle* **7**, 57-62.

**Mathan, M., Moxey, P. C. and Trier, J. S.** (1976). Morphogenesis of fetal rat duodenal villi. *Am J Anat* **146**, 73-92.

**Matsumoto, A., Hashimoto, K., Yoshioka, T. and Otani, H.** (2002). Occlusion and subsequent re-canalization in early duodenal development of human embryos: integrated organogenesis and histogenesis through a possible epithelial-mesenchymal interaction. *Anat Embryol (Berl)* **205**, 53-65.

**Miyata, T.** (2008). Development of three-dimensional architecture of the neuroepithelium: role of pseudostratification and cellular 'community'. *Dev Growth Differ* **50 Suppl 1**, S105-12.

**Miyata, T., Kawaguchi, A., Okano, H. and Ogawa, M.** (2001). Asymmetric inheritance of radial glial fibers by cortical neurons. *Neuron* **31**, 727-41.

**Muzumdar, M. D., Tasic, B., Miyamichi, K., Li, L. and Luo, L.** (2007). A global double-fluorescent Cre reporter mouse. *Genesis* **45**, 593-605.

**Nishimura, T. and Takeichi, M.** (2008). Shroom3-mediated recruitment of Rho kinases to the apical cell junctions regulates epithelial and neuroepithelial planar remodeling. *Development* **135**, 1493-502.

**Picone, R., Ren, X., Ivanovitch, K. D., Clarke, J. D., McKendry, R. A. and Baum, B.** (2010). A polarised population of dynamic microtubules mediates homeostatic length control in animal cells. *PLoS Biol* **8**, e1000542.



**Plageman, T. F., Jr., Chung, M. I., Lou, M., Smith, A. N., Hildebrand, J. D., Wallingford, J. B. and Lang, R. A.** (2010). Pax6-dependent Shroom3 expression regulates apical constriction during lens placode invagination. *Development* **137**, 405-15.

**Saito, K., Kawaguchi, A., Kashiwagi, S., Yasugi, S., Ogawa, M. and Miyata, T.** (2003). Morphological asymmetry in dividing retinal progenitor cells. *Dev Growth Differ* **45**, 219-29.

**Saotome, I., Curto, M. and McClatchey, A. I.** (2004). Ezrin is essential for epithelial organization and villus morphogenesis in the developing intestine. *Dev Cell* **6**, 855-64.

**Sauer, F. C.** (1936). The Interkinetic migration of embryonic epithelial nuclei. *J Morphol.* **60**, 1-11.

**Sbarbati, R.** (1982). Morphogenesis of the intestinal villi of the mouse embryo: chance and spatial necessity. *J Anat* **135**, 477-99.

**Schenk, J., Wilsch-Brauninger, M., Calegari, F. and Huttner, W. B.** (2009). Myosin II is required for interkinetic nuclear migration of neural progenitors. *Proc Natl Acad Sci U S A* **106**, 16487-92.

**Smart, I. H.** (1972). Proliferative characteristics of the ependymal layer during the early development of the spinal cord in the mouse. *J Anat* **111**, 365-80.

**Sternlicht, M. D.** (2006). Key stages in mammary gland development: the cues that regulate ductal branching morphogenesis. *Breast Cancer Res* **8**, 201.

**Taylor, J., Chung, K. H., Figueroa, C., Zurawski, J., Dickson, H. M., Brace, E. J., Avery, A. W., Turner, D. L. and Vojtek, A. B.** (2008). The scaffold protein POSH regulates axon outgrowth. *Mol Biol Cell* **19**, 5181-92.

**Toofanian, F. and Targowski, S. P.** (1982). Morphogenesis of rabbit small intestinal mucosa. *Am J Vet Res* **43**, 2213-9.

**Toyota, T., Yamamoto, M. and Kataoka, K.** (1989). Light and electron microscope study on developing intestinal mucosa in rat fetuses with special reference to the obliteration of the intestinal lumen. *Arch Histol Cytol* **52**, 51-60.

**Tucker, A. S.** (2007). Salivary gland development. *Semin Cell Dev Biol* **18**, 237-44.

**Ueno, M., Katayama, K., Yamauchi, H., Nakayama, H. and Doi, K.** (2006). Cell cycle progression is required for nuclear migration of neural progenitor cells. *Brain Res* **1088**, 57-67.

**Villasenor, A., Wang, Z. V., Rivera, L. B., Ocal, O., Asterholm, I. W., Scherer, P. E., Brekken, R. A., Cleaver, O. and Wilkie, T. M.** (2010). Rgs16 and Rgs8 in embryonic endocrine pancreas and mouse models of diabetes. *Dis Model Mech* **3**, 567-80.

**Walker, J. L., Menko, A. S., Khalil, S., Rebustini, I., Hoffman, M. P., Kreidberg, J. A. and Kukuruzinska, M. A.** (2008). Diverse roles of E-cadherin in the morphogenesis of the submandibular gland: insights into the formation of acinar and ductal structures. *Dev Dyn* **237**, 3128-41.

**Wells, J. M. and Melton, D. A.** (1999). Vertebrate endoderm development. *Annu Rev Cell Dev Biol* **15**, 393-410.

**Yamada, M., Udagawa, J., Matsumoto, A., Hashimoto, R., Hatta, T., Nishita, M., Minami, Y. and Otani, H.** (2010). Ror2 is required for midgut elongation during mouse development. *Dev Dyn* **239**, 941-53.

**Zorn, A. M. and Wells, J. M.** (2009). Vertebrate endoderm development and organ formation. *Annu Rev Cell Dev Biol* **25**, 221-51.

## Chapter 3

### **Specialized divisions extend the apical surface of the intestinal lumen and direct the formation of villus structures**

#### **Abstract**

An important step in intestinal development is the remodeling of the epithelium into villi, the functional absorptive units of the intestine. The current accepted model for intestinal epithelial remodeling is that cell rearrangement and secondary lumen formation, in the context of a stratified epithelium, are required for proper villus development. However, we recently established that the intestinal epithelium is pseudostratified, and that secondary lumen formation does not occur. Thus, the mechanisms underlying luminal expansion and villus formation must be reevaluated. Here, we present data that support a new hypothesis: that luminal expansion is driven by a specialized cell division that delivers apical surface proteins to the cytokinetic furrow, a process we have termed an extending- (or e-) division. We show that, during a specific window of developmental time, Zona occludens (ZO-1) first localizes on both sides of the cytokinetic furrow, followed by delivery of apical protein atypical protein kinase C (aPKC) between the two daughter cells. E-divisions deposit the daughter cells onto two separate villi, effectively carving out the villi, while also extending the lumen.

## **Introduction**

The functional absorptive unit of the adult vertebrate intestine is a finger-like structure called a villus. A single layer of polarized, columnar epithelial cells covers the surface of each villus, protecting a mesenchymally-derived core that consists of blood vessels, nerves, muscle, fibroblasts and immune cells. Villi are first generated in fetal life, during a complex morphogenic remodeling process that begins at embryonic day (E)14.5 (Mathan et al., 1976). Prior to this time, the endodermally derived epithelial tube consists of a single layer of highly elongated and apicobasally (AB) polarized cells with a flat luminal surface (Grosse et al.). The cellular and molecular processes responsible for the dramatic remodeling of this epithelium to produce the villus structures are critical for the generation of a functional absorptive surface.

Multiple models of tube formation and tubular remodeling have been identified in various tissues [reviewed in (Andrew and Ewald, 2009)]. In the context of the intestine, the prevailing notion has been that the epithelium remodels via *de novo* polarization of stratified epithelial cells, coupled with rearrangement of these cells to form villi (Saotome, et al, 2004). Secondary lumina, islands of newly generated apical surface independent from the primary lumen, are thought to form within the deep stratified cell layers and subsequently connect with it to carve out the villi (Mathan et al., 1976). Evidence from several studies support this model. First, electron microscopic and freeze fracture studies document small lumina, apparently

unconnected to the primary lumen, that are surrounded by tight junctions and small cytoplasmic vesicles (some of which appear to be fusing with the secondary lumen) (Madara et al., 1981; Mathan et al., 1976). Second, analysis of mice deficient in Ezrin, an apical scaffolding protein, display connected villi, a phenotype posited to result from failure of proper polarization during secondary lumen expansion and coalescence (Saotome et al., 2004). Third, a genetic analysis of zebrafish gut tube organogenesis reveals that multiple small lumens converge to form a single primary lumen and identify some of the genes required for *de novo* polarization (Bagnat et al., 2007).

The models of intestinal lumen formation described above are based on the idea that the intestinal epithelium is stratified. However, in a recent study of fetal intestinal epithelial cell dynamics and polarity, we discovered that this epithelium is in fact pseudostratified, i.e., the majority of cells maintain contact with the basal and apical surfaces (Grosse et al.). Importantly, we demonstrated that this single layered, pseudostratified morphology is maintained throughout epithelial thickening between E12.5 and E14.5. Given this single layered constraint on epithelial morphology, the current model for intestinal morphogenesis, i.e., remodeling of a stratified epithelium to form secondary lumina, is not possible. However, two other potential models might explain intestinal remodeling: apical transformation (generation of apical surface at previously lateral domains) and apical expansion (further extension of the existing apical surface).

First, in a slight variation on the secondary lumen formation model, apical transformation would involve the *de novo* formation of apical domains at deep lateral surfaces between adjacent elongated epithelial cells, thus transforming the lateral domain into apical membrane. This model requires each cell to have, at least transiently, two apical surfaces; the original apical surface that touches the main lumen as well as a newly generated apical surface at a previously lateral domain. Cells with more than one apical domain are indeed the norm in the liver, where each cell may contribute to more than one apical bile canaliculus (Cohen et al., 2004; Cohen et al., 2007). This model would preserve the formation of *de novo* lumen as a mechanism for generation of the new apical surface.

A second possibility is that epithelial remodeling occurs by expansion of the primary lumen rather than by secondary lumen formation. If this apical expansion model is correct, then the so-called secondary lumina observable in TEM or histological sections are artifacts of the two dimensional analysis; each of these lumina would in fact be connected to the primary lumen at all times. Among known mechanisms for creating new apical surfaces is co-option of cytokinesis, a mechanism that is utilized in three dimensional (3D) cysts generated *in vitro* from intestinal epithelial CaCo2 cells (Jaffe et al., 2008). In this system, an “apical patch,” formed by the delivery of apical proteins to the cytokinetic furrow, is established at the first cell division, thus creating luminal identity. This process has also been observed in growing MDCK cysts and shown to require vesicular transport (Martin-Belmonte et al., 2007; Schluter and Margolis, 2009; Schluter et al., 2009). A relevant *in vivo* example of

apical surface generation *via* cytokinesis has been documented in the developing zebrafish neural keel, an epithelium that, like the intestinal epithelium, is pseudostratified (Ciruna et al., 2006; Tawk et al., 2007). As the left and right sides of the neural keel converge medially, a new apical surface is formed *via* specialized cell divisions called crossing (or c-) divisions. These divisions are so named because the dividing cell comes from one side of the neural tube, but the two resulting daughter cells are deposited with mirror symmetry, one on either side of the forming neural seam. C-divisions occur within a specific window of time, coinciding with the first appearance of apical surfaces, as identified by the apical marker Pard3.

Here, we identify specialized mitotic divisions that occur in a specific window of time during apical surface expansion in the mammalian intestine. We demonstrate that the apical markers ZO-1 and aPKC localize to the newly forming apical surface, at the cytokinetic furrow, segregating the two daughter cells to two different villi. Since these divisions result in the expansion of the apical surface, we name them extending (e)-divisions and propose that oriented e-divisions, rather than formation of *de novo* secondary lumina, provide the morphogenetic mechanism that controls villus emergence.

## **Results**

*Luminal surface does not extend by apical transformation.* The single-layered, pseudostratified intestinal epithelium challenges the previous theory that secondary lumina form between multiple stratified layers of cells (Madara et al.,

1981; Mathan et al., 1976; Moxey and Trier, 1979; Toyota et al., 1989; Trier and Moxey, 1979). Instead, the epithelium either transforms the lateral surface into apical, creating isolated pockets of lumen, or the lumen is expanded by apical extension defining new apical surface contiguous with the central lumen. In order to examine the isolated vs. connected structure of the lumen, vibratome sections of the intestine were stained for apical F-actin using phalloidin-488. In confocal z-stacks of E14.5 intestines, individual optical sections appear to contain isolated lumina, but examination of the entire z-stack reveals that the vast majority of luminal islands are in fact connected to the primary lumen (Fig. 3.1, arrows). Therefore, isolated lumina result from a plane of section artifact. No independent lumina were found, except at the extreme edges of the 100  $\mu\text{m}$  vibratome sections, where it was not possible to follow their connection to the main lumen. These findings rule out the possibility of apical transformation; the alternative morphogenetic mechanism of apical expansion was therefore examined.

*Luminal surface extends by apical expansion.* We first examined the earliest time points of intestinal remodeling after staining intestinal sections with the apical markers, aPKC and ZO-1, as well as E-cadherin (Ecad) to visualize cell outlines. As epithelial remodeling begins, it is possible to detect small branches of apical surface that appear to extend like cracks from the main lumen (Fig. 3.2A). We noted that mitotic figures often appeared to be associated with these cracks. Interestingly, in the intestine, as in all pseudostratified epithelia, mitotic cells are restricted to the apical surface (Baye and Link, 2008; Miyata, 2008). Since it has been demonstrated



that mitosis can be co-opted to create new apical surface, the appearance of these extending cracks near dividing cells was intriguing.

To quantitate the apparent association between mitotic cells and extending cracks, we analyzed the localization of phospho-HistoneH3 (pHH3) positive cells relative to the apical surface stained with aPKC in E14.5 intestines that are undergoing cracking (Fig 3.2A). Of the total apically localized pHH3-positive mitotic nuclei, 40% are found at the tip of a luminal extension, 15% are tip associated (within a 2-cell radius of the tip) and 45% are unassociated with the crack tip (Fig 3.2B-C). The luminal surface area of the crack tip is very small compared to the entire apical surface circumference; thus, the concentration of 60% of pHH3 nuclei at or near the extending luminal tip is striking. These data demonstrate that cell division is preferentially localized at extending apical surfaces and supports the idea that these dividing cells may be responsible for apical expansion during epithelial remodeling.

*Apical proteins localize to the cytokinetic furrow of dividing intestinal cells.* If apical surface is added at the cytokinetic furrow of these dividing cells, apical proteins should localize to the furrow in cells completing cytokinesis. The localization of apical proteins ZO-1, aPKC, and Crumbs3 (Crb3) as well as the localization of the midbody protein Acetylated  $\alpha$ -tubulin (Ac- $\alpha$ -tub), were analyzed in dividing cells of WT E14.5 intestine were analyzed. In the anaphase cycle of cell division at the beginning of the cracking stage, punctate ZO-1 on both sides of the cytokinetic furrow is the first indication of apical surface between the daughter cells (Fig. 3.3).

Interestingly, others had previously noted the sudden appearance (at E14.5) of long tight junctions between adjacent cells just prior to intestinal remodeling (Madara et al., 1981; Mathan et al., 1976). During anaphase, Crb3 and aPKC do not localize between the daughter cells at the cytokinetic furrow (Fig 3.3 A,F).

Analysis of E14.75 cells undergoing abscission revealed that the apical surface marker, aPKC, is expressed on both sides of the Ac- $\alpha$ -tub positive midbody (Fig. 3.4, arrow). The placing of apical surface between the two daughter cells puts them, by definition, on separate villi. These data support apical expansion and co-option of cytokinesis as the mechanism of luminal extension. Since mitosis localizes to the apical surface and delivers apical proteins to the cytokinetic furrow to extend the apical surface, these specialized divisions are termed e-divisions. For the lumen to extend in the proper direction, the cytokinetic furrow of the first e-division must be oriented perpendicular to the luminal slit while sequential e-divisions must be oriented parallel to the growing luminal crack. Future studies will examine if alterations in the axis and angle of cell division result in aberrant lumen expansion.

## **Discussion**

*A new model for intestinal remodeling.* We recently presented evidence that the mouse intestinal epithelium consists of a single layer of pseudostratified cells that maintain their polarity throughout the remodeling process (Grosse et al.). This finding itself rules out the most well accepted model of intestinal remodeling: that

the epithelium is stratified and uses cellular rearrangements to carve out the villi (Cervantes et al., 2008; Kim et al., 2007; Mathan et al., 1976; Saotome et al., 2004). Here, we examine two different remodeling models that are consistent with the single-layered nature of the intestine. The data indicate that the morphogenetic mechanism controlling luminal expansion in the intestine is cell division and reveal that e-divisions mediate luminal expansion.

In MDCK 3D cultures, the creation of a lumen between the first two cells of the cyst require endosomal Crb3, also termed the vacuolar apical compartment of VAC (Howe et al.), to be delivered to the cytokinetic furrow and fuse with the membrane during cell division to form a lumen between the daughter cells (Schluter et al., 2009; Vega-Salas et al., 1987). Cdc42, a RhoGTPase with an evolutionarily conserved function in cytoskeletal arrangement and cell polarity, is required in MDCK and CaCo2 cyst cultures to properly position the apical surface and to orient cell division (Bayless and Davis, 2002; Jaffe et al., 2008; Kamei et al., 2006; Rodriguez-Fraticelli et al., 2010). In conjunction with oriented division, Cdc42 is also required for exocytosis of VAC's in multiple systems (Bayless and Davis, 2002; Kamei et al., 2006; Malacombe et al., 2006; Martin-Belmonte et al., 2007). Small cytoplasmic vacuoles have also been noted at the intestinal epithelial junctions during lumen formation (Madara et al., 1981; Mathan et al., 1976). It will be important to test whether Cdc42 plays a role in proper lumen expansion by controlling vacuole exocytosis and oriented division in the intestine.

*Ezrin mutant intestines*. Improper localization of apical surface resulting in a multiple lumen phenotype was observed in the intestine of the *Ezrin* knockout mouse (Saotome et al., 2004). Ezrin is part of the ERM family of proteins, which include important scaffolding proteins. Ezrin is the only ERM protein expressed in the mouse intestine (Berryman et al., 1993; Ingraffea et al., 2002; Saotome et al., 2004). A striking aspect of the *Ezrin* null phenotype is the appearance of cellular bridges that connect adjacent villi; the villus connections separate islands of lumina, which apparently do not connect to the main lumen. Thus, the authors concluded that loss of Ezrin inhibited the process in which secondary lumina connect with the primary lumen (Saotome et al., 2004). However, in light of the both the pseudostratified intestinal epithelial cell shape and cell division as a mechanism for apical expansion, another explanation for fused villi in the *Ezrin* mutant could be failure to complete cytokinesis. In fact, in a recent high-throughput phenotypic screen of human genes involved in cell division, knockdown of *Ezrin* was found to cause a defect in metaphase alignment [(Neumann et al., 2010), [mitocheck.org](http://mitocheck.org)]. Since misoriented divisions in Caco2 and MDCK cultures also cause multiple lumen phenotypes, it will be important to examine the *Ezrin* mutant intestine for possible defects in cell division.

The e-divisions have other attributes that deserve further study. For example, these mitotic events require precise timing and alignment in order to carve out villi of regular size and shape. E-division is a highly regulated process that is not detected prior to E14.5, occurs for a short period of time to carve out the villi, and then is not

observed thereafter. These characteristics suggest that a specific, but short-lived molecular trigger is responsible for initiating these specialized cell divisions.

It is likely that spindle orientation in these cell divisions is also tightly controlled. One signaling pathway that might be involved in modulating these processes is planar cell polarity (PCP) signaling. Indeed, mutations in core PCP genes have been shown to disrupt spindle orientation in the stomach and kidney (Matsuyama et al., 2009; Saburi et al., 2008). Moreover, mutations in PCP components have also been shown to disrupt the analogous c-divisions during zebrafish neural keel formation (Ciruna et al., 2006; Tawk et al., 2007).

The identification of the e-division as the cellular driver of intestinal remodeling can be easily reconciled with previous morphological evidence (Madara et al., 1981; Mathan et al., 1976). The formation of specialized tight junctions and the observation of vesicular trafficking near lumina that appear to resemble canaliculi can all be attributed to the process of adding apical membrane at the cytokinetic furrow. The only aspect of the previous model that must be discarded is the formation of secondary lumina, which appear to represent artifacts of thin sectioning. Further investigation of the molecules that pattern and orient e-divisions, and the triggers that induce them are important future goals.

## **Materials and Methods**

### *Mice*

Embryonic tissues were obtained from C57BL6/J (Jackson Labs 000664). The morning of vaginal plug was recorded as day E0.5.

### *Tissue preparation*

Tissues were fixed 1 hour to overnight in 4% paraformaldehyde and prepared for paraffin or agarose embedding. For paraffin, tissue was rinsed with PBS, dehydrated in ethanol, and infused with paraffin. Agarose samples were rinsed in 1x PBS and embedded in 7% low melt agarose. Paraffin blocks were sectioned at 5  $\mu\text{m}$  and agarose embedded tissue was vibratome sectioned at 100  $\mu\text{m}$ . Sections were stained and imaged on an Olympus FluoView 500 laser scanning confocal microscope or Nikon eclipse E800 widefield fluorescent microscope.

### *Immunostaining*

Sections were deparaffinized in xylene, rehydrated, washed with PBS, and boiled in 10mM sodium citrate at pH=6 for antigen retrieval. Sections were incubated for 30 minutes in blocking buffer (1% BSA, 10% goat serum, and 0.3% Triton X-100 in TBS). Primary antibodies (details below) were diluted in blocking buffer and incubated overnight at 4°C. Molecular Probes Alexafluor conjugated secondary antibodies (Invitrogen; 1:1000; 488, 568, 647) with 10  $\mu\text{g}/\text{mL}$  Hoechst (Invitrogen) were diluted in blocking buffer for 30 minutes at RT; slides were mounted with Prolong Gold (Invitrogen).

Vibratome sections were permeabilized in 0.5% Triton X-100 in PBS, blocked (4% goat serum and 0.1% Tween 20 in PBS), incubated with primary antibody at 4°C overnight, incubated with Molecular Probes Alexafluor conjugated secondary antibodies (Invitrogen;1:1000) and 10ug/mL Hoechst (Invitrogen) for 45 minutes at RT, and mounted with Prolong Gold between two glass coverslips. Images were obtained on an Olympus FluoView 500 laser scanning confocal microscope.

### *Antibodies*

Ac- $\alpha$ -tub (Sigma T7451, 1:100, primary incubated at 37°C). Crb3 (Dr. Ben Margolis, 1:5000), Ecad (Invitrogen ECCD2 13-1900, 1:1000), Ecad (BD 610181, 1:1000), Phalloidin-488 (Molecular Probes A12379, 1:50), pHH3 (Millipore 6-570, 1:400), pHH3 (Millipore 05-806; 1:200), PKC $\zeta$  (aPKC; Santa Cruz sc-216, 1:500), ZO-1 (Invitrogen 33-9100; 1:1000).

### **Acknowledgements**

This work will be part of a paper designed for submission later this year. Significant intellectual and experimental input from Mark F. Pressprich contributed greatly to this work. The authors are also grateful for excellent technical assistance provided by Chris Edwards, Shelley Almburg, Dotty Sorenson, and Sasha Meshinchi in the Microscopy and Image Analysis Laboratory as well as Marta Dzaman and Maria Ripberger in the Organogenesis Morphology Core at the University of Michigan.

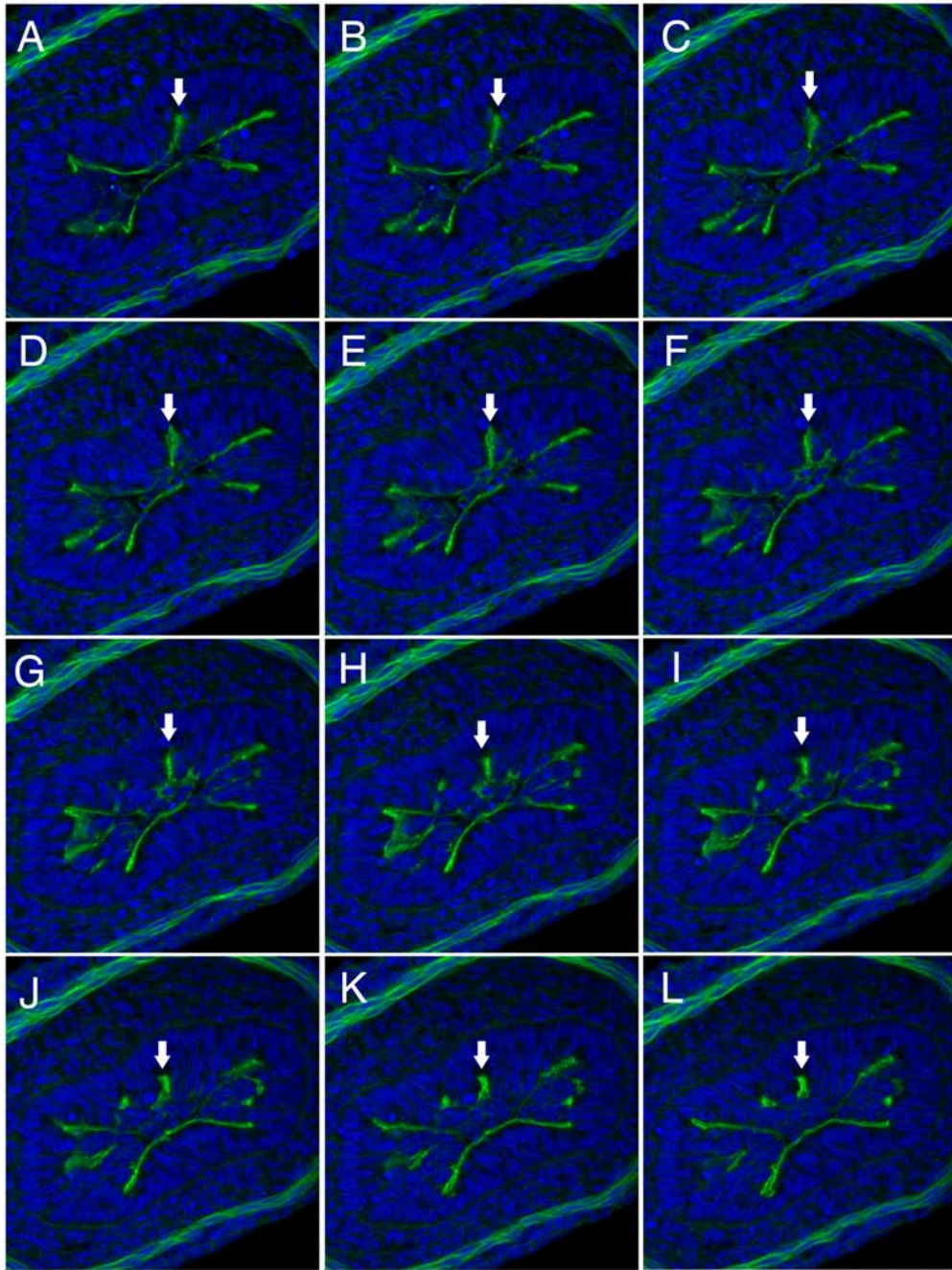


**Figure 3.1. Lumina are connected.** A-L) Intestinal vibratome sections stained with phalloidin (green) and DAPI (blue). Individual 1  $\mu\text{m}$  consecutive slices from a confocal z-stack are shown. The arrows identify an apparently isolated lumen (J-K) that connects to the main lumen in a different plane (A-C).



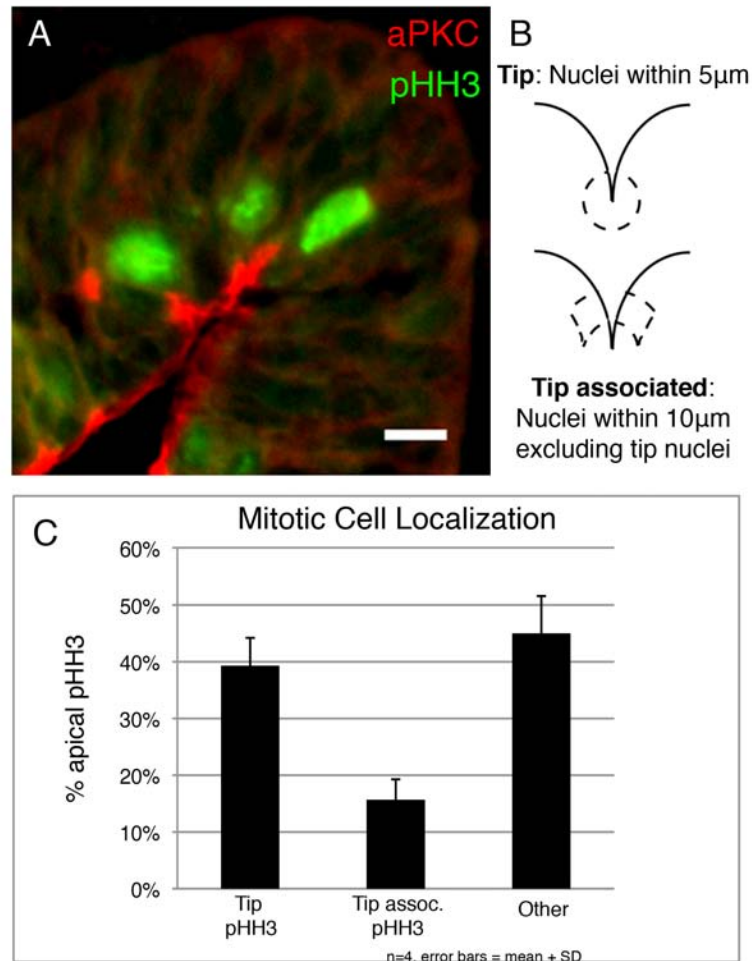


**Figure 3.2. At E14.5, pHH3 positive nuclei localize to the tips of forming luminal cracks.** A) Consecutive paraffin sections were stained with pHH3 (green) and aPKC (red) and z-stacks were imaged. B-C) Optical slices from 10 consecutive 6 $\mu$ m paraffin sections and were analyzed and apical pHH3 positive cells were quantified as crack tip, tip associated, or unassociated. n=4 different intestines, 20 separate z-stacks. Error bars = S.D. Panels A-C were obtained by Mark Pressprich.

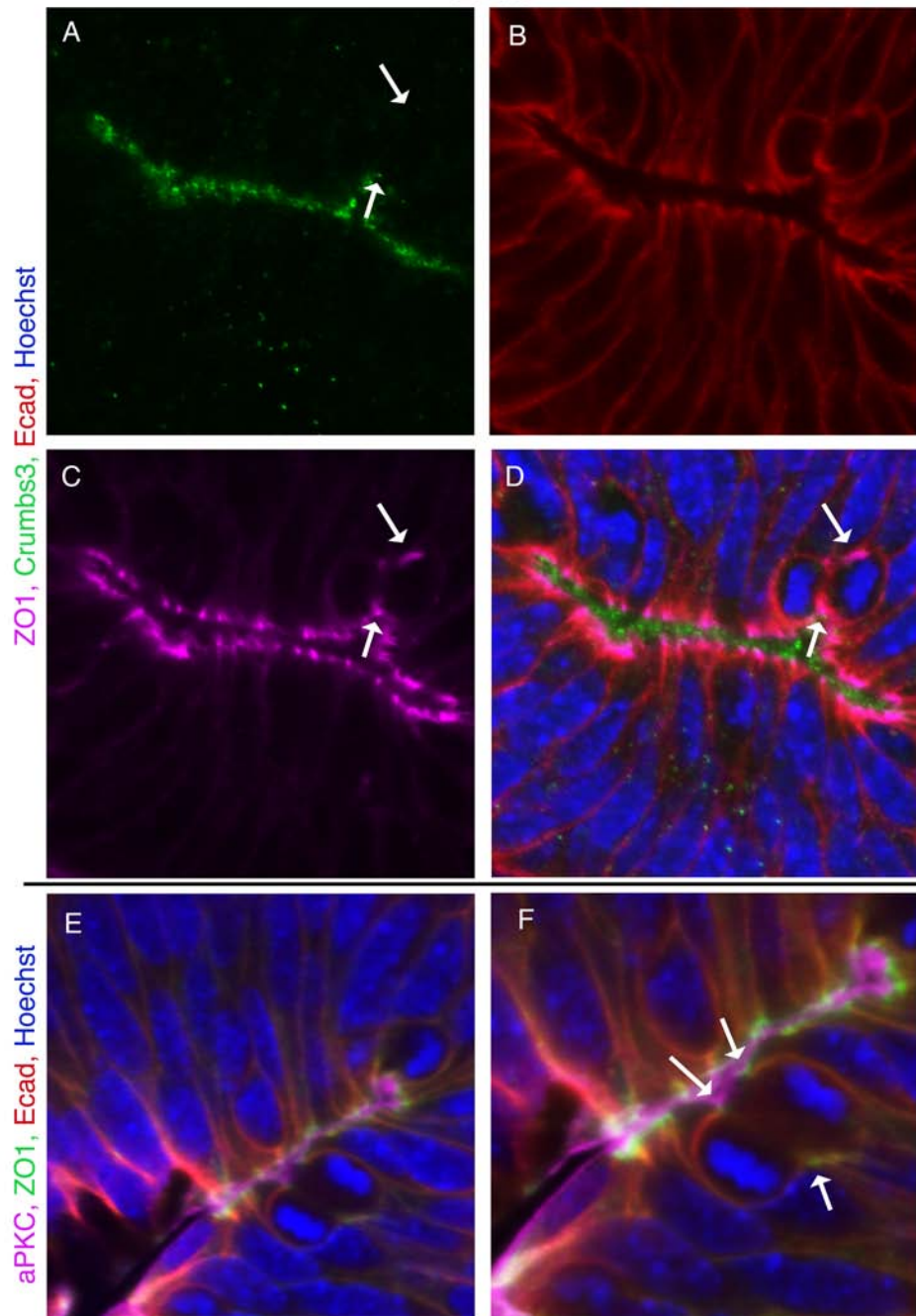


**Figure 3.3. ZO-1 is the first apical marker during cell division.** A-F) Intestinal paraffin section with a dividing cell in anaphase. ZO-1 marks both ends of the cytokinetic furrow (arrows) A-D) Sections are stained for Hoechst (blue), Crb3 (green), Ecad (red), and ZO-1 (pink). E-F) Sections are stained for Hoechst (blue), ZO-1 (green), Ecad (red), and aPKC (pink).

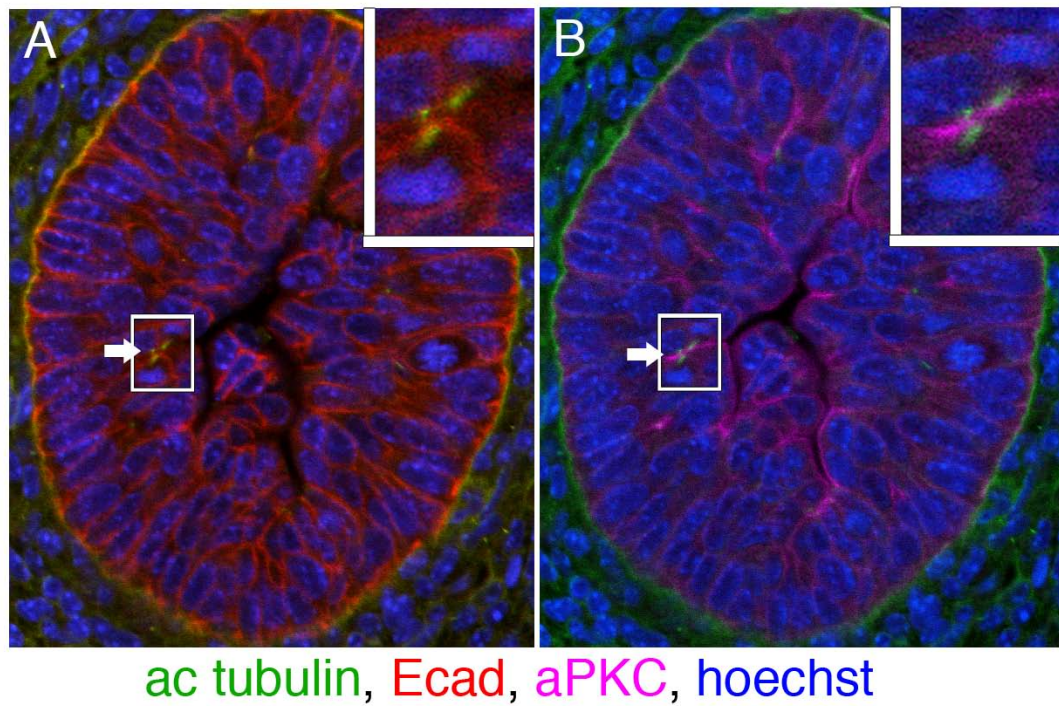


**Figure 3.4. Apical proteins localize to the cytokinetic furrow.** A-B) During abscission, apical protein aPKC (pink) localizes to the cytokinetic furrow and through the acetylated tubulin stained midbody (green) of the telophase cell. Ecad (red), Hoechst (blue). Panels A and B were obtained by Mark Pressprich.

## **Literature Cited**

- Andrew, D. J. and Ewald, A. J.** (2009). Morphogenesis of epithelial tubes: Insights into tube formation, elongation, and elaboration. *Dev Biol*.
- Bagnat, M., Cheung, I. D., Mostov, K. E. and Stainier, D. Y.** (2007). Genetic control of single lumen formation in the zebrafish gut. *Nat Cell Biol* **9**, 954-60.
- Baye, L. M. and Link, B. A.** (2008). Nuclear migration during retinal development. *Brain Res* **1192**, 29-36.
- Bayless, K. J. and Davis, G. E.** (2002). The Cdc42 and Rac1 GTPases are required for capillary lumen formation in three-dimensional extracellular matrices. *J Cell Sci* **115**, 1123-36.
- Berryman, M., Franck, Z. and Bretscher, A.** (1993). Ezrin is concentrated in the apical microvilli of a wide variety of epithelial cells whereas moesin is found primarily in endothelial cells. *J Cell Sci* **105 ( Pt 4)**, 1025-43.
- Cervantes, S., Yamaguchi, T. P. and Hebrok, M.** (2008). Wnt5a is essential for intestinal elongation in mice. *Dev Biol*.
- Ciruna, B., Jenny, A., Lee, D., Mlodzik, M. and Schier, A. F.** (2006). Planar cell polarity signalling couples cell division and morphogenesis during neurulation. *Nature* **439**, 220-4.
- Cohen, D., Brennwald, P. J., Rodriguez-Boulan, E. and Musch, A.** (2004). Mammalian PAR-1 determines epithelial lumen polarity by organizing the microtubule cytoskeleton. *J Cell Biol* **164**, 717-27.
- Cohen, D., Tian, Y. and Musch, A.** (2007). Par1b promotes hepatic-type lumen polarity in Madin Darby canine kidney cells via myosin II- and E-cadherin-dependent signaling. *Mol Biol Cell* **18**, 2203-15.
- Grosse, A. S., Pressprich, M. F., Curley, L. B., Margolis, B., Hildebrand, J. D. and Gumucio, D. L.** (2011). Cell dynamics in fetal intestinal epithelium: implications for intestinal growth and morphogenesis. *Development, In revision*.
- Howe, J. R., Sayed, M. G., Ahmed, A. F., Ringold, J., Larsen-Haidle, J., Merg, A., Mitros, F. A., Vaccaro, C. A., Petersen, G. M., Giardiello, F. M. et al.** (2004). The prevalence of MADH4 and BMPR1A mutations in juvenile polyposis and absence of BMPR2, BMPR1B, and ACVR1 mutations. *J Med Genet* **41**, 484-91.
- Ingraffea, J., Reczek, D. and Bretscher, A.** (2002). Distinct cell type-specific expression of scaffolding proteins EBP50 and E3KARP: EBP50 is generally expressed with ezrin in specific epithelia, whereas E3KARP is not. *Eur J Cell Biol* **81**, 61-8.
- Jaffe, A. B., Kaji, N., Durgan, J. and Hall, A.** (2008). Cdc42 controls spindle orientation to position the apical surface during epithelial morphogenesis. *J Cell Biol* **183**, 625-33.
- Kamei, M., Saunders, W. B., Bayless, K. J., Dye, L., Davis, G. E. and Weinstein, B. M.** (2006). Endothelial tubes assemble from intracellular vacuoles in vivo. *Nature* **442**, 453-6.
- Kim, B. M., Mao, J., Taketo, M. M. and Shivdasani, R. A.** (2007). Phases of canonical Wnt signaling during the development of mouse intestinal epithelium. *Gastroenterology* **133**, 529-38.

**Madara, J. L., Neutra, M. R. and Trier, J. S.** (1981). Junctional complexes in fetal rat small intestine during morphogenesis. *Dev Biol* **86**, 170-8.

**Malacombe, M., Ceridono, M., Calco, V., Chasserot-Golaz, S., McPherson, P. S., Bader, M. F. and Gasman, S.** (2006). Intersectin-1L nucleotide exchange factor regulates secretory granule exocytosis by activating Cdc42. *EMBO J* **25**, 3494-503.

**Martin-Belmonte, F., Gassama, A., Datta, A., Yu, W., Rescher, U., Gerke, V. and Mostov, K.** (2007). PTEN-mediated apical segregation of phosphoinositides controls epithelial morphogenesis through Cdc42. *Cell* **128**, 383-97.

**Mathan, M., Moxey, P. C. and Trier, J. S.** (1976). Morphogenesis of fetal rat duodenal villi. *Am J Anat* **146**, 73-92.

**Matsuyama, M., Aizawa, S. and Shimono, A.** (2009). Sfrp controls apicobasal polarity and oriented cell division in developing gut epithelium. *PLoS Genet* **5**, e1000427.

**Miyata, T.** (2008). Development of three-dimensional architecture of the neuroepithelium: role of pseudostratification and cellular 'community'. *Dev Growth Differ* **50 Suppl 1**, S105-12.

**Moxey, P. C. and Trier, J. S.** (1979). Development of villus absorptive cells in the human fetal small intestine: a morphological and morphometric study. *Anat Rec* **195**, 463-82.

**Neumann, B., Walter, T., Heriche, J. K., Bulkescher, J., Erfle, H., Conrad, C., Rogers, P., Poser, I., Held, M., Liebel, U. et al.** (2010). Phenotypic profiling of the human genome by time-lapse microscopy reveals cell division genes. *Nature* **464**, 721-7.

**Rodriguez-Fraticelli, A. E., Vergarajauregui, S., Eastburn, D. J., Datta, A., Alonso, M. A., Mostov, K. and Martin-Belmonte, F.** (2010). The Cdc42 GEF Intersectin 2 controls mitotic spindle orientation to form the lumen during epithelial morphogenesis. *J Cell Biol* **189**, 725-38.

**Saburi, S., Hester, I., Fischer, E., Pontoglio, M., Eremina, V., Gessler, M., Quaggin, S. E., Harrison, R., Mount, R. and McNeill, H.** (2008). Loss of Fat4 disrupts PCP signaling and oriented cell division and leads to cystic kidney disease. *Nat Genet* **40**, 1010-5.

**Saotome, I., Curto, M. and McClatchey, A. I.** (2004). Ezrin is essential for epithelial organization and villus morphogenesis in the developing intestine. *Dev Cell* **6**, 855-64.

**Schluter, M. A. and Margolis, B.** (2009). Apical Lumen Formation in Renal Epithelia. *J Am Soc Nephrol*.

**Schluter, M. A., Pfarr, C. S., Pieczynski, J., Whiteman, E. L., Hurd, T. W., Fan, S., Liu, C. J. and Margolis, B.** (2009). Trafficking of Crumbs3 during cytokinesis is crucial for lumen formation. *Mol Biol Cell* **20**, 4652-63.

**Tawk, M., Araya, C., Lyons, D. A., Reugels, A. M., Girdler, G. C., Bayley, P. R., Hyde, D. R., Tada, M. and Clarke, J. D.** (2007). A mirror-symmetric cell division that orchestrates neuroepithelial morphogenesis. *Nature* **446**, 797-800.

**Toyota, T., Yamamoto, M. and Kataoka, K.** (1989). Light and electron microscope study on developing intestinal mucosa in rat fetuses with special reference to the obliteration of the intestinal lumen. *Arch Histol Cytol* **52**, 51-60.

**Trier, J. S. and Moxey, P. C.** (1979). Morphogenesis of the small intestine during fetal development. *Ciba Found Symp*, 3-29.

**Vega-Salas, D. E., Salas, P. J. and Rodriguez-Boulan, E.** (1987). Modulation of the expression of an apical plasma membrane protein of Madin-Darby canine kidney epithelial cells: cell-cell interactions control the appearance of a novel intracellular storage compartment. *J Cell Biol* **104**, 1249-59.

## Chapter 4

### The role of *Wnt5a* and PCP genes in intestinal lengthening and villus formation

#### Abstract

Adequate absorption of nutrients by the intestine requires an extensive epithelial absorptive surface. During embryonic development, this surface is generated by the formation of intestinal villi and by elaboration of remarkable intestinal length. Mice null for *Wnt5a* exhibit very short intestines and it has been proposed that this is due to aberrant radial intercalation movements, a planar cell polarity defect. Here, we re-examine the mechanisms underlying gut lengthening in wild type and *Wnt5a* null intestines, in light of new evidence that the intestinal epithelium is pseudostratified and therefore does not undergo radial intercalation. At E14.5, *Wnt5a* null intestines exhibit disorganized epithelium with misoriented nuclei. Patterns of INM that characterize the pseudostratified epithelium of WT mice are altered in *Wnt5a*  $-/-$  epithelium. Villi in *Wnt5a* null intestines are misshapen and display aberrant Golgi localization. Furthermore, mice deficient in the PCP genes *Vangl2* and *Fat4* also display a short gut phenotype and *Wnt5a* $^{-/-}$ , *Vangl2* $^{-/-}$ , *Fat4* $^{-/-}$ , and *Vangl2* $^{-/+};Wnt5a$  $^{-/-}$  mice all exhibit epithelial disorganization, with ectopic cells. Data on length and villus organization suggest that genetic interactions exist between these genes,

Mechanistically, we tie lengthening defects to perturbation of INM movements and speculate that misshapen villi are due to misoriented cell divisions during intestinal remodeling.

## **Introduction**

The intestine is highly specialized to carry out its main function, the absorption of nutrients. Since absorption occurs at the membrane surface of intestinal epithelial cells, an enormous epithelial surface area is critical. To generate this surface, the mucosa is formed into villi, fingerlike projections that represent the functional unit of absorption, and the intestinal organ itself grows to an impressive length (nearly 25 feet in the human). Diseases that compromise villus structure (e.g., Celiac disease, an inflammatory reaction to dietary gluten that results in loss of villi) or significantly reduced intestinal length (e.g., short bowel syndrome) can result in malabsorption (Goulet and Ruemmele, 2006). Despite the critical importance of appropriate surface area to absorptive function, the cellular control of villus formation and the molecular mechanisms that generate intestinal length are poorly understood.

Wnt ligands comprise a large family of secreted glycoproteins that are responsible for tissue patterning, cell fate, and cell proliferation that fall into two broad classes: canonical and noncanonical. Canonical Wnts signal through Frizzled (Visel et al.) receptors to inhibit a  $\beta$ -catenin ( $\beta$ -cat) destruction complex, allowing translocation of  $\beta$ -cat to the nucleus, where it can interact with Tcf/Lef transcription factors to



activate target gene transcription [reviewed in (Clevers and van de Wetering, 1997; Gordon and Nusse, 2006)]. Canonical Wnt signaling is often associated with cell proliferation and not surprisingly, with many cancers. In contrast, non-canonical Wnts signal instead through  $\beta$ -catenin-independent pathways to alter morphogenetic movements [reviewed in (Wallingford et al., 2002)]. Canonical and non-canonical pathways were originally described as two separate pathways, but additional studies demonstrate that non-canonical Wnts can both activate and inhibit the canonical signaling pathway (Cha et al., 2008; Mikels and Nusse, 2006). Reciprocal repression between canonical and non-canonical Wnts may depend upon competition for Fz binding at the cell surface (Grumolato et al., 2010).

Wnt5a was originally identified as part of the noncanonical pathway because its role in elongation in *Xenopus* was distinct and had no effect on canonical Wnt – dependent cell differentiation (Moon et al., 1993; Ungar et al., 1995). Body axis elongation occurs when multiple layers of cells mediolaterally converge and intercalate to convert a short, fat organism into an extended long, thin embryo; hence these movements are termed convergent extension (CE). In *Xenopus*, zebrafish, and mice, defects in non-canonical Wnt ligands, Wnt5a and Wnt11, alter CE movements and consequently disturb AP axis elongation (Djiane et al., 2000; Heisenberg et al., 2000; Kilian et al., 2003; Moon et al., 1993; Yamaguchi et al., 1999). *Wnt5a* mouse mutants display general outgrowth defects of multiple structures including the limbs, tail, and snout (Yamaguchi et al., 1999), suggesting that a common Wnt5a-dependent morphogenetic mechanism links axis and organ-

specific elongation. Accordingly, non-canonical Wnt5a is required for a variety of cellular processes associated with morphogenesis and metastasis including cell migration (Dissanayake et al., 2008; Hardy et al., 2008; He et al., 2008; Jonsson and Andersson, 2001; Kim et al., 2005; Kurayoshi et al., 2006; Nomachi et al., 2008; Safholm et al., 2008; Schlessinger et al., 2007), cell polarity (Montcouquiol et al., 2006; Witze et al., 2008), tubulogenesis (Loscertales et al., 2008), and tubular branching (Allgeier et al., 2008; Huang et al., 2009; Roarty and Serra, 2007).

Interestingly, *Wnt5a* null mice also have very short intestines with increased width (Cervantes et al., 2008). To examine the cellular mechanisms underlying the short gut phenotype, Cervantes *et al.* tracked cells by labeling S-phase nuclei in E11.5 intestinal epithelium with a Bromodeoxyuridine (BrdU) pulse followed by a chase of thymidine. In this experiment, BrdU labeled nuclei accumulate at the lumen in *Wnt5a* null intestines as compared to the mixture of labeled and unlabeled nuclei throughout the epithelium in the wild type. Building on the classical studies that the intestinal epithelium is stratified (Mathan et al., 1976; Moxey and Trier, 1979; Toyota et al., 1989; Trier and Moxey, 1979), the authors put forth the model that the luminal BrdU positive nuclei in the mutant are cells that transiently delaminated to divide, but failed to re-intercalate into the basal layer. In opposition to this interpretation, we recently demonstrated that the intestinal epithelium is not stratified. Rather, at all times during early development, the intestinal epithelium is a single, pseudostratified layer that maintains junctions and polarity during remodeling (Grosse et al., 2011). The fact that intestinal epithelium, like other

pseudostratified epithelia, undergoes interkinetic nuclear migration (INM) may explain the BrdU labeling results of Cervantes *et al.* That is, in INM, nuclei move from the basal surface (where they synthesize DNA) to the apical surface (where they undergo mitosis) in a continuous manner. Thus, the presence of excess BrdU-labeled cells at the luminal surface may represent defects in INM movements rather than aberrant re-intercalation of post-mitotic cells. This means that the shortened intestines of *Wnt5a* null mice cannot be explained by defective radial intercalation as proposed (Cervantes *et al.*, 2008). However, given the other outgrowth defects in these mice and the previously demonstrated involvement of *Wnt5a* in planar cell polarity (PCP) signaling, the observed gut phenotype may still be connected to PCP signaling in some manner.

The PCP pathway was discovered in *Drosophila* and controls the coordination of cellular polarization within a plane of tissue. For example, PCP signaling is required to orient actin-rich hairs on the *Drosophila* wing and to properly organize the photoreceptors of the complex eye (Gubb and Garcia-Bellido, 1982; Lawrence and Shelton, 1975). In *Drosophila*, two arms of the PCP pathway have been identified: a *Frizzled*-dependent core PCP signaling pathway and a *Fat*-dependent *Fat/Dachsous* (*Ds*; mammalian orthologue is *Dsch1*) pathway (McNeill, 2009). The core PCP genes are involved broadly in multiple tissue types and include *Frizzled* (Visel *et al.*), a seven-pass transmembrane receptor; *Dishevelled* (*Dsh*, mammalian orthologue is *Dvl*), a cytoplasmic signaling protein; *Strabismus* or *van Gogh* (*Vang*), membrane proteins; *Flamingo*, a membrane protein with cadherin like domains; and *Prickle*, a

cytoplasmic protein. The *Fat/Ds* PCP genes include the large cadherins *Fat* and *Ds* along with the Golgi-associated kinase, four jointed (*Fj*; mammalian orthologue is *Fjx1*). In *Drosophila*, *Ds* and *Fat* also participate in the *Hippo* pathway, a transcriptional signaling pathway that controls organ size [reviewed in (Halder and Johnson, 2011)].

In vertebrates, the PCP pathway controls the morphogenetic movements of CE, apical constriction, cell shape, and migration (Chen et al., 2003; Habas et al., 2001; He et al., 2008; Kawasaki et al., 2007; Kilian et al., 2003; Kim et al., 2005; Loscertales et al., 2008; Nomachi et al., 2008; Oishi et al., 2003; Schambony and Wedlich, 2007; Witze et al., 2008). The non-canonical Wnt ligands (*Wnt5a* and *Wnt11*) signal through *Ror2*, a receptor tyrosine kinase, or several of the Fz receptors (*Fz2*, *Fz3*, *Fz4* and *Fz7*), to activate downstream Wnt/PCP. PCP orthologues (*Vangl2*, *Fz*, *Fat4*) regulate similar phenotypes to *Drosophila* PCP, including stereocilia actin bundle orientation and mouse fur patterns as well as unique phenotypes such as axis elongation [reviewed in (McNeill; Simons and Mlodzik, 2008)]. In addition, loss of *Wnt5a*, *Vangl2*, or *Fat4* alone causes the classical vertebrate PCP phenotypic defect of disorganized stereocilia of the mouse inner ear (Montcouquiol et al., 2003; Qian et al., 2007; Saburi et al., 2008). Complete loss of either *Wnt5a* or *Vangl2* also perturbs CE during axis elongation (Goto and Keller, 2002; Heisenberg et al., 2000; Kilian et al., 2003; Moon et al., 1993; Tada and Smith, 2000; Yamaguchi et al., 1999).

Interactions among the Wnt, PCP, and Fat PCP pathways are just beginning to be studied. Genetic interactions between *Wnt5a* and *Vangl2* are revealed by increased severity of stereocilia disorganization and cochlear shortening in the mouse inner ear in mice deficient for both proteins (Qian et al., 2007). Additionally, genetic interactions between *Fat4* and *Vangl2* have been demonstrated to control oriented cell division in the mouse kidney (Saburi et al., 2008). Tubule lengthening requires properly oriented mitotic spindle poles, and in *Fat4/Vangl2* double mutants, kidneys are smaller and tubules are wider, resulting in cysts similar to those seen in polycystic kidney disease (Saburi et al., 2008).

It is striking that shortened intestines have been observed in mice null for *Wnt5a* (Cervantes et al., 2008), *Fat4* (Mao et al., 2011), *Dchs* (Mao et al., 2011), and *Ror2* (Yamada et al., 2010). It is not clear whether these proteins act in separate but parallel pathways or whether they genetically interact to control morphogenetic mechanisms of PCP and gut length. Moreover, since the short intestinal phenotype of *Wnt5a* null mice is NOT the result of perturbed radial intercalation, the mechanism underlying this interesting phenotype in *Wnt5a*<sup>-/-</sup> animals (as well as in the other mutants with short guts) remains obscure.

This chapter represents our initial investigations of these questions. We evaluate mouse intestinal lengthening between embryonic day (E)12.5 and E18.5 and define a rapid growth phase between E14.5 and E16.5, coinciding with intestinal remodeling and villus formation. This accelerated growth phase is diminished in

*Wnt5a* null animals, and we present preliminary evidence that INM is perturbed in this model. We also show that *Wnt5a* is required for intestinal epithelial intracellular polarity and epithelial cell organization between E14.5 and E16.5. Finally, examination of the cellular phenotype in E16.5 *Fat4* deficient mice reveals disorganized villi and improperly localized cells, similar to those seen in the *Wnt5a* null animals. Thus, preliminary data that suggest that *Wnt5a* may genetically interact in the same pathway as *Fat4* and *Vangl2* during intestinal elongation. Based on these preliminary studies, we posit that *Wnt5a* interacts with both core and Fat-dependent PCP signaling pathways to control epithelial cell dynamics during epithelial remodeling and gut lengthening.

## Results

*The Wnt5a deficient mouse.* Our analysis of the *Wnt5a* knockout mouse confirmed many of the published findings (Cervantes et al., 2008; Yamaguchi et al., 1999). Mutant mice display generalized outgrowth defects of the body axis, snout, and limbs (Fig. 4.1A). Similarly, the *Wnt5a* mutant intestine exhibits shortened length in addition to a midgut tubular duplication, truncated colon, and an imperforate anus as early as E10.5 (Fig. 4.1B-D). The short gut phenotype persists until birth, at which time the embryo is not viable. Cervantes *et al.* reported epithelial thickening and defective radial intercalation at E11.5 as the sole explanation for the short gut phenotype of the *Wnt5a* mutant (Cervantes et al., 2008). No additional epithelial defects were reported after E11.5, but we present here an in depth examination of the *Wnt5a*<sup>-/-</sup> model that does indeed reveal unique phenotypes after E11.5.

*Intestinal elongation.* Though *Wnt5a* null intestines are dramatically shortened, it is not clear when during development this length deficit actually occurs. Therefore, we carefully analyzed the growth of *Wnt5a* null intestines compared to WT littermates between E12.5 and E18.5. Intestinal length was measured from the proximal duodenum through the distal ileum. In WT animals three separate phases of growth were observed (Fig. 4.1B), including two slower growth phases separated by an accelerated phase.

The first slow lengthening phase takes place between E12.5 and E14.5, a developmental period associated with epithelial thickening caused by apicobasal (AB) lengthening and dense packing of the pseudostratified cells (Grosse et al., 2011). The accelerated growth in length occurs between E14.5 and E16.5. Histologically, this rapid phase corresponds to intestinal epithelial remodeling and villus formation, a process that begins in the proximal E14.5 intestine and proceeds distally in a wave-like fashion. Finally, a second slow phase of lengthening accompanies further growth of the villi after E16.5. Strikingly, the *Wnt5a* deficient intestine is shorter at all time points examined. Though growth is nearly constant, the *Wnt5a* null intestine lacks the accelerated lengthening phase between E14.5 and 16.5, suggesting that the morphogenetic changes at this time are particularly important for AP lengthening.

*Wnt5a expression in the intestine.* *Wnt5a* is reportedly expressed in the mesenchyme as determined from whole mount *in situ* analysis of the small intestine (Lickert et al., 2001; Yamaguchi et al., 1999), but expression at the cellular level will provide a better clue to the function of *Wnt5a*. To determine the cellular localization of *Wnt5a* between E12.5 and E16.5, *Wnt5a* transcripts were identified by *in situ* hybridization (Fig. 4.2). At E12.5 (Fig. 4.2A) and E14.5 (Fig. 4.2B), *Wnt5a* mRNA localizes diffusely throughout mesenchymal cells adjacent to the epithelium. By E15.5 (Fig. 4.2C) and E16.5 (Fig. 4.2D), however, a dynamic change in expression compartmentalizes *Wnt5a* mRNA to discrete clusters of mesenchymal cells that are associated with the growing villi. These clusters are believed to be important signaling centers responsible for epithelial/mesenchymal signaling during villus formation (Karlsson et al., 2000). Thus, a dynamic change in *Wnt5a* expression coincides with villus formation and length generation, suggesting that the *Wnt5a* ligand may be a crucial mesenchymal signal that is required for both processes.

*Epithelial disorganization in mice lacking Wnt5a.* In order to investigate the role of *Wnt5a* in villus organization, we examined *Wnt5a* null mice at E16.5. Normally, villi evaginate into the lumen in an evenly spaced, sized, and organized pattern as shown by scanning electron microscopy (SEM), whole mount, and hematoxylin and eosin (H&E) in WT intestines (Fig 4.3A-C). The villi of *Wnt5a* null mice, however, are disorganized and vary drastically in size and spacing (Fig. 4.3D-F). For example, in Figure 3D, a large, irregular villus occupies the majority of the field and is surrounded by a crowd of small asymmetric villi. The distorted villi are also



apparent in whole mount preparations (Fig. 4.3E). Upon histological analysis, *Wnt5a* deficient villi were misshapen and branched (Fig. 4.3F).

To investigate the possible basis for the disorganized villus phenotype, we examined the epithelial organization of *Wnt5a*<sup>-/-</sup> mice prior to villus emergence. At E14.5, the WT intestinal epithelium is made up of tall, pseudostratified cells that stretch from the apical to the basal surface (Grosse et al., 2011). The long axes of the nuclei in the WT epithelium are radially oriented towards the center of the gut tube (Fig 4.3D); nuclei closest to the basement membrane are uniform in size, shape, and orientation. In *Wnt5a* null epithelium, however, nuclei are disorganized and misoriented (Fig 4.3H). Mutant nuclei in histological sections are varied in shape and size, likely corresponding to their altered orientation in three dimensional space.

The misoriented nuclei at E14.5 and the disorganized villi at E16.5 may represent a general epithelial polarity defect. Epithelial intracellular polarity and organelle localization of the nucleus, Golgi, and centrosomes are controlled by the microtubule cytoskeletal network [reviewed in (Bornens, 2008; Thyberg and Moskalewski, 1999)]. Epithelial AB polarity is maintained by directed protein sorting in the Golgi to either the apical or basolateral plasma membrane by traveling along the AB polarized microtubules (Ku et al., 1999; Mogensen et al., 2002; Rodriguez-Boulan and Nelson, 1989). In the E16.5 intestine, the columnar villus tip epithelium has withdrawn from the cell cycle and is highly polarized. We reasoned that polarity

defects, if present, would be easily detectable in this population of cells. Thus, E16.5 WT and *Wnt5a*<sup>-/-</sup> intestinal samples were stained with the apical marker, Ezrin (Fig. 4.4A-B), the lateral marker,  $\beta$ -cat (Fig 4.4C-D), the basal marker, Collagen IV (CollIV; Fig. 4.4E-F), and the *cis*-Golgi marker, gm130 (Fig 4.4G-H).

Ezrin,  $\beta$ -cat, and Coll IV localize properly to the apical, lateral, and basal membranes in both the control and mutant. However, while WT *cis*-Golgi are localized in an apical position relative to the nucleus, *Wnt5a* deficient epithelial cells exhibit randomly localized nuclei with fragmented, perinuclear *cis*-Golgi. Golgi are known to fragment and adopt a perinuclear localization in prophase cells when microtubules depolymerize; after completion of mitosis, Golgi are again rebuilt into stacks in both daughter cells (Thyberg and Moskalewski, 1999). At E16.5, the villus tip epithelial cells are differentiated and are no longer proliferative, so the persisting Golgi fragmentation and mislocalization in the *Wnt5a* mutant may be the consequence of failure to properly orient the Golgi following the last mitotic event prior to differentiation.

*Altered INM in Wnt5a null epithelia.* In WT intestinal epithelium, as in other pseudostratified epithelia, nuclei are not static, but migrate constantly from the basal surface, where they synthesize DNA, to the apical surface, where they divide, a process called INM. To examine INM in *Wnt5a* null intestines, pregnant dams carrying E14.5 fetuses were given a single intraperitoneal (IP) injection of BrdU.

Twenty minutes after the BrdU pulse, a chase of thymidine was administered. After another 20 min. (40 min. after BrdU injection), tissues were harvested.

Samples pooled from multiple experiments demonstrate that in WT samples, only 30% of BrdU positive nuclei localize one or more nuclear lengths away from the basal surface. However, in *Wnt5a* null mice, 60% of BrdU positive nuclei are away from the basal surface. Thus, either nuclei migrate faster in mutant animals, or S-phase nuclei are positioned aberrantly in those animals. In this context, it is interesting to note that Cervantes *et al.*, also using a BrdU pulse chase strategy, found that BrdU positive nuclei collect aberrantly at the luminal surface of *Wnt5a* deficient intestines. Thus, in concert with our data, the most likely explanation is that INM movements are altered in *Wnt5a* null animals. An important next question, which we are currently investigating, is to determine the length of time required for mitotic nuclei, labeled by phospho-HistoneH3 (pHH3) to be double-labeled with BrdU. This will reveal whether the pace of cell cycling is aberrant in this model (as we suspect).

*Increased cell death without apparent changes in proliferation in Wnt5a null epithelium.* Because intestines in *Wnt5a* null mice are shorter, we tested whether the apoptotic index was higher in these animals. Analysis of E14.5 intestines stained with the apoptotic marker Caspase3 (Fig. 4.5E,F) reveal that loss of *Wnt5a* results in increased apoptosis in the lumen. In the *Wnt5a* mutant, levels of mitotic cells stained with pHH3 appear similar to WT and no nuclei display mitotic arrest

phenotypes (data not shown). We are currently evaluating cell number/area in *Wnt5a* null intestines, as well as the percentage of mitotic cells. If the proliferation rate is similar in WT and *Wnt5a* deficient guts, the increased apoptotic index may contribute to the reduced length of *Wnt5a* null intestines.

*Luminal expansion is delayed in Wnt5a null animals.* We showed in Chapter 3 of this thesis that luminal expansion during intestinal remodeling at E14.5 involves a new type of cell division called the extending (e)-division; these mitotic events require delivery of apical proteins to the cytokinetic furrow of dividing cells in a time dependent manner in order to extend the lumen and carve out the villi. To examine lumen expansion, E14.5 intestines were stained with Ezrin and atypical protein kinase C ( $\alpha$ PKC) to mark the apical surface and Zona occludens (ZO-1) to identify tight junctions (Fig. 4.6) At early E14.5 stages of luminal expansion, *Wnt5a* mutant intestines have fewer luminal cracks, as if e-divisions are perturbed. At later E14.75 and E15 stages, luminal expansion in the WT has defined regularly-shaped villi, while the villus pattern in mutant intestines appears very disorganized without clear segregation of villi. Lumen expansion defects may be due to a developmental delay resulting from the altered rate of INM and the cell cycle. Because the villi are abnormally shaped in *Wnt5a* null animals, we also predict that e-divisions (which are responsible for shaping the villi) are abnormally oriented or aberrantly positioned. We are currently examining these aspects more carefully.

*Evidence supporting disruption of PCP in Wnt5a null animals.*

Wnt5a is well known to signal in the non-canonical Wnt pathway and some aspects of the phenotype of *Wnt5a* null mice suggest modulation of PCP signaling (abnormal Golgi orientation, disrupted nuclear orientation, and aberrant pattern of villus appendages). To test this, we examined genetic interactions between *Wnt5a* and the *Fz*-dependent core PCP pathway (*Vangl2*) as well as the *Fat*-dependent PCP pathway (*Fat4*).

*Expression of PCP pathway molecules in the intestine.* To determine whether genes of the PCP pathway are expressed during intestinal morphogenesis, we examined localization of *Fz6*, *Fz7*, *Fat4*, and *Dchs1* mRNAs at E14.5 (Fig. 4.7). The mRNA for *Fz6* (Djiane et al., 2005), a non-canonical Wnt5a receptor, localizes weakly to the epithelium (Fig. 4.7A). *Fz7* (Djiane et al., 2000; Medina et al., 2000; Medina and Steinbeisser, 2000) another Wnt5a receptor, localizes most strongly in the epithelium at E14.5 with some expression throughout the mesenchyme (Fig. 4.7B). Previous studies had shown that *Ror2* (Grumolato et al., 2010; He et al., 2008; Mikels and Nusse, 2006; Oishi et al., 2003), another receptor that is commonly used by Wnt5a in non-canonical signaling, is also epithelial. Finally, mRNAs for *Fat4* and *Dchs1* both localize exclusively in the mesenchyme (Fig 4.7C,D). Our attempts to localize *Vangl2* mRNA were not conclusive; however, repeated *in situ* results suggest that this mRNA is expressed weakly in the epithelium (Åsa Kolterud, data not shown). Based on these expression patterns, it is feasible that mesenchymal Wnt5a could control epithelial morphogenetic movements by directly modulating core PCP

pathways in the intestinal epithelium. Also, Wnt5a could modulate mesenchymal Fat/Dchs1 signaling to indirectly control epithelial morphogenesis.

*Vangl2* mutant mice have short guts and genetic interaction can be demonstrated between *Vangl2* and *Wnt5a*. If alterations in core PCP signaling cause shortened intestines, then we would expect that animals mutant for *Vangl2* (*Looptail* or *Lp/Lp* mice) would also show this phenotype and that, depending on whether one pathway or parallel pathways are at work, mice mutant for both *Vangl2* and *Wnt5a* might show similar or worse phenotypes. Thus, E16.5 intestines were measured in *Vangl2*<sup>Lp/Lp</sup> mice and in *Vangl2;Wnt5a* crosses. A trend of progressive shortening of the intestine was observed in the following order: WT, *Vangl2*<sup>Lp/+</sup>, *Vangl2*<sup>Lp/Lp</sup>, (*Vangl2*<sup>Lp/Lp</sup>; *Wnt5a*<sup>+/-</sup>), *Wnt5a*<sup>-/-</sup>, (*Vangl2*<sup>Lp/Lp</sup>; *Wnt5a*<sup>-/-</sup>) (Fig 4.8). The additive shortening effect between *Vangl2* and *Wnt5a* suggests that *Vangl2* and *Wnt5a* may genetically interact to control intestinal elongation.

*Vangl2* mutants display epithelial disorganization. To further examine genetic interactions between the *Wnt5a* and core PCP/*Vangl2* pathway, we compared H&E stained sections of the various genotypes (Figure 4.9A-F). Preliminary data suggest that like *Wnt5a* null animals, *Vangl2* homozygotes also display luminal epithelial aggregation. Interestingly, this phenotype also seems to be present in double heterozygotes. Additional experiments are needed to examine epithelial polarity, apical expansion, and the morphogenetic mechanisms affected in these double mutants.

Further analysis of *Vangl2*<sup>Lp/Lp</sup> sections by staining with gm130 reveals mislocalization of Golgi at E16.5, similar to that seen in *Wnt5a* null animals, indicating that intracellular polarity of the villus epithelium is not organized properly (Fig. 4.9G,H). Thus, loss of these two genes seem to result in similar phenotypes and genetic interactions can be demonstrated between them, but given the additive shortening effects in double mutants, there is not a simple epistatic relationship between them.

*Fat4* villus phenotype at E16.5. As demonstrated previously, *Fat4* null intestines are short (Mao et al., 2011). We confirmed this phenotype, but in our initial studies, we did not see that loss of an additional *Wnt5a* allele additively affected *Fat4* null intestinal length or *vice versa* (Fig. 4.10). We obtained no double knockout embryos in more than 70 total embryos, suggesting that the double mutant might be embryonic lethal. Thus, the current intestinal length data are insufficient to definitively establish or rule out genetic interactions between *Wnt5a* and *Fat4*. However, in E16.5 intestinal sections stained with H&E, we observed some apparently overlapping phenotypes (Fig. 4.11). The villus epithelium at this time point should consist of a single layer of columnar cells, but in both the *Fat4* and the *Wnt5a* mutants, villi are wider, disorganized, and present epithelial accumulations that may reflect additional layers of cells. Interestingly, this aspect of the phenotype seems to be somewhat ameliorated in animals that are *Fat4*<sup>+/-</sup>; *Wnt5a*<sup>-/-</sup> as well as those that are the *Fat4*<sup>-/-</sup>; *Wnt5a*<sup>+/-</sup>, but in these cases, villi appear thinner than

normal with fewer mesenchymal cells filling the core. These preliminary data suggest that *Fat4* and *Wnt5a* may indeed interact, but that a complex relationship may exist. It will be important to test whether *Wnt5a* levels are perturbed in *Fat4* null animals and *vice versa*. We are further examining the *Fat4* null phenotype as well as the hypothesis that the *Fat4* pathway partially rescues epithelial organization defect of the *Wnt5a* mutant. We also have not yet tested potential interactions between *Fat4* and *Vangl2* in the intestinal system.

## **Discussion**

Previous studies of *Wnt5a* deficient intestines led to a description of the short gut phenotype and to the hypothesis that defective radial interaction is the mechanism underlying reduced length (Cervantes et al., 2008). Yet, our findings that the epithelium is single pseudostratified layer contradict this hypothesis. To identify the morphogenetic mechanisms responsible for gut length, we investigated intestinal development in mouse models deficient in gut elongation, including mice deficient in *Wnt5a*, *Vangl2*, and *Fat4*. We identified the embryonic stage E14.5 to 16.5 as the developmental time period with the greatest increase in length, and we discovered that *Wnt5a* mutants lack this accelerated growth pattern. Since this period of rapid growth is also linked to villus emergence and since we saw clear evidence that this process is perturbed in *Wnt5a* null mice, we posit that a mechanistic link exists between villus formation and gut lengthening. Based on our findings of potential genetic interactions between *Wnt5a* and *Vangl2* and between *Wnt5a* and *Fat4*, we also propose that this link involves, at least in part, the regulation of PCP signaling



*via* at least two pathways. While these data are still preliminary, they have interesting implications for the understanding of intestinal growth, villus remodeling and the regulation of PCP signaling in the developing gut.

*Intestinal growth during early development.* Our studies of WT intestinal lengthening identified three periods of growth, defined by different rates of lengthening.

Between E12.5 and E14.5, growth is slow (relative to mid-fetal growth), but steady.

During this entire time, we have shown that the intestinal epithelium is pseudostratified and that its cells are highly proliferative. The cell divisions that occur during this time give rise to progressively taller, more tightly packed epithelial cells. Thus, measurable differences in intestinal girth occur, but it is reasonable to predict that these active cell divisions also contribute to intestinal lengthening. We are currently working with Dr. Santiago Schnell to model the resulting effects of this early proliferation on intestinal length.

A characteristic of the proliferating pseudostratified epithelium is that its nuclei are constantly moving within the AB plane of the epithelium in the process known as INM. Examination of the WT epithelium prior to E14.5 reveals that nuclei are highly elongated and radially arranged, with their long axes pointing toward the luminal surface. As epithelial cells elongate between E12.5 and E14.5, additional layers of stacked nuclei are visible, but the radial arrangement remains. This arrangement likely facilitates the INM movements as the elongated nuclei can easily slide past one another in the growing epithelium. In *Wnt5a* null epithelia, however, this radial

arrangement of nuclei is disrupted. Though we need to perform more careful 3D reconstructions of nuclear shapes in this model, it is clear that either nuclei are aberrantly shaped or that they are mis-oriented. It will be important to examine microtubular networks in these cells, since microtubules serve to orient both nuclei and Golgi, and we have also detected mis-oriented Golgi in both *Wnt5a* and *Vangl2* null animals. Furthermore, in the zebrafish model, PCP signaling has recently been shown to regulate the polarity of microtubules (Sepich et al., 2011); thus PCP signaling may directly regulate the polarity of these organelles in the intestinal epithelium.

The lack of a regular radial orientation of nuclei in *Wnt5a* mutant mice could conceivably slow INM movements, an event that could in turn interfere with cell cycle length. We have already found evidence that INM is perturbed in *Wnt5a* null animals and experiments are underway to determine whether this slows the cell cycle as measured by the time from S-phase to M-phase. A slower cell cycle in *Wnt5a* deficient intestinal epithelium, in association with the increased apoptosis, could account for the slower lengthening of these mutant guts in the early phase of intestinal growth.

*Intestinal growth during villus emergence.* The period of villus emergence occurs in a wave-like fashion from duodenum to ileum between E14.5 and E16.5 and is accompanied by accelerated growth in intestinal length. We find that this accelerated growth period is greatly diminished in *Wnt5a* null animals. This growth

in length must be at least due to the dramatic change in cell shape that occurs in concert with villus formation, as very tall thin pseudostratified cells become converted to more columnar ones. However, in *Wnt5a* null intestines, this cell shape conversion is accomplished effectively and therefore must not be the primary cause of the shortened intestines. Examination of the growth and development of other pseudostratified epithelia, such as the neural tube, have led to the speculation that the pseudostratified cell shape and the accompanying INM movements are adaptations that allow packing of a large number of progenitors into a small space (Miyata, 2008; Smart, 1972). If INM and cell cycling rate are indeed perturbed in *Wnt5a* null animals, then this might reduce the total number of cells in the epithelium, thereby affecting total length. We are working to mathematically model the degree to which small perturbances in proliferation, coupled with significant increases in apoptosis could account for reduced lengthening during this period.

*Additional potential modifiers of intestinal length.* Three other elements may play into the reduction in length seen in *Wnt5a* null mice. First, we have reconfirmed evidence that loss of *Fat4*, which like *Wnt5a* is a mesenchymal protein, also leads to short guts. Moreover, we have preliminary evidence for potential interactions between *Wnt5a* and *Fat4* at the cellular level that suggest that loss of one allele of either protein might partially rescue mice that are null for the other. These interactions are likely complex and we have not yet found the basis for this proposed mesenchymal contribution. A role for *Hippo* signaling is a possibility,

given the known role of *Fat4* in this signaling pathway, but there is currently no literature suggesting a link between *Wnt5a* and *Hippo* signaling.

Another consideration could be the potential for non-canonical signaling *via* *Wnt5a* to modulate canonical,  $\beta$ -cat signaling. *Wnt5a* is known to activate both canonical and non-canonical Wnt pathways depending on the receptor (Cha et al., 2008; Grumolato et al., 2010; Mikels and Nusse, 2006). Therefore, *Wnt5a* might directly activate canonical Wnt signaling; loss of *Wnt5a* in this scenario would prevent successful activation of canonical Wnt. Alternatively, *Wnt5a* might compete for Fz binding with other Wnts, thereby inhibiting canonical Wnt signaling, in which case, loss of *Wnt5a* signal would cause inappropriate activation of canonical Wnt pathways.

Most studies agree that  $\beta$ -cat-dependent Wnt signaling is required for stem cell maintenance in the E16.5 (and later) pre-crypt proliferative region as well as in adult crypts (Barker et al., 2007; Gregorieff et al., 2005; Kim et al., 2007; Korinek et al., 1998). However,  $\beta$ -cat-dependent Wnt signaling does not appear to be active in the intestine at E14.5 (and earlier); deletion of the transcription factor downstream of the Wnt signal, *Tcf4*, in mice and overexpression of  $\beta$ -cat cause phenotypes only after E16.5 (Gregorieff et al., 2005; Kim et al., 2007; Korinek et al., 1998).

Additionally, activation of the canonical Wnt target gene, *Axin2*, is first observed at E16.5 and not expressed at E14.5 (Cervantes et al., 2008; Kim et al., 2007; Korinek et al., 1998; Li et al., 2009). Thus, it is highly unlikely that reduced growth in E12.5 to

E14.5 *Wnt5a* mutant intestines is due to modulation of canonical Wnt signaling since the latter pathway does not seem to be active at this time. Additionally, given the fairly well accepted role for canonical Wnt signaling in maintenance of stem cells at E16.5 and later (likely starting at E15.5 during villus emergence), it seems unlikely that *Wnt5a* loss further modulates  $\beta$ -cat-dependent signaling in mid-fetal life, since this should result in either hyperproliferation of intervillus cells (if *Wnt5a* normally suppresses canonical Wnts) or reduced intervillus proliferation (if *Wnt5a* normally activates canonical Wnt signaling); neither of these phenotypes is observed.

We have performed initial experiments assessing canonical Wnt signaling activity by analyzing *Axin2* expression. We confirmed that *Axin2* is not expressed normally at E14.5 and established that it is also not expressed in *Wnt5a* null intestines at E14.5. Likewise, *Axin2* mRNA is localized to the pre-crypt region at E16.5 and this pattern is not affected in the *Wnt5a* deficient intestine. Furthermore, localization and levels of proliferation in E16.5 and E18.5 *Wnt5a* knockout intestinal epithelium are identical to those seen in WT villi [unpublished data; (Cervantes et al., 2008)], suggesting that *Wnt5a* does not interact or signal through the canonical Wnt pathway. Thus, we conclude that *Wnt5a* is signaling through a  $\beta$ -cat independent mechanism during intestinal morphogenesis.

*Wnt5a/PCP effector molecules.* One of the next questions is, what are the targets of *Wnt5a* signaling in the intestine? During vertebrate gastrulation and CE movements,

both regulated by noncanonical Wnt/PCP signaling, the downstream effectors are commonly RhoGTPases. Additionally, in cultured cells, non-canonical Wnts have been described to target RhoGTPases including Rho, Rac, and Cdc42 to alter the actin cytoskeleton and thereby affect cell shape, migration and cell polarity (Dejmek et al., 2006; Habas et al., 2003; Habas et al., 2001; Schlessinger et al., 2007; Witze et al., 2008). Wnt5a in particular can signal through Cdc42 in fibroblast and cancer cell lines to remodel the actin and microtubule cytoskeleton (Dejmek et al., 2006; Schlessinger et al., 2007). Our initial attempts to stain and analyze the cytoskeletal organization in fixed tissue were not successful; additional studies with non-conventional fixation protocols designed to preserve these delicate structures are underway.

*Oriented cell division and PCP.* We demonstrated that INM and epithelial orientation is abnormal in *Wnt5a* deficient intestines. We also found abnormal collections of cells near the lumen in the *Wnt5a* as well as in animals mutant for both *Vangl2* and *Wnt5a*. Though this remains to be further studied, we speculate that this phenotype might result from abnormalities in the timing or orientation of e-divisions that are required for lumen expansion and villus definition. Defective PCP pathways in mice are associated with problems in oriented cell division and result in abnormally shaped, small organs in the stomach and the kidney (Matsuyama et al., 2009; Saburi et al., 2008). In the adult intestine, orientation of division is important for stem cell maintenance and orientation preference is lost in precancerous tissues (Fleming et al., 2007; Quyn et al., 2010). In light of the importance of oriented division during

organ development and maintenance, it will be interesting to explore the role of oriented division in the fetal intestine in the context of disrupted PCP signaling.

## **Materials and Methods**

### *Mice*

Embryonic tissues were obtained from *Wnt5a* (Jackson 004758), *Vangl2* (kindly provided by Dr. Helen McNeill), or *Fat4* (kindly provided by Dr. Helen McNeill) mice. The morning of vaginal plug was recorded as day E0.5. Intestines for whole mount imaging were cut open and imaged shortly following the dissection.

### *Tissue preparation*

Tissues were fixed 1 hour to overnight in 4% paraformaldehyde and prepared for paraffin embedding. For paraffin, tissue was rinsed with PBS, dehydrated in ethanol, and infused with paraffin. Paraffin blocks were sectioned at 5  $\mu$ m. For staining, sections were deparaffinized, rehydrated and either H&E or immunostained. Stained samples were imaged on an Olympus FluoView 500 laser scanning confocal microscope or Nikon eclipse E800 widefield fluorescent microscope.

### *Immunostaining*

Sections were deparaffinized in xylene, rehydrated, washed with PBS, and boiled in 10mM sodium citrate at pH=6 for antigen retrieval. Sections were incubated for 30 minutes in blocking buffer (1% BSA, 10% goat serum, and 0.3% Triton X-100 in TBS). Primary antibodies (details below) were diluted in blocking buffer and

incubated overnight at 4°C. Molecular Probes Alexafluor conjugated secondary antibodies (Invitrogen; 1:1000; 488, 568, 647) with 10 ug/mL Hoechst (Invitrogen) were diluted in blocking buffer for 30 minutes at RT; slides were mounted with Prolong Gold (Invitrogen).

### *Antibodies*

Activated  $\beta$ -cat (ABC; Millipore, 1:100), BrdU (Accurate Chemical and Scientific Corp clone BU1/75, 1:200), BrdU (DSHB clone G3G4, 1:400), Casp 3 (R&D AF835, 1:500), CollIV (Millipore AB756P, 1:500), Ecad (Invitrogen ECCD2 13-1900, 1:1000), Ecad (BD 610181, 1:1000), Ezrin [Thermo Scientific MS-661-P1, 1:100; blocking from M.O.M. kit (Vector Labs)], gm130 (BD 610822; 1:250), pHH3 (Millipore 6-570, 1:400), pHH3 (Millipore 05-806; 1:200), PKC $\zeta$  (aPKC; Santa Cruz sc-216, 1:500), ZO-1 (Invitrogen 33-9100; 1:1000).

### *BrdU labeling studies*

Pregnant females were IP injected with a pulse of 50 mg/kg BrdU, chased at various times with 500 mg/kg thymidine. Tissues were paraffin embedded and stained with anti-BrdU. BrdU positive nuclei were counted manually, and significance was determined using ANOVA and unpaired t-tests.

### *SEM*



Intestinal tissue samples were fixed in Bouin's solution and dehydrated in EtOH followed by hexamethyldisilazane. Samples were critical point dried and mounted using double-sided tape. The intestinal surface was exposed by cracking with a sharp razor blade. Samples were then coated with gold/palladium under vacuum and imaged on an AMRAY 1910 Field Emission Scanning Electron Microscope (FEG-SEM) using X-STREAM imaging software.

*In situ hybridization.*

RNA probes were synthesized by rtPCR, cloned into PCR4 TOPO vectors (Invitrogen) and sequenced for confirmation. The following templates were used: Wnt5a, Fz7, Fat4, and Dchs1. Sense and antisense probes were generated from each template and tested in parallel. Paraffin sections were deparaffinized, rehydrated, incubated with 10 µg/ml proteinase K in PBS (15 min, RT), post fixed (10 min in 4% PFA), and treated with acetic anhydride solution. After 4h prehybridization at RT, the sections were hybridized at 70°C O/N with specific probes in 50% deionized formamide, 5 x SSC, 5x Denhardt's solution, 250 µg/ml yeast tRNA, 0.5 mg/ml herring sperm DNA and 2% blocking reagent (Roche). Slides were washed in 5 x SSC at 70°C, 0.2 x SSC at 70°C for 1h, 0.2 x SSC at RT for 5 min and B1 (100 mM Tris-HCl pH 7.5, 150 mM NaCl) at RT for 5 min. Sections were blocked for 1 h in B1 containing 10% heat-inactivated FCS and 2% blocking reagent (Roche) and incubated with alkaline phosphatase-conjugated anti-digoxigenin antibody (Roche), 1:5000 in blocking solution at 4°C O/N. After several washes in B1, the slides were equilibrated in B3 (100 mM Tris-HCl pH 9.5, 100 mM NaCl, 50 mM MgCl<sub>2</sub>) and color

reaction was performed in the dark in B3 supplemented with 100 mg/ml NBT (4-nitro blue tetrazolium chloride), 50 mg/ml BCIP (5-bromo-4-chloro-3-indolyl-phosphate), 0.05% Tween-20 and 1mM levamisole for 10–20 h. The color reaction was stopped in PBS, and the slides were mounted with 70% glycerol/PBS.

### **Acknowledgements**

This work will be part of a paper designed for submission later this year. Significant intellectual and experimental input from Lauren B. Curley and Mark F. Pressprich contributed greatly to this work. *Vangl2* and *Fat4* mice were kindly provided by Dr. Helen McNeill, University of Toronto, Toronto, Canada. The authors are also grateful for excellent technical assistance provided by Chris Edwards, Shelley Almburg, Dotty Sorenson, and Sasha Meshinchi in the Microscopy and Image Analysis Laboratory as well as Marta Dzaman and Maria Ripberger in the Organogenesis Morphology Core at the University of Michigan.

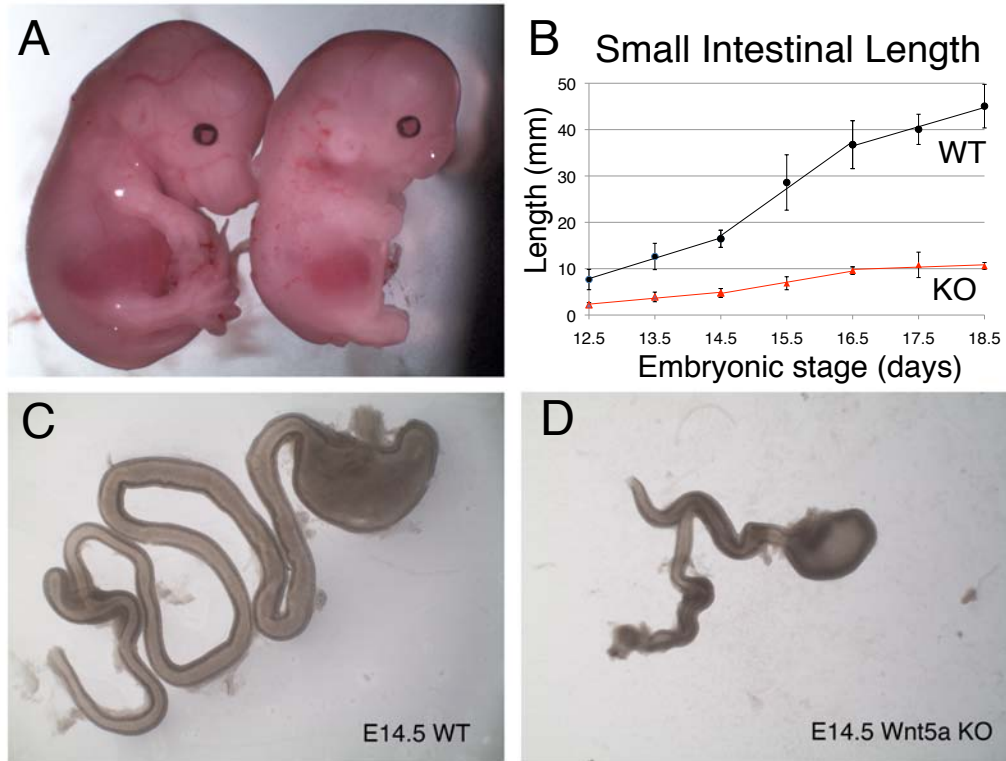


**Figure 4.1. Growth in length of the fetal intestine.** A) The comparison of E14.5 WT (left) and Wnt5a KO (right) mouse embryos demonstrates the mutant gross phenotype. B) Measurement of WT and KO intestinal epithelial length at E12.5 (n=7), E13.5 (n=5), E14.5 (n=3), E15.5 (n=11), E16.5 (n=7), E17.5 (n=3), and E18.5 (n=3). C-D) Dissected E14.5 WT and Wnt5a KO intestines display the shortened mutant intestine with a tubular duplication and imperforate anus.

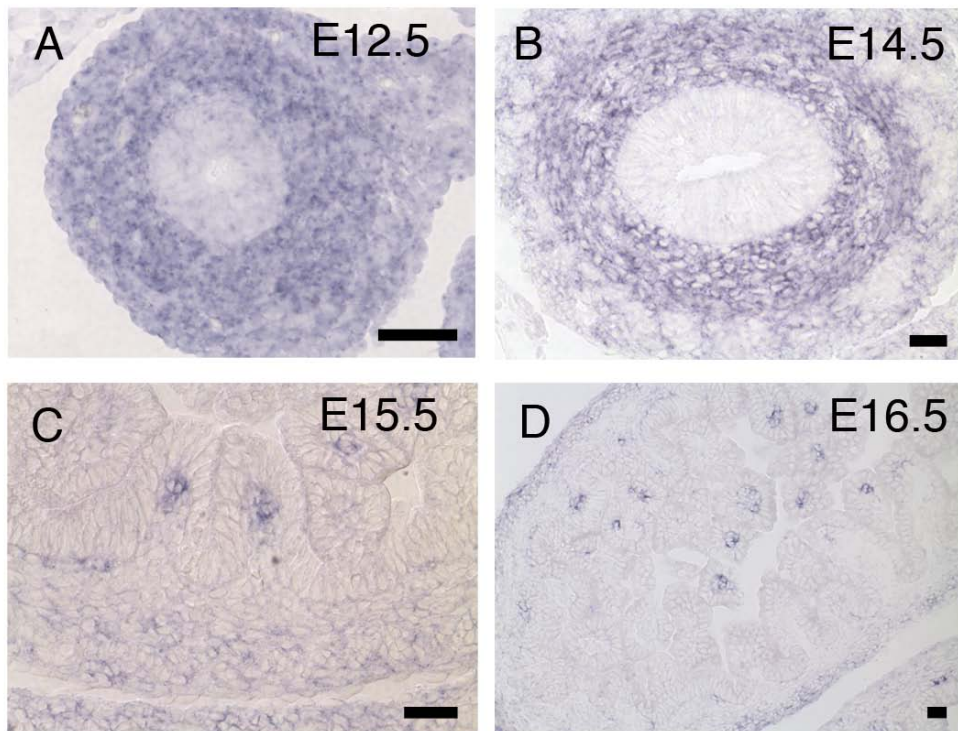


**Figure 4.2. Wnt5a expression in the intestine.** In situ hybridization reveals the expression of Wnt5a in the mesenchyme at E12.5 (A), 14.5 (B), 15.5 (C), and E16.5 (D). The Wnt5a transcript starts out as a diffuse signal surrounding the epithelium that with time specifically localizes to mesenchymal clusters before and during villus formation. Scale bars = 20  $\mu\text{m}$ . Panels A-D were obtained by Asa Kolterud.

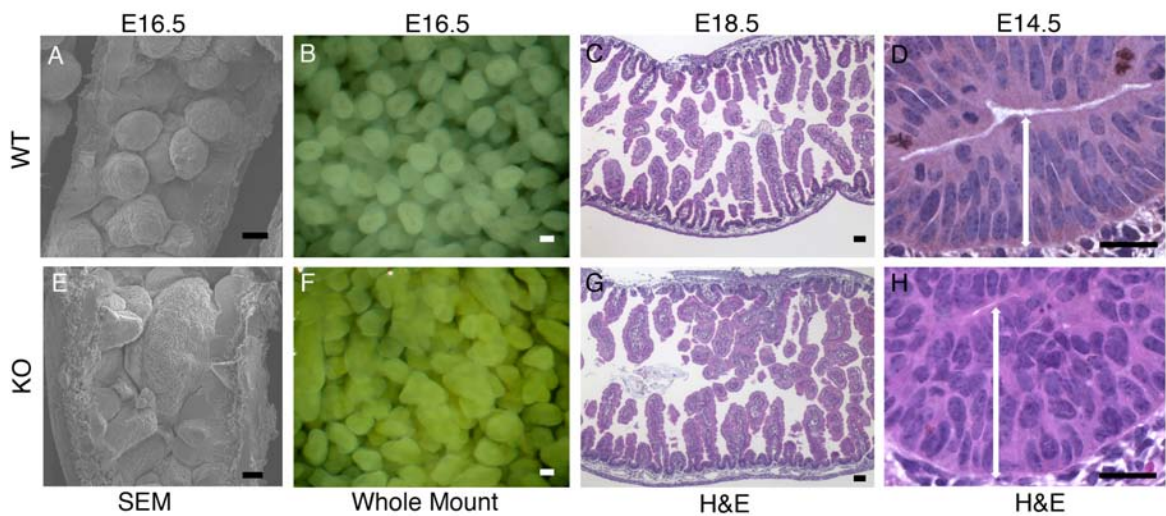


**Figure 4.3. Analysis of villus development and organization.** WT villi analyzed by SEM (A), whole mount (B), and H&E staining (C) are uniformly spaced and organized with tall, finger-like projections into the lumen. E14.5 intestinal sections were H&E stained (D) with the white double headed arrow indicating girth. The long axes of E14.5 WT nuclei are arranged radially toward the central lumen with a girth of 3-4 nuclei. Wnt5a KO villi analyzed by SEM (E), whole mount (F), and H&E staining (G) are varied in size, shape, and spacing. Additionally, the villi are disorganized with projections and branches in multiple directions. E14.5 intestinal sections were H&E stained (H) with the white double headed arrow indicating girth. Wnt5a KO nuclei are more varied in size, shape, and orientation with a thicker girth of 8-10 nuclei. Scale bars = 20  $\mu$ m.



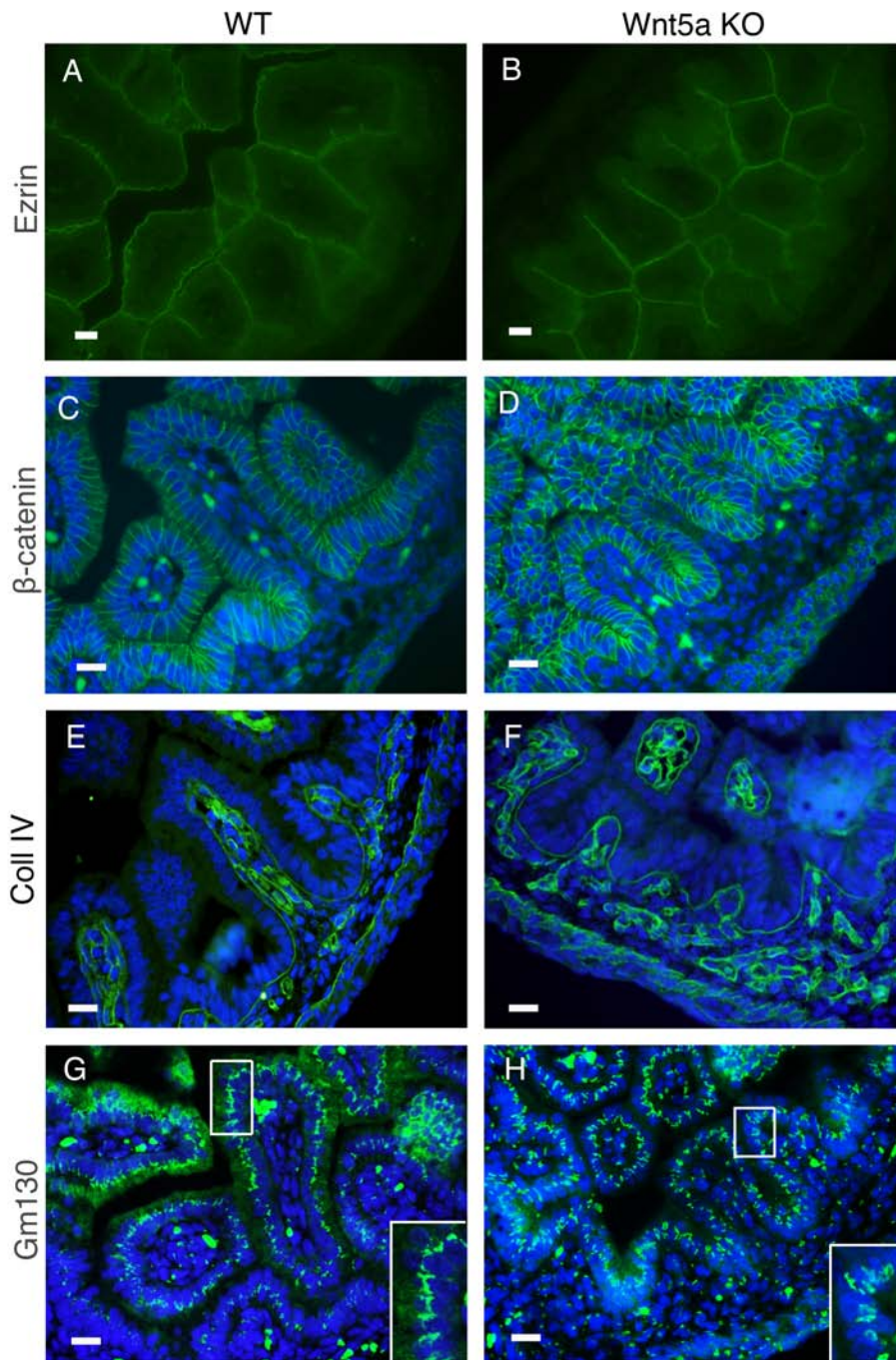


**Figure 4.4. Epithelial cell polarity at E16.5.** A-F) In both the WT and the mutant E16.5 intestines, AB markers localize normally. Ezrin (A,B) stains the apical surface,  $\beta$ -cat (C,D) demarcates the basolateral surface, and CollagenIV (E,F) identifies the basement membrane and blood vessels. G-H) Intestinal sections stained with Gm130, identify Golgi localized to the apical side of the nucleus in the WT and short, mislocalized Golgi in the Wnt5a mutant. Scale bars = 20  $\mu$ m.

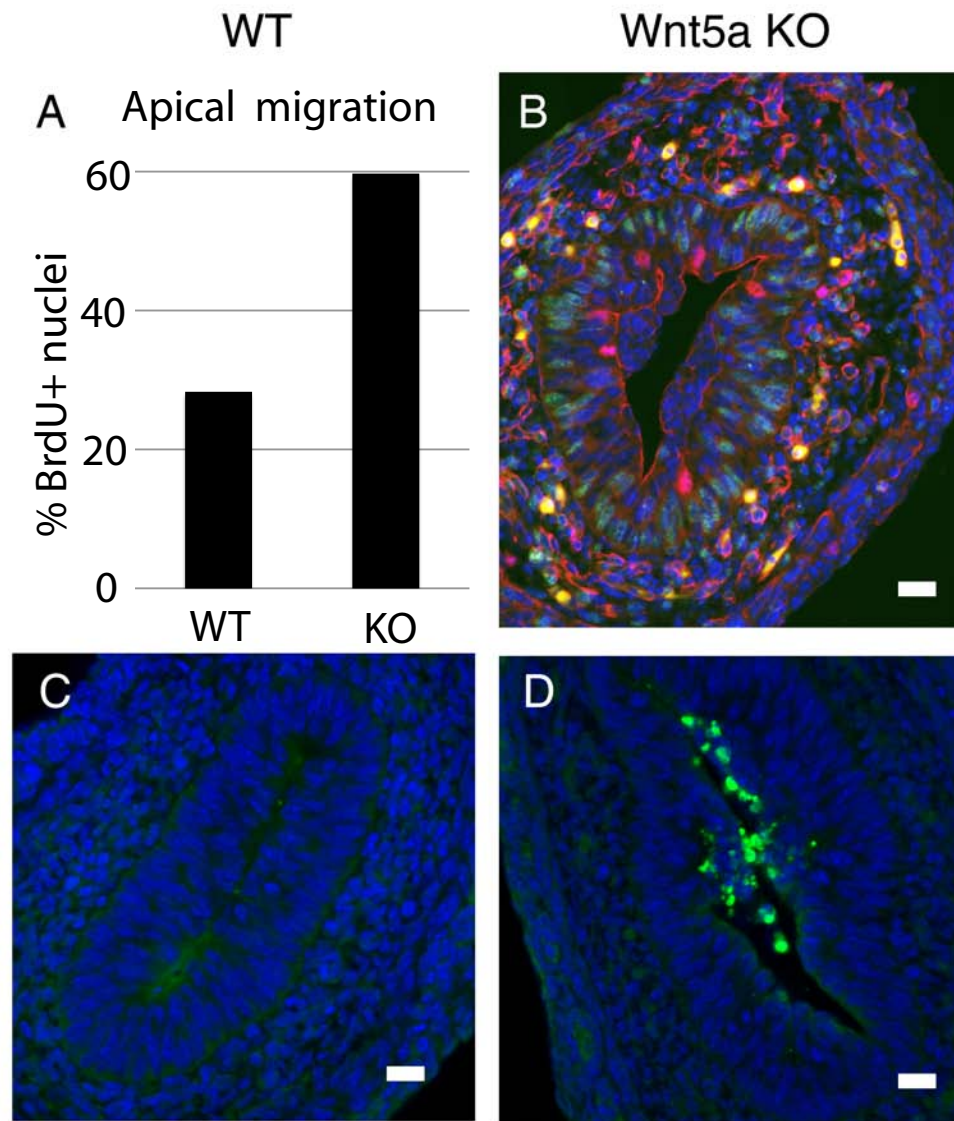


**Figure 4.5. Epithelial INM and cell death at E14.5.** A,B) A greater percentage of BrdU positive nuclei localize non-basally in the epithelial cells of the *Wnt5a* mutant. Intestines were pulsed with BrdU for 20 min. followed by a 20 min. chase and quantified for non-basal BrdU. Intestines were stained with Hoechst (blue), BrdU (green), pHH3 (red), collIV (red), and aPKC (red). Data from C and D were generated by Mark Pressprich. C,D) Intestinal sections were stained for apoptotic marker Caspase 3 (green). Intestinal sections identify increased apoptosis in the *Wnt5a* null intestine. Scale bars = 20  $\mu$ m.

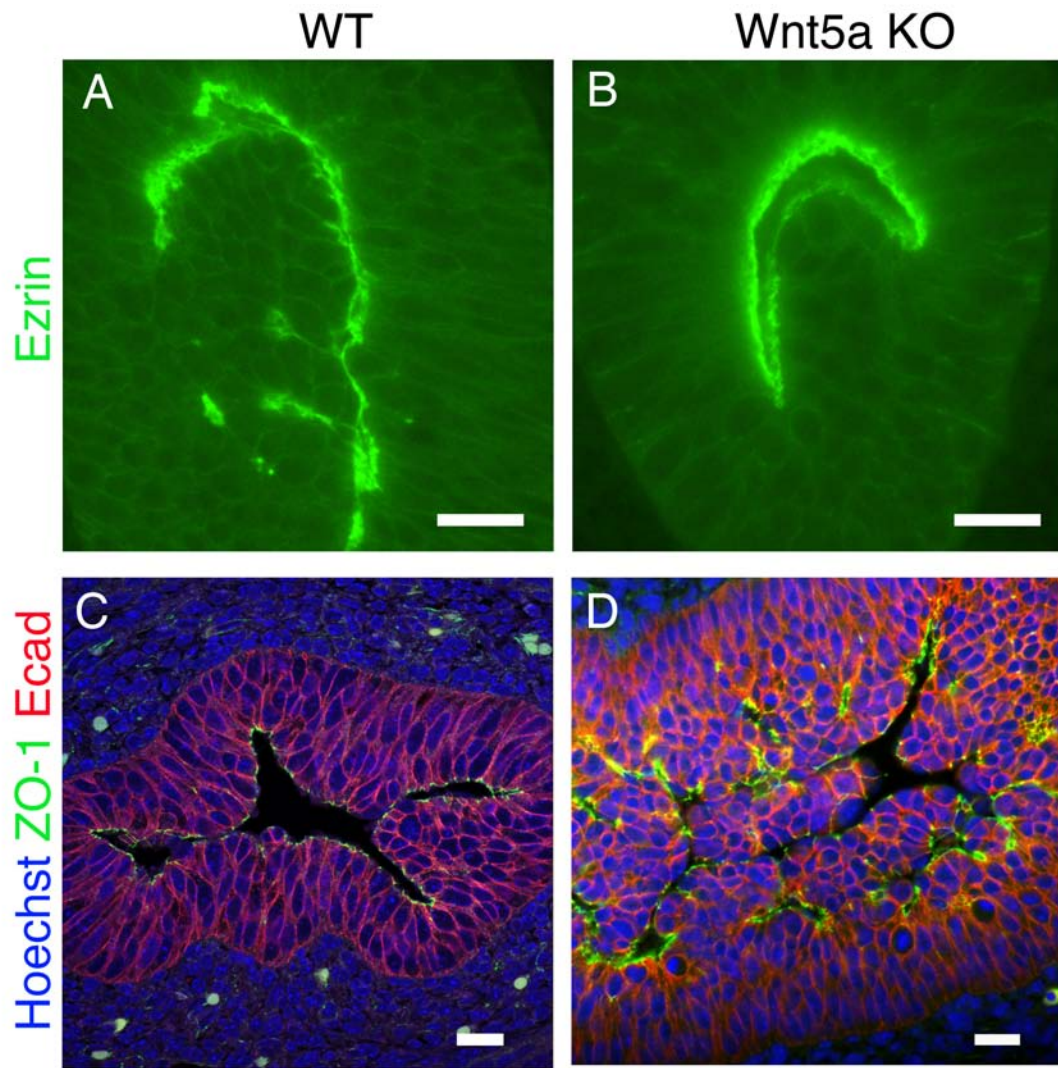


**Figure 4.6. Apical expansion is defective in *Wnt5a* mutants.** A-B) WT and *Wnt5a* deficient intestines at E14.5 are stained with apical marker Ezrin (green) to demarcate the expanding lumen. C-D) WT and *Wnt5a* deficient intestines at E14.75 are stained with Hoechst (blue), tight junction marker ZO-1 (green), and lateral membrane marker E-cadherin (red) to identify luminal cracks and apical expansion. Scale bars = 20 $\mu$ m.



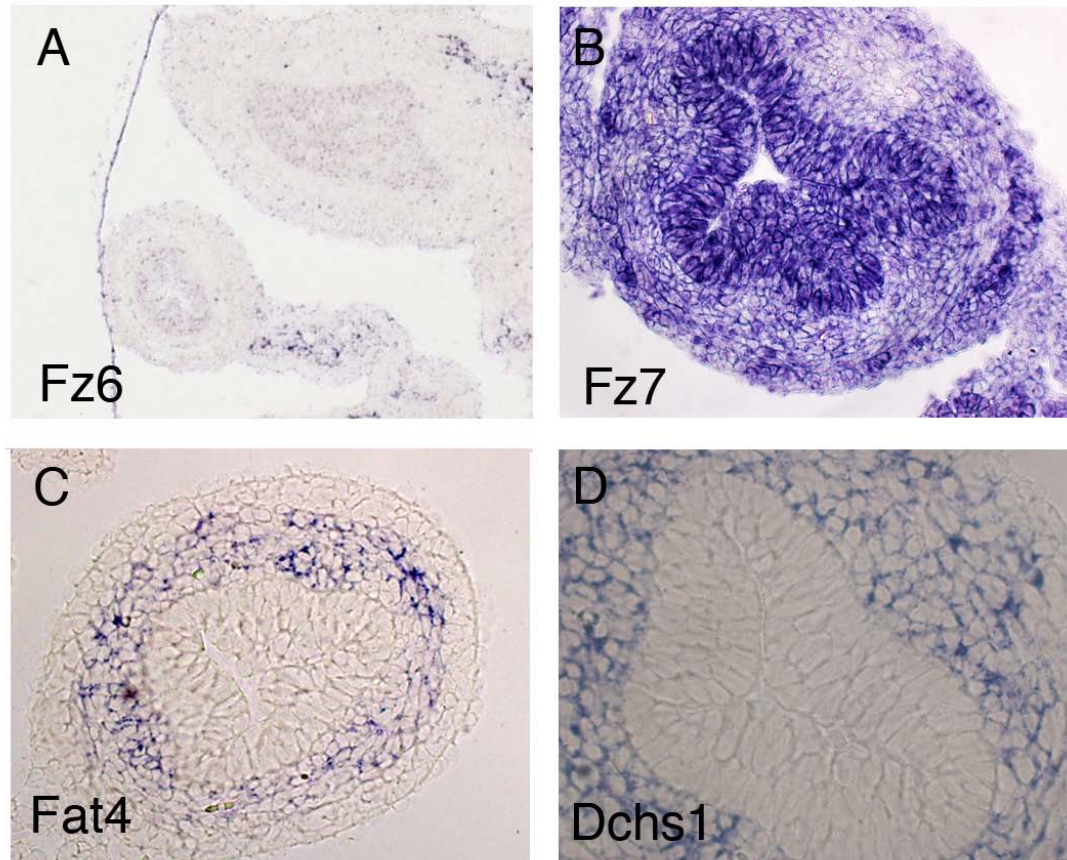


**Figure 4.7. PCP expression in the intestine.** In situ hybridization determines that PCP receptors Fz6 (A; [genepaint.org](http://genepaint.org)) and Fz7 (B) localize most strongly to the epithelium. Fat4 (C) and Dchs1 (D) localize to the mesenchyme. Panels B-D were obtained by Asa Kolterud and Kate Walton.

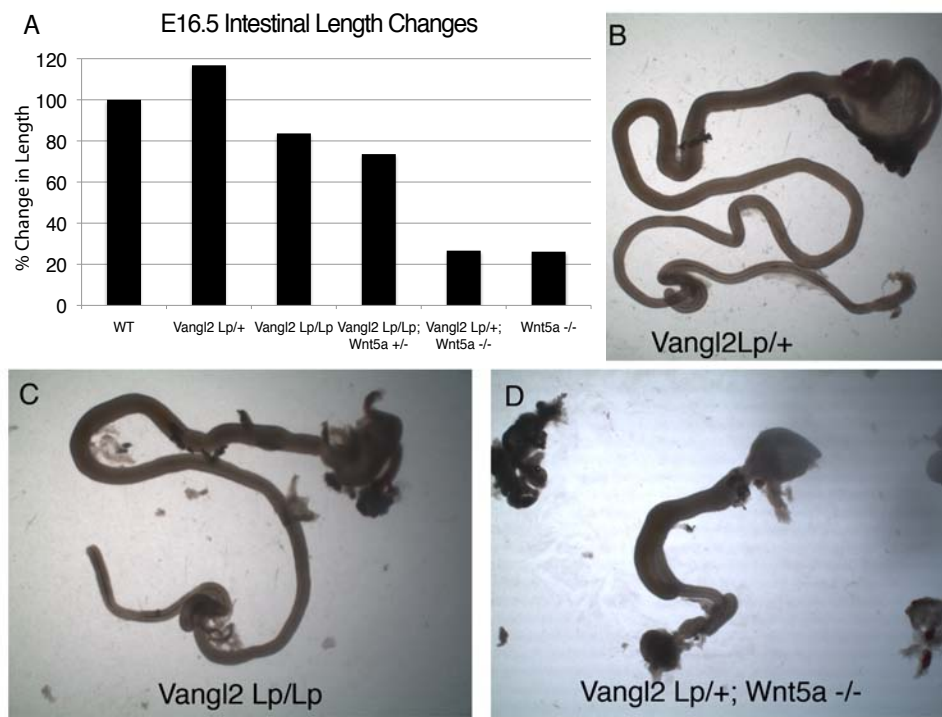


**Figure 4.8. Core PCP defects in gut elongation.** A) Comparison of intestinal length at E16.5 in Vangl2;Wnt5a reveals elongation defects. B-D) Whole mount E16.5 intestines from Vangl2<sup>Lp/+</sup>, Vangl2<sup>Lp/Lp</sup>, and Vangl2<sup>Lp/+</sup>; Wnt5a<sup>-/-</sup> mice. n=1 for all genotypes.

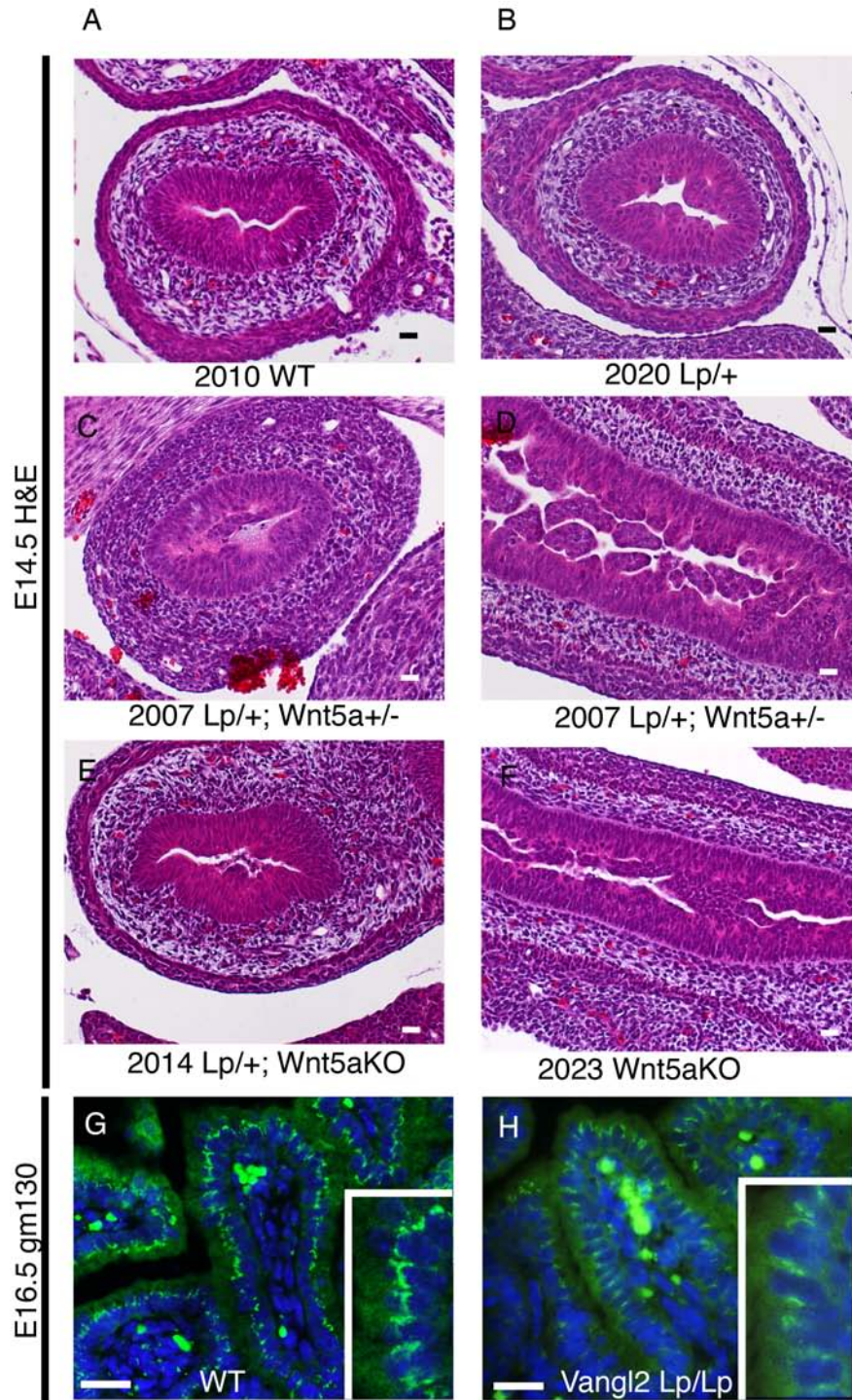


**Figure 4.9. Vangl2;Wnt5a epithelial defects.** A-F) H&E stained E14.5 intestines from Vangl2;Wnt5a crosses exhibit increased severity of cellular accumulation in the lumen with additional Vangl2 and Wnt5a alleles. G,H) Epithelial defects are apparent in e16.5 Vangl2 deficient intestines with laterally mislocalized cis-Golgi stained with gm130 (green). Scale bars = 20 $\mu$ m.



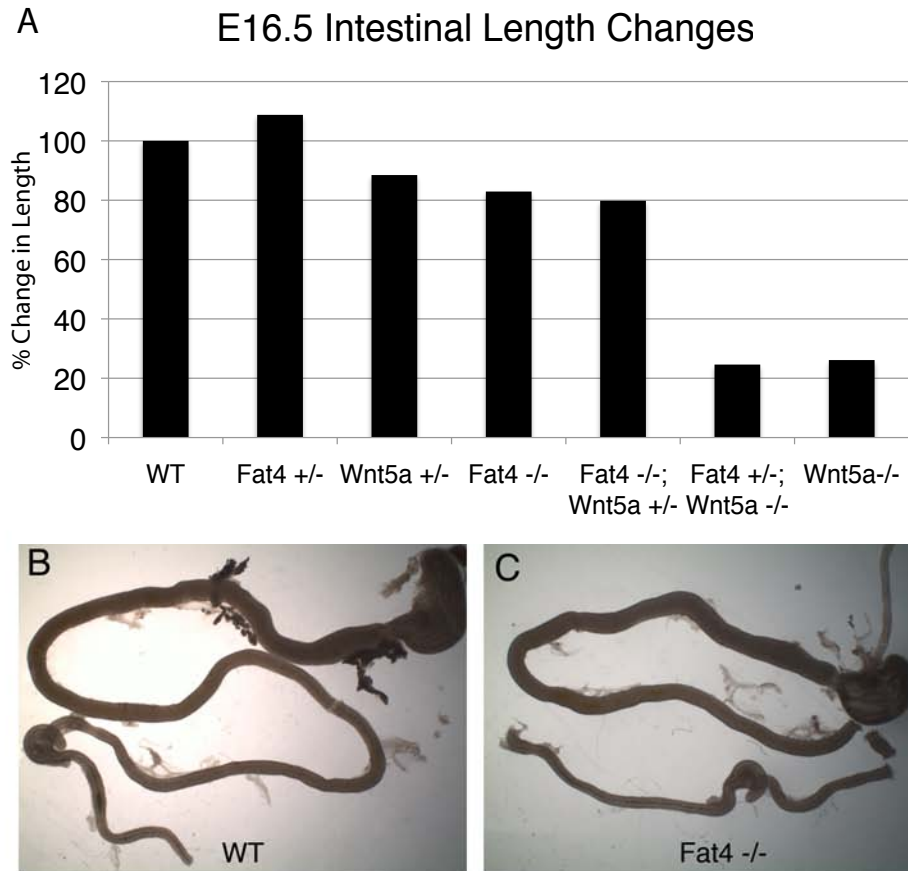


**Figure 4.10. Fat4 PCP defects in gut elongation.** A) Comparison of intestinal length at E16.5 in Fat4;Wnt5a to WT reveals elongation defects. Fat4<sup>-/-</sup> intestines are 80% the length of WT littermates. B-C) Whole mount intestines from WT and Fat4<sup>-/-</sup> mice. n=1 for all genotypes.

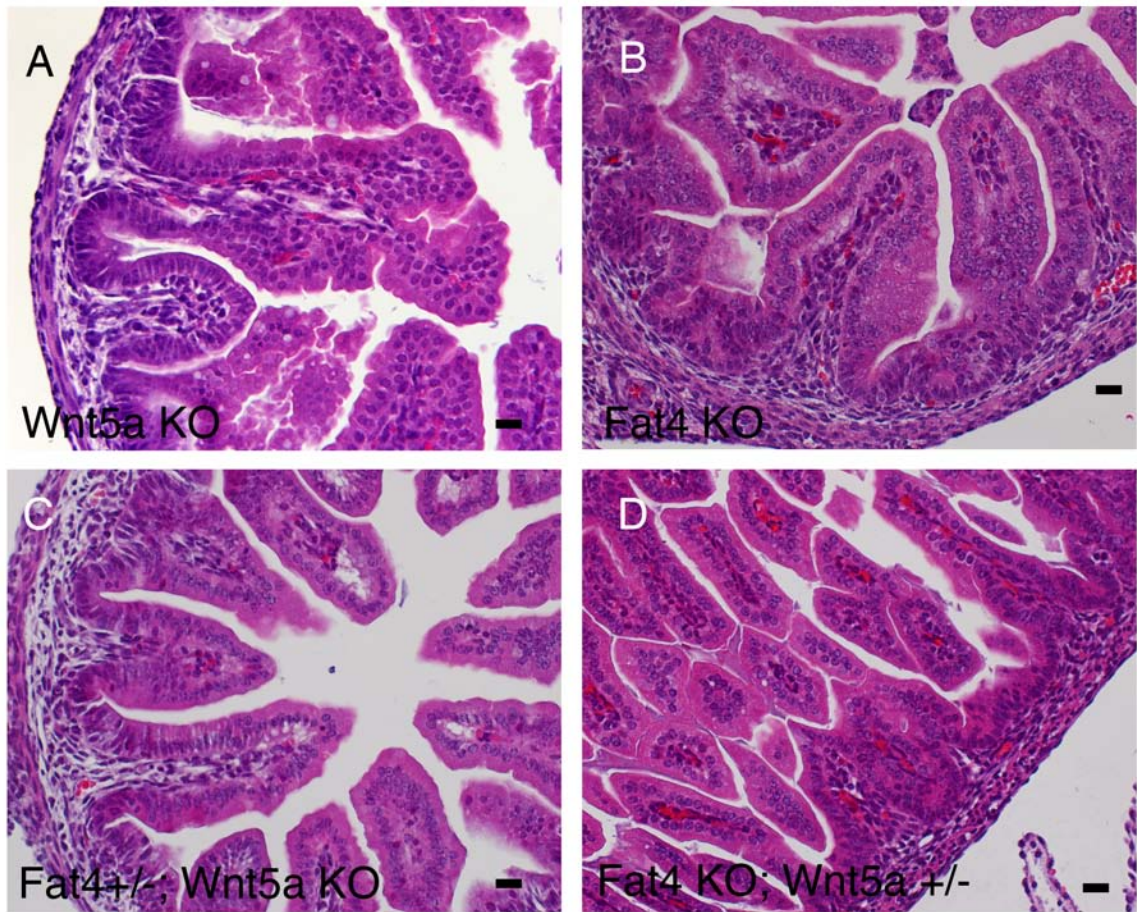


**Figure 4.11. Epithelial accumulation in *Fat4* mutant intestines.** Intestines were H&E stained to examine histology. A) E18.5 *Wnt5a*<sup>-/-</sup> and B) E16.5 *Fat4*<sup>-/-</sup> villi display epithelial accumulation. C) E16.5 *Fat4*<sup>+/-</sup>; *Wnt5a*<sup>-/-</sup> villi appear normal. D) *Fat4*<sup>-/-</sup>; *Wnt5a*<sup>+/-</sup> villi are thin and tightly packed together. Scale bars = 20 $\mu$ m.

## Literature Cited

- Allgeier, S. H., Lin, T. M., Vezina, C. M., Moore, R. W., Fritz, W. A., Chiu, S. Y., Zhang, C. and Peterson, R. E.** (2008). WNT5A selectively inhibits mouse ventral prostate development. *Dev Biol* **324**, 10-7.
- Barker, N., van Es, J. H., Kuipers, J., Kujala, P., van den Born, M., Cozijnsen, M., Haegebarth, A., Korving, J., Begthel, H., Peters, P. J. et al.** (2007). Identification of stem cells in small intestine and colon by marker gene Lgr5. *Nature* **449**, 1003-7.
- Bornens, M.** (2008). Organelle positioning and cell polarity. *Nat Rev Mol Cell Biol* **9**, 874-86.
- Cervantes, S., Yamaguchi, T. P. and Hebrok, M.** (2008). Wnt5a is essential for intestinal elongation in mice. *Dev Biol*.
- Cha, S. W., Tadjuidje, E., Tao, Q., Wylie, C. and Heasman, J.** (2008). Wnt5a and Wnt11 interact in a maternal Dkk1-regulated fashion to activate both canonical and non-canonical signaling in Xenopus axis formation. *Development* **135**, 3719-29.
- Chen, W., ten Berge, D., Brown, J., Ahn, S., Hu, L. A., Miller, W. E., Caron, M. G., Barak, L. S., Nusse, R. and Lefkowitz, R. J.** (2003). Dishevelled 2 recruits beta-arrestin 2 to mediate Wnt5A-stimulated endocytosis of Frizzled 4. *Science* **301**, 1391-4.
- Clevers, H. and van de Wetering, M.** (1997). TCF/LEF factor earn their wings. *Trends Genet* **13**, 485-9.
- Dejmek, J., Saffholm, A., Kamp Nielsen, C., Andersson, T. and Leandersson, K.** (2006). Wnt-5a/Ca<sup>2+</sup>-induced NFAT activity is counteracted by Wnt-5a/Yes-Cdc42-casein kinase 1alpha signaling in human mammary epithelial cells. *Mol Cell Biol* **26**, 6024-36.
- Dissanayake, S. K., Olkhanud, P. B., O'Connell, M. P., Carter, A., French, A. D., Camilli, T. C., Emeche, C. D., Hewitt, K. J., Rosenthal, D. T., Leotlela, P. D. et al.** (2008). Wnt5A regulates expression of tumor-associated antigens in melanoma via changes in signal transducers and activators of transcription 3 phosphorylation. *Cancer Res* **68**, 10205-14.
- Djiane, A., Riou, J., Umbhauer, M., Boucaut, J. and Shi, D.** (2000). Role of frizzled 7 in the regulation of convergent extension movements during gastrulation in Xenopus laevis. *Development* **127**, 3091-100.
- Djiane, A., Yogev, S. and Mlodzik, M.** (2005). The apical determinants aPKC and dPatj regulate Frizzled-dependent planar cell polarity in the Drosophila eye. *Cell* **121**, 621-31.
- Fleming, E. S., Zajac, M., Moschenross, D. M., Montrose, D. C., Rosenberg, D. W., Cowan, A. E. and Tirnauer, J. S.** (2007). Planar spindle orientation and asymmetric cytokinesis in the mouse small intestine. *J Histochem Cytochem* **55**, 1173-80.
- Gordon, M. D. and Nusse, R.** (2006). Wnt signaling: multiple pathways, multiple receptors, and multiple transcription factors. *J Biol Chem* **281**, 22429-33.
- Goto, T. and Keller, R.** (2002). The planar cell polarity gene strabismus regulates convergence and extension and neural fold closure in Xenopus. *Dev Biol* **247**, 165-81.
- Goulet, O. and Ruemmele, F.** (2006). Causes and management of intestinal failure in children. *Gastroenterology* **130**, S16-28.

**Gregorieff, A., Pinto, D., Begthel, H., Destree, O., Kielman, M. and Clevers, H.** (2005). Expression pattern of Wnt signaling components in the adult intestine. *Gastroenterology* **129**, 626-38.

**Grosse, A. S., Pressprich, M. F., Curley, L. B., Margolis, B., Hildebrand, J. D. and Gumucio, D. L.** (2011). Cell dynamics in fetal intestinal epithelium: implications for intestinal growth and morphogenesis. *Development*, *In revision*.

**Grumolato, L., Liu, G., Mong, P., Mudbhary, R., Biswas, R., Arroyave, R., Vijayakumar, S., Economides, A. N. and Aaronson, S. A.** (2010). Canonical and noncanonical Wnts use a common mechanism to activate completely unrelated coreceptors. *Genes Dev* **24**, 2517-30.

**Gubb, D. and Garcia-Bellido, A.** (1982). A genetic analysis of the determination of cuticular polarity during development in *Drosophila melanogaster*. *J Embryol Exp Morphol* **68**, 37-57.

**Habas, R., Dawid, I. B. and He, X.** (2003). Coactivation of Rac and Rho by Wnt/Frizzled signaling is required for vertebrate gastrulation. *Genes Dev* **17**, 295-309.

**Habas, R., Kato, Y. and He, X.** (2001). Wnt/Frizzled activation of Rho regulates vertebrate gastrulation and requires a novel Formin homology protein Daam1. *Cell* **107**, 843-54.

**Halder, G. and Johnson, R. L.** (2011). Hippo signaling: growth control and beyond. *Development* **138**, 9-22.

**Hardy, K. M., Garriock, R. J., Yatskievych, T. A., D'Agostino, S. L., Antin, P. B. and Krieg, P. A.** (2008). Non-canonical Wnt signaling through Wnt5a/b and a novel Wnt11 gene, Wnt11b, regulates cell migration during avian gastrulation. *Dev Biol* **320**, 391-401.

**He, F., Xiong, W., Yu, X., Espinoza-Lewis, R., Liu, C., Gu, S., Nishita, M., Suzuki, K., Yamada, G., Minami, Y. et al.** (2008). Wnt5a regulates directional cell migration and cell proliferation via Ror2-mediated noncanonical pathway in mammalian palate development. *Development* **135**, 3871-9.

**Heisenberg, C. P., Tada, M., Rauch, G. J., Saude, L., Concha, M. L., Geisler, R., Stemple, D. L., Smith, J. C. and Wilson, S. W.** (2000). Silberblick/Wnt11 mediates convergent extension movements during zebrafish gastrulation. *Nature* **405**, 76-81.

**Huang, L., Pu, Y., Hu, W. Y., Birch, L., Luccio-Camelo, D., Yamaguchi, T. and Prins, G. S.** (2009). The role of Wnt5a in prostate gland development. *Dev Biol* **328**, 188-99.

**Jonsson, M. and Andersson, T.** (2001). Repression of Wnt-5a impairs DDR1 phosphorylation and modifies adhesion and migration of mammary cells. *J Cell Sci* **114**, 2043-53.

**Karlsson, L., Lindahl, P., Heath, J. K. and Betsholtz, C.** (2000). Abnormal gastrointestinal development in PDGF-A and PDGFR-(alpha) deficient mice implicates a novel mesenchymal structure with putative instructive properties in villus morphogenesis. *Development* **127**, 3457-66.

**Kawasaki, A., Torii, K., Yamashita, Y., Nishizawa, K., Kanekura, K., Katada, M., Ito, M., Nishimoto, I., Terashita, K., Aiso, S. et al.** (2007). Wnt5a promotes adhesion of human dermal fibroblasts by triggering a phosphatidylinositol-3 kinase/Akt signal. *Cell Signal* **19**, 2498-506.

- Kilian, B., Mansukoski, H., Barbosa, F. C., Ulrich, F., Tada, M. and Heisenberg, C. P.** (2003). The role of Ppt/Wnt5 in regulating cell shape and movement during zebrafish gastrulation. *Mech Dev* **120**, 467-76.
- Kim, B. M., Mao, J., Taketo, M. M. and Shivdasani, R. A.** (2007). Phases of canonical Wnt signaling during the development of mouse intestinal epithelium. *Gastroenterology* **133**, 529-38.
- Kim, H. J., Schleiffarth, J. R., Jessurun, J., Sumanas, S., Petryk, A., Lin, S. and Ekker, S. C.** (2005). Wnt5 signaling in vertebrate pancreas development. *BMC Biol* **3**, 23.
- Korinek, V., Barker, N., Moerer, P., van Donselaar, E., Huls, G., Peters, P. J. and Clevers, H.** (1998). Depletion of epithelial stem-cell compartments in the small intestine of mice lacking Tcf-4. *Nat Genet* **19**, 379-83.
- Ku, N. O., Zhou, X., Toivola, D. M. and Omary, M. B.** (1999). The cytoskeleton of digestive epithelia in health and disease. *Am J Physiol* **277**, G1108-37.
- Kurayoshi, M., Oue, N., Yamamoto, H., Kishida, M., Inoue, A., Asahara, T., Yasui, W. and Kikuchi, A.** (2006). Expression of Wnt-5a is correlated with aggressiveness of gastric cancer by stimulating cell migration and invasion. *Cancer Res* **66**, 10439-48.
- Lawrence, P. A. and Shelton, P. M.** (1975). The determination of polarity in the developing insect retina. *J Embryol Exp Morphol* **33**, 471-86.
- Li, X., Udager, A. M., Hu, C., Qiao, X. T., Richards, N. and Gumucio, D. L.** (2009). Dynamic patterning at the pylorus: formation of an epithelial intestine-stomach boundary in late fetal life. *Dev Dyn* **238**, 3205-17.
- Lickert, H., Kispert, A., Kutsch, S. and Kemler, R.** (2001). Expression patterns of Wnt genes in mouse gut development. *Mech Dev* **105**, 181-4.
- Loscertales, M., Mikels, A. J., Hu, J. K., Donahoe, P. K. and Roberts, D. J.** (2008). Chick pulmonary Wnt5a directs airway and vascular tubulogenesis. *Development* **135**, 1365-76.
- Mao, Y., Mulvaney, J., Zakaria, S., Yu, T., Morgan, K. M., Allen, S., Basson, M. A., Francis-West, P. and Irvine, K. D.** (2011). Characterization of a Dchs1 mutant mouse reveals requirements for Dchs1-Fat4 signaling during mammalian development. *Development* **138**, 947-57.
- Mathan, M., Moxey, P. C. and Trier, J. S.** (1976). Morphogenesis of fetal rat duodenal villi. *Am J Anat* **146**, 73-92.
- Matsuyama, M., Aizawa, S. and Shimono, A.** (2009). Sfrp controls apicobasal polarity and oriented cell division in developing gut epithelium. *PLoS Genet* **5**, e1000427.
- McNeill, H.** Planar cell polarity: keeping hairs straight is not so simple. *Cold Spring Harb Perspect Biol* **2**, a003376.
- McNeill, H.** (2009). Planar cell polarity and the kidney. *J Am Soc Nephrol* **20**, 2104-11.
- Medina, A., Reintsch, W. and Steinbeisser, H.** (2000). Xenopus frizzled 7 can act in canonical and non-canonical Wnt signaling pathways: implications on early patterning and morphogenesis. *Mech Dev* **92**, 227-37.
- Medina, A. and Steinbeisser, H.** (2000). Interaction of Frizzled 7 and Dishevelled in Xenopus. *Dev Dyn* **218**, 671-80.



**Mikels, A. J. and Nusse, R.** (2006). Purified Wnt5a protein activates or inhibits beta-catenin-TCF signaling depending on receptor context. *PLoS Biol* **4**, e115.

**Miyata, T.** (2008). Development of three-dimensional architecture of the neuroepithelium: role of pseudostratification and cellular 'community'. *Dev Growth Differ* **50 Suppl 1**, S105-12.

**Mogensen, M. M., Tucker, J. B., Mackie, J. B., Prescott, A. R. and Nathke, I. S.** (2002). The adenomatous polyposis coli protein unambiguously localizes to microtubule plus ends and is involved in establishing parallel arrays of microtubule bundles in highly polarized epithelial cells. *J Cell Biol* **157**, 1041-8.

**Montcouquiol, M., Crenshaw, E. B., 3rd and Kelley, M. W.** (2006). Noncanonical Wnt signaling and neural polarity. *Annu Rev Neurosci* **29**, 363-86.

**Montcouquiol, M., Rachel, R. A., Lanford, P. J., Copeland, N. G., Jenkins, N. A. and Kelley, M. W.** (2003). Identification of Vangl2 and Scrb1 as planar polarity genes in mammals. *Nature* **423**, 173-7.

**Moon, R. T., Campbell, R. M., Christian, J. L., McGrew, L. L., Shih, J. and Fraser, S.** (1993). Xwnt-5A: a maternal Wnt that affects morphogenetic movements after overexpression in embryos of *Xenopus laevis*. *Development* **119**, 97-111.

**Moxey, P. C. and Trier, J. S.** (1979). Development of villus absorptive cells in the human fetal small intestine: a morphological and morphometric study. *Anat Rec* **195**, 463-82.

**Nomachi, A., Nishita, M., Inaba, D., Enomoto, M., Hamasaki, M. and Minami, Y.** (2008). Receptor tyrosine kinase Ror2 mediates Wnt5a-induced polarized cell migration by activating c-Jun N-terminal kinase via actin-binding protein filamin A. *J Biol Chem* **283**, 27973-81.

**Oishi, I., Suzuki, H., Onishi, N., Takada, R., Kani, S., Ohkawara, B., Koshida, I., Suzuki, K., Yamada, G., Schwabe, G. C. et al.** (2003). The receptor tyrosine kinase Ror2 is involved in non-canonical Wnt5a/JNK signalling pathway. *Genes Cells* **8**, 645-54.

**Qian, D., Jones, C., Rzadzinska, A., Mark, S., Zhang, X., Steel, K. P., Dai, X. and Chen, P.** (2007). Wnt5a functions in planar cell polarity regulation in mice. *Dev Biol* **306**, 121-33.

**Quyn, A. J., Appleton, P. L., Carey, F. A., Steele, R. J., Barker, N., Clevers, H., Ridgway, R. A., Sansom, O. J. and Nathke, I. S.** (2010). Spindle orientation bias in gut epithelial stem cell compartments is lost in precancerous tissue. *Cell Stem Cell* **6**, 175-81.

**Roarty, K. and Serra, R.** (2007). Wnt5a is required for proper mammary gland development and TGF-beta-mediated inhibition of ductal growth. *Development* **134**, 3929-39.

**Rodriguez-Boulan, E. and Nelson, W. J.** (1989). Morphogenesis of the polarized epithelial cell phenotype. *Science* **245**, 718-25.

**Saburi, S., Hester, I., Fischer, E., Pontoglio, M., Eremina, V., Gessler, M., Quaggin, S. E., Harrison, R., Mount, R. and McNeill, H.** (2008). Loss of Fat4 disrupts PCP signaling and oriented cell division and leads to cystic kidney disease. *Nat Genet* **40**, 1010-5.

**Safholm, A., Tuomela, J., Rosenkvist, J., Dejmek, J., Harkonen, P. and Andersson, T.** (2008). The Wnt-5a-derived hexapeptide Foxy-5 inhibits breast cancer metastasis in vivo by targeting cell motility. *Clin Cancer Res* **14**, 6556-63.

**Schambony, A. and Wedlich, D.** (2007). Wnt-5A/Ror2 regulate expression of XPAPC through an alternative noncanonical signaling pathway. *Dev Cell* **12**, 779-92.

**Schlessinger, K., McManus, E. J. and Hall, A.** (2007). Cdc42 and noncanonical Wnt signal transduction pathways cooperate to promote cell polarity. *J Cell Biol* **178**, 355-61.

**Sepich, D. S., Usmani, M., Pawlicki, S. and Solnica-Krezel, L.** (2011). Wnt/PCP signaling controls intracellular position of MTOCs during gastrulation convergence and extension movements. *Development* **138**, 543-52.

**Simons, M. and Mlodzik, M.** (2008). Planar cell polarity signaling: from fly development to human disease. *Annu Rev Genet* **42**, 517-40.

**Smart, I. H.** (1972). Proliferative characteristics of the ependymal layer during the early development of the mouse diencephalon, as revealed by recording the number, location, and plane of cleavage of mitotic figures. *J Anat* **113**, 109-29.

**Tada, M. and Smith, J. C.** (2000). Xwnt11 is a target of Xenopus Brachyury: regulation of gastrulation movements via Dishevelled, but not through the canonical Wnt pathway. *Development* **127**, 2227-38.

**Thyberg, J. and Moskalewski, S.** (1999). Role of microtubules in the organization of the Golgi complex. *Exp Cell Res* **246**, 263-79.

**Toyota, T., Yamamoto, M. and Kataoka, K.** (1989). Light and electron microscope study on developing intestinal mucosa in rat fetuses with special reference to the obliteration of the intestinal lumen. *Arch Histol Cytol* **52**, 51-60.

**Trier, J. S. and Moxey, P. C.** (1979). Morphogenesis of the small intestine during fetal development. *Ciba Found Symp*, 3-29.

**Ungar, A. R., Kelly, G. M. and Moon, R. T.** (1995). Wnt4 affects morphogenesis when misexpressed in the zebrafish embryo. *Mech Dev* **52**, 153-64.

**Visel, A., Blow, M. J., Li, Z., Zhang, T., Akiyama, J. A., Holt, A., Plajzer-Frick, I., Shoukry, M., Wright, C., Chen, F. et al.** (2009). ChIP-seq accurately predicts tissue-specific activity of enhancers. *Nature* **457**, 854-8.

**Wallingford, J. B., Fraser, S. E. and Harland, R. M.** (2002). Convergent extension: the molecular control of polarized cell movement during embryonic development. *Dev Cell* **2**, 695-706.

**Witze, E. S., Litman, E. S., Argast, G. M., Moon, R. T. and Ahn, N. G.** (2008). Wnt5a control of cell polarity and directional movement by polarized redistribution of adhesion receptors. *Science* **320**, 365-9.

**Yamada, M., Udagawa, J., Matsumoto, A., Hashimoto, R., Hatta, T., Nishita, M., Minami, Y. and Otani, H.** (2010). Ror2 is required for midgut elongation during mouse development. *Dev Dyn* **239**, 941-53.

**Yamaguchi, T. P., Bradley, A., McMahon, A. P. and Jones, S.** (1999). A Wnt5a pathway underlies outgrowth of multiple structures in the vertebrate embryo. *Development* **126**, 1211-23.

## **Chapter 5**

### **Conclusions and Future Directions**

The work in this thesis is the first in depth examination of the epithelial organization and the cellular dynamics of morphogenesis in the embryonic mouse intestine and identifies some of the cellular and genetic changes required for epithelial morphogenetic movements during intestinal development. Using mouse models combined with advanced microscopy and three dimensional (3D) reconstruction, this work overturns the previously accepted dogma to establish a new model of intestinal morphogenesis (Fig. 5.1). The studies presented in this thesis highlight the importance of cell dynamics in establishing, maintaining, and remodeling the pseudostratified intestinal epithelium, as well as generating intestinal length.

For many decades, the embryonic intestine was thought to be a stratified epithelium. In Chapter 2, we demonstrated that the intestinal epithelium is in fact pseudostratified and is maintained as a single layer throughout morphogenesis. Furthermore, we showed that between embryonic day (E)12.5 and E14.5, the thickening of the epithelium is an actinomyosin and microtubule dependent process that involves progressive lengthening of epithelial cells, and progressive apical

constriction. Using Cagg;mTmG mice, we utilized the variegated expression of the CaggCreERT2 after administration of a low tamoxifen dose to label individual epithelial cell membranes. This powerful, recently described tool (Muzumdar et al., 2007) will likely become the standard for cell shape analysis.

We found that the pseudostratified intestinal epithelium shares several characteristics with other embryonic pseudostratified epithelia. The epithelium is highly proliferative and characterized by specialized nuclear movements termed interkinetic nuclear migration (INM). The nuclei migrate between the apical cell surface and the basement membrane with S-phase occurring at the basal surface and mitosis at the apical surface. Thus, the INM results in staggering of nuclei within the epithelium, a characteristic that caused previous investigators to misinterpret of epithelial organization of the epithelium as stratified.

One protein required for both cellular elongation and apical constriction in the neuroepithelium and the lens epithelium is the actin binding protein Shroom3 (Lee et al., 2009). In the mouse intestine, Shroom3 activity seems to be most critical when cells exit mitosis and must re-establish their elongated and apically constricted shape. The *Shroom3* mutant gut contains rounded, lumenally located cells with expanded apical surfaces. During remodeling, the normally smooth apical surfaces of wild type villi are irregular, highly branched, and ramified in *Shroom3* knockouts. Interestingly, this phenotype is similar to the ramified lumen of the ductal pancreas, which assumes a temporary stratified morphology before resolving

the final ductal pattern (Villasenor et al., 2011). Our preliminary analysis of emerged villi in *Shroom3* mutant mice suggests that they have extra cells on their surfaces, indicating that the rounded luminal cells may result in a stratified organization prior to remodeling. It will be important to determine whether the *Shroom3* mutants maintain a pseudostratified epithelium or assume a stratified organization prior to remodeling.

During the remodeling of the epithelium, villus formation, apical expansion, and lumen extension occur synchronously, suggesting that these processes may be mechanistically linked. Previous studies described lumen formation as the *de novo* creation of apical surface at isolated junctions called secondary lumina (Mathan et al., 1976; Saotome et al., 2004). It was thought that these secondary lumina enlarged and eventually fused to create a single lumen in the intestine. However, in Chapter 3, our analysis of intestinal 3D reconstructions demonstrated that the apparent secondary lumina are actually connected to the primary lumen in a different plane. This Chapter therefore overturns the secondary lumen model and instead introduces a specialized form of cell division as the mechanism of luminal expansion. Delivery of apical membrane to the cytokinetic furrow had been previously described in MDCK cysts, Caco-2 organoids, and the zebrafish neural keel (Ciruna et al., 2006; Ferrari et al., 2008; Jaffe et al., 2008; Martin-Belmonte et al., 2007; Tawk et al., 2007). However, specialized extending divisions (which we term e-divisions) that deliver apical surface to the cytokinetic furrow to expand the apical surface and separate the intestinal villi are a novel observation. Our studies identify

an association between cytokinesis and lumen formation in about 60% of mitotic nuclei at E14.5/15, which are associated with the tips of extending lumina. Additionally, apical markers atypical protein kinase C (aPKC) and Zona occludens (ZO-1) are identified at the cytokinetic furrow of the e-divisions only during intestinal remodeling and not prior to this time. We propose that e-divisions drive the morphogenetic process responsible for lumen remodeling, apical expansion, and villus emergence.

Finally, Chapter 4 presents initial findings from a study of the genetic pathways responsible for intestinal morphogenesis and gut lengthening. The previous dogma stated that intestinal thickening is accomplished by temporary epithelial stratification and that intestinal remodeling occurs by radial intercalation, creating a single-layered columnar epithelium that defines evaginating villi. Since we demonstrate here that the early intestinal epithelium is pseudostratified, the theory of radial intercalation is not feasible and a new mechanism of intestinal remodeling and gut lengthening needs to be investigated. To begin to address this, we analyzed intestinal growth in wild type embryos and found that the most accelerated period of lengthening coincides with the period of epithelial remodeling between E14.5 and E16.5. To further explore this apparent link between remodeling and lengthening, we examined the growth patterns of the *Wnt5a* null mouse model. These mice are known to have very short intestines (Cervantes et al., 2008). Since *Wnt5a* can signal through the non-canonical Wnt/planar cell polarity (PCP) pathway, we also

examined mice carrying genetic mutations in other components of this pathway, including *Vangl2* and *Fat4*.

Analysis of growth of the *Wnt5a* deficient intestines revealed that these mutants maintained a slow, but steady rate of lengthening between E12.5 and E18.5 and without the standard accelerated growth rate between E14.5 and E16.5. These studies are also ongoing for *Vangl2* and *Fat4* mutants, both of which have shortened intestines. Additionally, in *Wnt5a* and *Vangl2*, as well as in *Fat4* null mice, disorganized nuclear orientation, Golgi mislocalization, and abnormal villus shape and pattern were identified. These initial observations once again suggest a link between intestinal remodeling and length generation and suggest that PCP signaling is critical for both (Fig. 5.2).

This work will not only have a tremendous impact on the field of intestinal development, but it will be important in the broader field of cell biology. These studies influence our understanding of epithelial cell dynamics and may offer insight into genetic pathways and molecular mechanisms utilized by epithelial cells during wound healing, cancer metastasis, and disease progression.

### **Future Studies**

The studies in this thesis have opened several new questions for further investigation. In the following discussion, I will review some of the most interesting of these and suggest experiments that could be used to address these new questions.

### **Why Pseudostratification?**

Why is it important that the intestine thickens in a pseudostratified organization as compared to a stratified organization? The data on pseudostratified epithelia are limited, but they include *Drosophila* imaginal disks, the primary neural tube (zebrafish, *Xenopus*, chick, mouse), and the mouse retina (Baye and Link, 2008; Meyer et al., 2011; Miyata, 2008). All of these pseudostratified epithelia also undergo INM, a process in which the nuclei migrate along the apical-basal axis of the cell and localization depends on the stage of the cell cycle. From the developmental biologist's perspective, it is probably not just coincidence that these tissues are so similar in their organization; there is likely an evolutionary advantage for these tissues to be pseudostratified.

The first advantage of a pseudostratified cell shape is that, in part because of INM, it is possible to pack a large number of cells into a small space. The pupa stage *Drosophila* imaginal wing disk is 50,000 cells, and it has been speculated that the pseudostratified cell shape is required for massive proliferation without a proportional growth in area (Bittig et al., 2009). Likewise, it has been postulated that pseudostratification of the neural tube is an adaptation to allow increased packing of progenitors, so as to expand brain size (Miyata, 2008; Smart et al., 2002). The fact that the remodeling of the mouse intestine is associated with a burst in length fits nicely with the idea that the pseudostratified shape creates a cell reservoir that, when cell shape is changed, can turn girth into length. We have



initiated some mathematical modeling experiments, with Dr. Santiago Schnell, to further explore this question.

Another advantage of pseudostratification may be that all of the cells are able to receive and respond to cellular signals from both the basement membrane and the apical surface. Initially, this may keep all of the cells essentially the same: highly proliferative stem or multipotent cells with great regenerative capacity. At a specific time in development (E14), however, some trigger must instruct the remodeling of this pseudostratified and therefore rather uniform collection of progenitors into an epithelium that contains islands of progenitors separated by regions of differentiated cells (the villi). This trigger seems to be linked to the formation of mesenchymal clusters (Karlsson et al., 2000), and the formation of these clusters is controlled by Hh signals from the epithelium (Drs. Kate Walton and Åsa Kolterud, Gumucio laboratory, unpublished data). But since the level of Hh signaling does not change during this time, we can predict that, while Hh is necessary for the formation of villi (because it is necessary for cluster formation), it is probably not the trigger for the process.

So, how does the epithelium sense that it is time to remodel and initiate the Hh-dependent clustering of nearby mesenchymal cells? One intriguing idea is that hypoxia is involved. The pseudostratified cell shape demands that the cells be thinner and thinner as they become more densely packed. Does the increasingly limited connection to the basement membrane (the area in touch with blood

vessels) result in development of a hypoxic state in the epithelial cells that triggers their remodeling? This could be tested in culture systems in reduced oxygen to determine whether limiting oxygen could accelerate villus formation, or whether increased oxygen tension could delay this process. Additionally, *in vivo* probes exist that allow the use of histochemical techniques to measure hypoxic states. Preliminary experiments suggest that changes in oxygen tension do occur at the time of intestinal remodeling.

### **Is pseudostratification required for proliferation?**

Pseudostratification allows tight packing of progenitors and pseudostratified epithelia are often highly proliferative, but is this cell shape necessary for proliferation in the developing intestine? It is interesting that, as the villi emerge, cells in the intervillus regions remain pseudostratified and they retain their proliferative status. These intervillus regions will later be remodeled to form mature crypts and function as the home for adult intestinal stem cells. Currently, it is not clear what relationship exists between the progenitors that inhabit the unremodeled early epithelium, the progenitors that occupy the fetal intervillus/pre-crypt regions, and the final adult stem cells in the crypt.

So far, we can only say that pseudostratification correlates with the maintenance of proliferation in embryonic and fetal stages. For example, loss of *Tcf4* (an effector of Wnt signaling) causes intervillus cells in the E16.5 mouse to lose their proliferative abilities; interestingly, these cells become cuboidal (Korinek et al., 1998). Similarly,

in our studies with Mitomycin C, we saw that loss of proliferation also resulted in a shape change from pseudostratified to columnar. Thus, it appears that loss of proliferation leads to failure to maintain the pseudostratified cell shape, but testing whether the converse is true must necessarily await the definition of the factors that control pseudostratification.

**What genes are responsible for maintaining the pseudostratified cell shape?**

*Shroom3* has clearly been shown in other models to be important in this context (Chung et al., 2010; Hildebrand, 2005; Hildebrand and Soriano, 1999; Lee et al., 2009; Lee et al., 2007; Plageman et al., 2010). However, in the mouse intestine, *Shroom3* seems to be required for rounded post-mitotic cells to re-acquire a pseudostratified shape, but it does not seem to be necessary, for the maintenance of pseudostratification in most of the cells. It is noteworthy though, that *Shroom2* is also expressed in the intestinal epithelium, and it is possible that the two genes act redundantly. Currently, a *Shroom2* knockout is not available, but the culture system that we have developed could be used in conjunction with dominant negative Shroom constructs [described in (Fairbank et al., 2006)] to test the role of Shroom signaling in pseudostratification. Apart from Shroom, other potential candidates might be identified in the laser capture microarray experiments described below.

**What role do cell shape changes play in villus development? How are these cell shape changes triggered? What controls their spatial organization?**

We showed that the epithelium remains single layered during the period of villus growth; no secondary lumina are formed and the cells do not “rearrange” as suggested in earlier models (Cervantes et al., 2008; Kim et al., 2007; Saotome et al., 2004). Rather, we favor a model in which e-divisions carve out the villi. As expected, given the rather uniform shapes of emerging villi, we have observed that the “cracking” of the epithelium that is driven by e-divisions is very regular and patterned. Interestingly, this cracking process always results in the extension of luminal cracks toward the future intervillus regions. Thus, we propose that the placement and orientation of e-divisions simultaneously controls both the shapes of emerging villi and the location of intervillus regions.

The emergence of villi, however, is also accompanied by changes in both cell shape and proliferation, particularly in the regions over the emerging villi, where the epithelial cells transition from pseudostratified and proliferative to columnar and post-mitotic. These dramatic changes are likely to be triggered by specific signaling programs. Though this thesis has been focused on the epithelium, in the search for the sources of these signals, it will be important to consider both the epithelium and the underlying mesenchyme.

Epithelial-mesenchymal crosstalk is known to be crucial for villus development (Gao et al., 2009; Kaestner et al., 1997; Karlsson et al., 2000; Kolterud et al., 2009; Li et al., 2007; Madison et al., 2005; Ormestad et al., 2006). Data from our lab indicate that one important signal for the initiation of villus growth is Hedgehog (Kolterud et al.,

2009; Madison et al., 2005). We previously demonstrated that Hedgehog ligands, expressed by the epithelium, signal to the underlying mesenchyme and are required for villus development (Kolterud et al., 2009; Madison et al., 2005). Expression of the Hh receptor *Patched1* and the downstream target gene *Gli1* is found exclusively in the mesenchyme, demonstrating that mesenchymal cells are responsive to the Hh signal, but epithelial cells are not. Therefore, a Hh-induced mesenchymal factor likely signals back to the epithelium to induce villus formation.

Dr. Kate Walton in our laboratory has found that a number of Hh target genes are expressed within mesenchymal aggregates of cells that we call “mesenchymal clusters.” These clusters, which had also been noted by other investigators (Karlsson et al., 2000), appear immediately subadjacent to the epithelium, just prior to intestinal remodeling. Interestingly, inhibition of Hh signals by cyclopamine or by over-expression of a pan-Hh inhibitor in cultured intestines results in the loss of these clusters. Under these conditions, the epithelium fails to remodel and remains as a pseudostratified proliferative epithelium (unpublished results). Thus, these mesenchymal clusters likely drive epithelial remodeling and Hh signals from the epithelium are required for their formation. Interestingly, the clusters are precisely positioned relative to the cracking epithelium, so that clusters appear beneath the epithelial regions that will become the future villi.

Whether the clusters pattern the cracking or *vice versa* is an interesting question for further exploration. We have observed that clusters are very tightly adherent to the

sub-epithelial surface. One could imagine that, as the clusters attach to the epithelium, the epithelial cells that are directly contacted may be induced to exit the cell cycle by signals from the clusters. In a zone surrounding this contact area, epithelial cells may be encouraged (by cluster signals?) to undergo e-divisions to separate villi.

But what signals do the clusters secrete that might talk back to the epithelium? The top candidate is Bmp. Both Drs. Åsa Kolterud and Kate Walton in the Gumucio lab have found that mesenchymal clusters express Bmp2, Bmp4 and Bmp5, but they also express Bmp modulators such as Twgs1 and Bmp1 (a tolloid-related metalloprotease that cleaves the Bmp inhibitor, chordin). Drs. Kolterud and Walton have also extensively studied the effects of Bmp signaling on the epithelium and villus formation. Bmp4 or Bmp2 recombinant protein added to intestinal explant cultures inhibit villus emergence and promote the formation of villus free epithelium, while Bmp inhibitors induce the formation of densely packed clusters and more villi. In the fly, decreased Dpp (Bmp) signal transduction in the pseudostratified epithelium of wing imaginal disks produces localized evaginations with columnar epithelium; shaped like intestinal villi (Widmann and Dahmann, 2009). We posit that the pattern of clusters, which is highly regular, sets up zones of high and low Bmp signaling; high Bmp signaling favors intervillus regions while lower Bmp signaling favors cell shape changes (from pseudostratified to columnar) that promote villus emergence. Analysis of clusters by electron microscopy has revealed a very tight association between the cluster and the epithelial cells at the

point of the emerging villus. Thus, other signals such as Notch, which are involved in direct cell-to-cell signaling, might also be important.

To further identify the factors that are made in the cluster and might be important in villus emergence and epithelial remodeling, it would be useful to perform a microarray on tissue isolated by laser capture microdissection. Since the signaling may be quite different in epithelium over the clusters and epithelium in intervillus regions, it would be important to separately examine the transcriptome of these two samples, as well as their underlying mesodermal regions.

Given that we believe that Bmp signals are highest in intervillus regions, it is interesting that we have observed that a subset of late stage mitotic nuclei that localize to the apical surface at E14.5 are positive for phosphorylated Smad1/5/8 (data not shown), suggesting that Bmp signals may be regulating the proliferation of these cells. We also know that e-divisions localize to extending luminal “cracks” that point toward intervillus regions. Are the e-divisions (but not the other earlier girth-building cell divisions, called g-divisions) driven by Bmp signaling? Are the clusters responsible for elaborating the Bmp signals? Experiments analyzing the effects of Bmp signals on epithelial proliferation and the localization of mitotic nuclei will be critical. To start, staining E13.5 and E14.5 intestines with pSmad1/5/8 in association with midbody markers will identify whether e-divisions vs. g-divisions are associated with high Bmp signals. Additionally, explant intestinal cultures treated with Bmp recombinant protein or Bmp inhibitors during remodeling and

analyzed for e-divisions, degree of luminal expansion, and cell shape will be essential to understand the role of Bmp in promoting e-divisions. Finally, the use of epithelial-specific *Bmpr1a* floxed mice and Cre-activatable constitutive active *Bmpr1a* (both underway) will allow us to directly examine the effects of altered Bmp signaling on the remodeling epithelium.

It is likely that other growth factors besides Bmp are important during intestinal epithelial remodeling. To assess the role of additional ligands, a screen of intestinal organ cultures treated with Shh, Notch, Wnt, and FGF pathway activators and inhibitors will be conducted. The treated samples will be screened after 24 hrs. for epithelial height, apical constriction, cell cycle (BrdU, pHH3, Ki67), and INM/nuclear stacking alterations. Additionally 48hr post treatment, intestines will be assessed for villus formation, epithelial cell shape, cell cycle localization, epithelial differentiation markers, and the presence of Lgr5+ stem cells. After screening the treated cultures, candidate pathways will be investigated in greater detail.

### **How can the luminal expansion alterations in the *Shroom3* null model be explained?**

Lumen formation and ductal branching in the embryonic mouse pancreas occur by transient stratification which produces a highly branched ramified apical surface (Villasenor et al.). In comparison, *Shroom3* null mouse intestines form a lumen that is also highly branched and ramified. The similarities in the two models may be explained if the *Shroom3* deficient epithelium is actually stratified. This can be



tested with a *Shroom3*<sup>-/-</sup>;Cagg;mTmG intestine or by electroporating a *Shroom3* null intestine with a CMV-EGFP plasmid injected into the lumen of an E13.5 intestine. Additionally, the Cagg;mTmG background will be crucial to understand the epithelial cell shape and organization of all models with defective morphogenesis including those mutant for *Wnt5a*, *Fat4*, and *Vangl2*.

### **What accounts for fused villi in the Ezrin null mouse?**

The *Ezrin* null mouse model is important since the interpretation of that phenotype as a failure of secondary lumen coalescence (Saotome et al., 2004) has been setting the dogma in the field with respect to the forces that shape emerging villi. In that study, the authors propose that villus formation occurs in the context of a stratified epithelium by “unzipping” the villi from one another *via* secondary lumen formation. That is, they posit that secondary lumina form in deep epithelial layers and that these lumina grow in size and then connect to the primary lumen. They also suggest that the fused villi in *Ezrin* null mice indicate a failure of this connection step. Of course, we know now that secondary lumina are essentially an artifact of thin sectioning. Thus, the *Ezrin* null phenotype needs to be re-evaluated.

Based on our identification of e-divisions as primary effectors of villus separation, we now propose that the *Ezrin* null phenotype is actually due to a failure of cytokinesis in cells undergoing the e-division. We would predict that, in the Cagg;mTmG model (induced with tamoxifen at E13.5 and harvested at E15.5), regions of fused villi will be characterized by cells of the same color (that is, we

expect that the two cells that bridge the villi are products of a single cell division in which cytokinesis, and thus apical extension, is stalled). We have obtained the *Ezrin* null mice and are currently testing this prediction.

### **Nocodazole synchronization to analyze dividing cells.**

Our analysis of e-division is technically demanding because, though many cells are dividing at the luminal cracks at the time when the tissue is fixed, cells are at vastly different stages of mitotic division. Stages such as cytokinesis and abscission are very short and difficult to “catch” in individual fixed tissue sections. Analyzing greater numbers of anaphase and telophase cells would improve our understanding of cell division and lumen expansion. In our studies of the effects of Nocodazole (Nocod) on epithelial cell height and INM, we noticed that the Nocod treatment could synchronize many cells at the same stage of the cell cycle in the context of cultured intestines. Furthermore, washing the intestines with fresh media releases this inhibition. We propose that treating intestinal organ cultures with Nocod should synchronize the epithelial cells in metaphase. Upon washing the intestines, we would be able to simultaneously analyze large numbers of dividing cells to examine cell shape, orientation, and apical surface proteins during division.

Nocod synchronization might allow us to determine how g-divisions differ from e-divisions. For example, we posit that midbody orientation might be different in the two divisions. We also predict that in g-divisions, the dividing cells maintain contact with the basal surface via a thin cytoplasmic process and that the cytokinetic furrow

splits this process. This has actually been documented in the neural tube (Ciruna et al., 2006; Tawk et al., 2007). However, in e-divisions, tethering both cells to the basement membrane is sterically impossible, since the two cells end up on different villi and will become separated by the intervening intervillus cells. In this case, then, at least one of the cells must release the basement membrane. It is likely however, that the release of the second cell is temporary and that this cell re-establishes contact with the basement membrane following the completion of mitosis. The same is seen in c-divisions in the neural tube (Tawk et al., 2007).

It is interesting to speculate that, in re-finding the basement membrane, the post-mitotic cell should follow radial cues. Failure to establish this contact has the potential to either result in cell death, or to result in a stratified epithelium. Mice deficient in *Wnt5a*, *Vangl2* or *Fat4* all have apparent areas of stratification as well as increased cell death. Thus, this might be a PCP-dependent process. The use of the Nocod block to see how often cells in these epithelia fail to re-establish basement membrane contact following mitosis will be of great interest.

### ***What is the role of cytoskeletal changes in intestinal remodeling?***

*Shroom3*, *Ezrin*, *Wnt5a*, *Fat4*, and *Vangl2* have all been associated with cytoskeletal rearrangement. In the mouse intestine, we have been unable so far to identify changes in the distribution of myosinII or microtubules since antibodies are unreliable and fixation protocols are tricky. However, alterations in cytoskeletal proteins after genetic and molecular manipulation need to be examined. One way to

circumvent the staining problem is to use transgenic or knockin mice carrying tagged cytoskeletal proteins or electroporate intestinal organ cultures with vectors carrying a fluorescently tagged cytoskeletal protein. Changes could then be examined in real time once the live imaging culture system is optimized as discussed below.

### **The use of live imaging to facilitate investigation of epithelial remodeling.**

Several events occur nearly concordantly during morphogenesis of the intestine: initiation of e-divisions, expansion of the apical surface, formation and patterning of the mesenchymal clusters cell shape change, and villus emergence. The ability to image these events in real time would certainly help to make sense of and temporally order these events. Current live imaging techniques use small, transparent embryos or organs. For live cell imaging in *Xenopus*, *C. elegans*, *Drosophila*, and zebrafish, the fluorescently labeled specimen is mounted on glass and various methods of immobilization are used to prevent embryo movement (Ellis et al., 2004; Keller et al., 2008; Kieserman and Wallingford, 2009; Ninov and Martin-Blanco, 2007). Current mouse live imaging is limited to studies of cells on the outside surface of the embryo or dissected organs including genetically labeled cells of the anterior visceral endoderm (Srinivas et al., 2004); the notochord (Yamanaka et al., 2007); branching morphogenesis of the kidney (Watanabe and Costantini, 2004), mammary glands (Ewald et al., 2008), and gonads (Coveney et al., 2008). Mouse imaging is limited because embryos develop internally, are not transparent,

and nutrient requirements are complex. Intestinal imaging will have many of the same challenges.

Because it is impossible to image through outer muscle layers of the mouse intestinal tube, I have established an intestinal slice culture system to analyze the epithelial cells lining the gut. Intestinal slice cultures, modeled after brain slices (Gahwiler et al., 1997), survive, develop, and contract on transwell plates and in glass bottom dishes. Individual epithelial cells in slice cultures at time zero can be imaged on the confocal microscope and imaged over time using a perfusion organ culture compression system created by our collaborator, Chris Janetopoulos, Ph.D., Assistant Professor of Biological Sciences at Vanderbilt University. The culturing device holds the intestinal slice between two glass plates while the intestine is perfused with warm media. By fluorescently labeling epithelial cell membranes, cytoplasm, and nuclei *in vivo*, I will be able to identify cell shape changes and follow nuclear movements in mouse tissue with and without genetic modifications.

Using this system, it would be possible to image changes in cell shape and cell movement. Changes in the epithelium can be visualized using mTmG mice (Muzumdar et al., 2007) with cell membranes stained either red with the fluorescent protein tomato or green with EGFP (after tamoxifen). Thus, cell shape changes in individual cells can be tracked. Nuclear movements can be visualized by using H2BEGFP, a tagged nuclear molecule. Briefly, intestines from E14 or E14.5 mouse embryos can be dissected in DMEM with Pen/Strep, immediately embedded

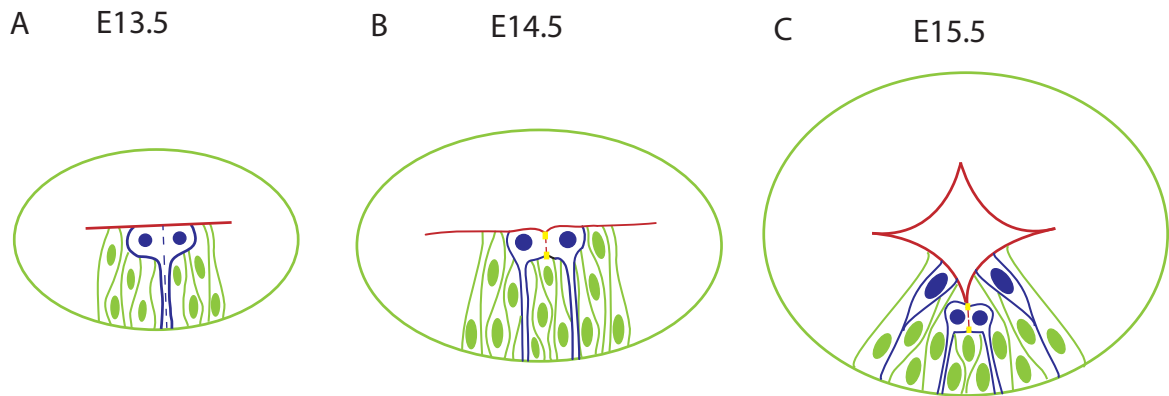
in 37°C 2% agarose and solidified at RT. Blocks sectioned at 100-200  $\mu\text{m}$  can be placed in the compression culture device. DMEM with P/S and 10% FBS, heated to 37°C, can be perfused across the intestinal slice using a perfusion pump and imaged on a confocal microscope for 2-4 hrs. XYZT images from the confocal can be analyzed using Imaris software and created into a movie to visualize dynamic cell shape changes and nuclear movements. These experiments will allow us to see INM, to follow the cell shape changes after mitosis in g-divisions as well as e-divisions, and to assess differences in these parameters in PCP mutants.

An alternative to the use of the mTmG mouse would be the use of Dendra2, a photoconvertible protein (Chudakov et al., 2007). That is, epithelial cells of E13.5 or E14 intestines can be transfected with Dendra2, by injecting the 2  $\mu\text{g}/\text{mL}$  Dendra2-EGFP construct into the lumen and electroporating with a square pulse electroporator. We have had initial success with this. Electroporated intestines can be cultured on transwell plates for 24 hrs and then embedded, sectioned, and live imaged as above. When excited at 405 nm, Dendra2 photoswitches from green to red, to allow identification and tracking of individual cells during live imaging. Such live imaging studies would greatly enhance our understanding of cell dynamics and morphogenetic movements in the intestinal epithelium.

## **Conclusions**

The data in this thesis present a novel model of intestinal morphogenesis in which the epithelium is pseudostratified and maintains its polarity as a single layer

throughout thickening and remodeling. We find that expansion of the intestinal lumen is driven by a specialized form of cell division, called the e-division, in which dividing cells deliver apical surface to the cytokinetic plane. The division of daughter cells therefore separates villi. We identify a number of genes required for various steps of intestinal morphogenesis including *Shroom3*, *Wnt5a*, *Vangl2*, and *Fat4*, and we redefine the role of *Ezrin* in this process. These findings, which necessitate the revision of several current and well-accepted ideas about intestinal organogenesis, have important implications for understanding villus development and length generation in the developing intestine and may eventually lead to improved treatments for absorptive disorders that result from loss of villi or disruption of intestinal length.



**Figures 5.1. New model of intestinal morphogenesis.** Multiple concurrent morphogenetic events drive epithelial remodeling including epithelial proliferation, AB thickening, apical expansion, and villus formation. The thickening process is a pseudostratification event between E12.5 and 14.5 with epithelial increasing to a height of up to 50 $\mu$ m. In the pseudostratified epithelium, nuclei migrate between the basal surface during S-phase and the apical surface to divide, a process termed interkinetic nuclear migration (INM). Also, the characteristic nuclear stacking makes the layer look stratified, but epithelial cells actually stretch from the basement membrane to the lumen. Between E13.5 and 14.5, the thickening process is aided by g-divisions (A), divisions that increase epithelial girth and maintain the current location and amount of apical surface. At E14.5, a specialized cell division termed an e-division (B) adds apical surface to the cytoketic furrow between dividing cells. The e-divisions effectively extend the apical surface while separating cells onto different villi (C). Mitosis preferentially localizes to the extending tips, the area that will become the proliferative intervillus/pre-crypt region.



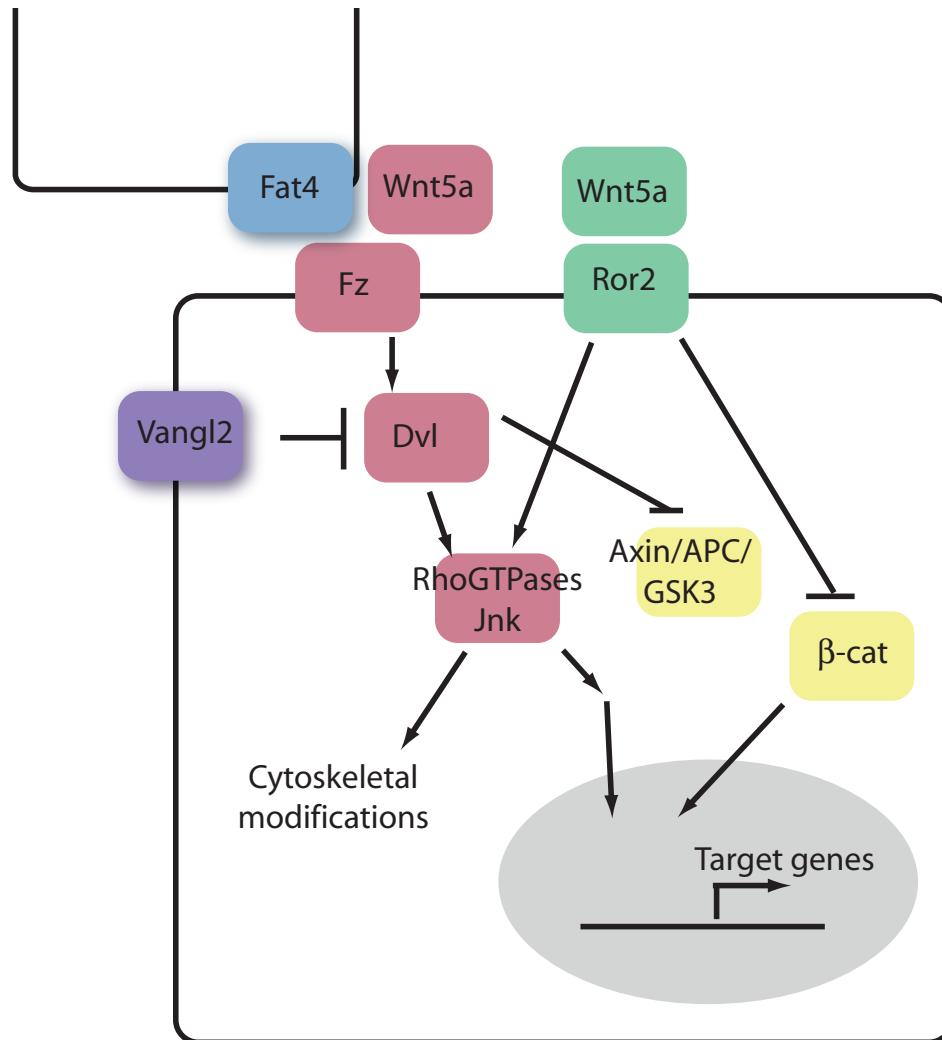


**Figure 5.2. The Wnt5a/PCP signaling pathway.** A model for mammalian Wnt and PCP signaling interactions based on genetic and molecular studies in *Drosophila*, *Xenopus*, zebrafish, and mice. Wnt5a can signal through the Ror2 to inhibit  $\beta$ -catenin dependent canonical Wnt signaling or activate noncanonical signaling. Binding of Wnt5a to Fz receptors activates canonical Wnt or noncanonical Wnt/PCP pathways. The membrane bound Fat4 cadherin may interact with Fz based on the similarity of phenotypes in Fat and Fz deficient flies. The core PCP protein Vangl2 can bind and interact with the noncanonical Wnt pathway at the level of Dvl.

## Literature Cited

- Baye, L. M. and Link, B. A.** (2008). Nuclear migration during retinal development. *Brain Res* **1192**, 29-36.
- Bittig, T., Wartlick, O., Gonzalez-Gaitan, M. and Julicher, F.** (2009). Quantification of growth asymmetries in developing epithelia. *Eur Phys J E Soft Matter* **30**, 93-9.
- Cervantes, S., Yamaguchi, T. P. and Hebrok, M.** (2008). Wnt5a is essential for intestinal elongation in mice. *Dev Biol*.
- Chudakov, D. M., Lukyanov, S. and Lukyanov, K. A.** (2007). Tracking intracellular protein movements using photoswitchable fluorescent proteins PS-CFP2 and Dendra2. *Nat Protoc* **2**, 2024-32.
- Chung, M. I., Nascone-Yoder, N. M., Grover, S. A., Drysdale, T. A. and Wallingford, J. B.** (2010). Direct activation of Shroom3 transcription by Pitx proteins drives epithelial morphogenesis in the developing gut. *Development* **137**, 1339-49.
- Ciruna, B., Jenny, A., Lee, D., Mlodzik, M. and Schier, A. F.** (2006). Planar cell polarity signalling couples cell division and morphogenesis during neurulation. *Nature* **439**, 220-4.
- Coveney, D., Cool, J., Oliver, T. and Capel, B.** (2008). Four-dimensional analysis of vascularization during primary development of an organ, the gonad. *Proc Natl Acad Sci U S A* **105**, 7212-7.
- Ellis, G. C., Phillips, J. B., O'Rourke, S., Lyczak, R. and Bowerman, B.** (2004). Maternally expressed and partially redundant beta-tubulins in *Caenorhabditis elegans* are autoregulated. *J Cell Sci* **117**, 457-64.
- Ewald, A. J., Brenot, A., Duong, M., Chan, B. S. and Werb, Z.** (2008). Collective epithelial migration and cell rearrangements drive mammary branching morphogenesis. *Dev Cell* **14**, 570-81.
- Fairbank, P. D., Lee, C., Ellis, A., Hildebrand, J. D., Gross, J. M. and Wallingford, J. B.** (2006). Shroom2 (APXL) regulates melanosome biogenesis and localization in the retinal pigment epithelium. *Development* **133**, 4109-18.
- Ferrari, A., Veligodskiy, A., Berge, U., Lucas, M. S. and Kroschewski, R.** (2008). ROCK-mediated contractility, tight junctions and channels contribute to the conversion of a preapical patch into apical surface during isochoric lumen initiation. *J Cell Sci* **121**, 3649-63.
- Gahwiler, B. H., Capogna, M., Debanne, D., McKinney, R. A. and Thompson, S. M.** (1997). Organotypic slice cultures: a technique has come of age. *Trends Neurosci* **20**, 471-7.
- Gao, N., White, P. and Kaestner, K. H.** (2009). Establishment of intestinal identity and epithelial-mesenchymal signaling by Cdx2. *Dev Cell* **16**, 588-99.
- Hildebrand, J. D.** (2005). Shroom regulates epithelial cell shape via the apical positioning of an actomyosin network. *J Cell Sci* **118**, 5191-203.
- Hildebrand, J. D. and Soriano, P.** (1999). Shroom, a PDZ domain-containing actin-binding protein, is required for neural tube morphogenesis in mice. *Cell* **99**, 485-97.
- Jaffe, A. B., Kaji, N., Durgan, J. and Hall, A.** (2008). Cdc42 controls spindle orientation to position the apical surface during epithelial morphogenesis. *J Cell Biol* **183**, 625-33.

**Kaestner, K. H., Silberg, D. G., Traber, P. G. and Schutz, G.** (1997). The mesenchymal winged helix transcription factor Fkh6 is required for the control of gastrointestinal proliferation and differentiation. *Genes Dev* **11**, 1583-95.

**Karlsson, L., Lindahl, P., Heath, J. K. and Betsholtz, C.** (2000). Abnormal gastrointestinal development in PDGF-A and PDGFR-(alpha) deficient mice implicates a novel mesenchymal structure with putative instructive properties in villus morphogenesis. *Development* **127**, 3457-66.

**Keller, P. J., Schmidt, A. D., Wittbrodt, J. and Stelzer, E. H.** (2008). Reconstruction of zebrafish early embryonic development by scanned light sheet microscopy. *Science* **322**, 1065-9.

**Kieserman, E. K. and Wallingford, J. B.** (2009). In vivo imaging reveals a role for Cdc42 in spindle positioning and planar orientation of cell divisions during vertebrate neural tube closure. *J Cell Sci* **122**, 2481-90.

**Kim, B. M., Mao, J., Taketo, M. M. and Shivdasani, R. A.** (2007). Phases of canonical Wnt signaling during the development of mouse intestinal epithelium. *Gastroenterology* **133**, 529-38.

**Kolterud, A., Grosse, A. S., Zacharias, W. J., Walton, K. D., Kretovich, K. E., Madison, B. B., Waghray, M., Ferris, J. E., Hu, C., Merchant, J. L. et al.** (2009). Paracrine Hedgehog signaling in stomach and intestine: new roles for hedgehog in gastrointestinal patterning. *Gastroenterology* **137**, 618-28.

**Korinek, V., Barker, N., Moerer, P., van Donselaar, E., Huls, G., Peters, P. J. and Clevers, H.** (1998). Depletion of epithelial stem-cell compartments in the small intestine of mice lacking Tcf-4. *Nat Genet* **19**, 379-83.

**Lee, C., Le, M. P. and Wallingford, J. B.** (2009). The shroom family proteins play broad roles in the morphogenesis of thickened epithelial sheets. *Dev Dyn* **238**, 1480-91.

**Lee, C., Scherr, H. M. and Wallingford, J. B.** (2007). Shroom family proteins regulate gamma-tubulin distribution and microtubule architecture during epithelial cell shape change. *Development* **134**, 1431-41.

**Li, X., Madison, B. B., Zacharias, W., Kolterud, A., States, D. and Gumucio, D. L.** (2007). Deconvoluting the intestine: molecular evidence for a major role of the mesenchyme in the modulation of signaling cross talk. *Physiol Genomics* **29**, 290-301.

**Madison, B. B., Braunstein, K., Kuizon, E., Portman, K., Qiao, X. T. and Gumucio, D. L.** (2005). Epithelial hedgehog signals pattern the intestinal crypt-villus axis. *Development* **132**, 279-89.

**Martin-Belmonte, F., Gassama, A., Datta, A., Yu, W., Rescher, U., Gerke, V. and Mostov, K.** (2007). PTEN-mediated apical segregation of phosphoinositides controls epithelial morphogenesis through Cdc42. *Cell* **128**, 383-97.

**Mathan, M., Moxey, P. C. and Trier, J. S.** (1976). Morphogenesis of fetal rat duodenal villi. *Am J Anat* **146**, 73-92.

**Meyer, E. J., Ikmi, A. and Gibson, M. C.** (2011). Interkinetic Nuclear Migration Is a Broadly Conserved Feature of Cell Division in Pseudostratified Epithelia. *Curr Biol*.

**Miyata, T.** (2008). Development of three-dimensional architecture of the neuroepithelium: role of pseudostratification and cellular 'community'. *Dev Growth Differ* **50 Suppl 1**, S105-12.

- Muzumdar, M. D., Tasic, B., Miyamichi, K., Li, L. and Luo, L.** (2007). A global double-fluorescent Cre reporter mouse. *Genesis* **45**, 593-605.
- Ninov, N. and Martin-Blanco, E.** (2007). Live imaging of epidermal morphogenesis during the development of the adult abdominal epidermis of *Drosophila*. *Nat Protoc* **2**, 3074-80.
- Ormestad, M., Astorga, J., Landgren, H., Wang, T., Johansson, B. R., Miura, N. and Carlsson, P.** (2006). *Foxf1* and *Foxf2* control murine gut development by limiting mesenchymal Wnt signaling and promoting extracellular matrix production. *Development* **133**, 833-43.
- Plageman, T. F., Jr., Chung, M. I., Lou, M., Smith, A. N., Hildebrand, J. D., Wallingford, J. B. and Lang, R. A.** (2010). Pax6-dependent Shroom3 expression regulates apical constriction during lens placode invagination. *Development* **137**, 405-15.
- Saotome, I., Curto, M. and McClatchey, A. I.** (2004). Ezrin is essential for epithelial organization and villus morphogenesis in the developing intestine. *Dev Cell* **6**, 855-64.
- Smart, I. H., Dehay, C., Giroud, P., Berland, M. and Kennedy, H.** (2002). Unique morphological features of the proliferative zones and postmitotic compartments of the neural epithelium giving rise to striate and extrastriate cortex in the monkey. *Cereb Cortex* **12**, 37-53.
- Srinivas, S., Rodriguez, T., Clements, M., Smith, J. C. and Beddington, R. S.** (2004). Active cell migration drives the unilateral movements of the anterior visceral endoderm. *Development* **131**, 1157-64.
- Tawk, M., Araya, C., Lyons, D. A., Reugels, A. M., Girdler, G. C., Bayley, P. R., Hyde, D. R., Tada, M. and Clarke, J. D.** (2007). A mirror-symmetric cell division that orchestrates neuroepithelial morphogenesis. *Nature* **446**, 797-800.
- Villasenor, A., Chong, D. C., Henkemeyer, M. and Cleaver, O.** (2011). Epithelial dynamics of pancreatic branching morphogenesis. *Development* **137**, 4295-305.
- Watanabe, T. and Costantini, F.** (2004). Real-time analysis of ureteric bud branching morphogenesis in vitro. *Dev Biol* **271**, 98-108.
- Widmann, T. J. and Dahmann, C.** (2009). Dpp signaling promotes the cuboidal-to-columnar shape transition of *Drosophila* wing disc epithelia by regulating Rho1. *J Cell Sci* **122**, 1362-73.
- Yamanaka, Y., Tamplin, O. J., Beckers, A., Gossler, A. and Rossant, J.** (2007). Live imaging and genetic analysis of mouse notochord formation reveals regional morphogenetic mechanisms. *Dev Cell* **13**, 884-96.